DELIVERY OF THERMOSTABILIZED CHONDROTINASE ABC

ENHANCES AXONAL SPROUTING AND

FUNCTIONAL RECOVERY AFTER SPINAL CORD INJURY

A Dissertation
Presented to
The Academic Faculty

by

Hyun-Jung Lee

In Partial Fulfillment
of the requirements for the Degree
Doctor of Philosophy in the
School of Biomedical Engineering

Georgia Institute of Technology
October 2009

DELIVERY OF THERMOSTABILIZED CHONDROTINASE ABC ENHANCES AXONAL SPROUTING AND FUNCTIONAL RECOVERY AFTER SPINAL CORD INJURY

Dr. Ravi V. Bellamkonda, Advisor
School of Biomedical Engineering
Georgia Institute of Technology

Dr. Andrés J. García
School of Mechanical Engineering
Georgia Institute of Technology

Dr. Andreas Bommarius
School of Chemical & Biomolecular Engineering
Georgia Institute of Technology

Dr. Robert J. McKeon
Department of Cell Biology
Emory University

Dr. Niren Murthy
School of Biomedical Engineering
Georgia Institute of Technology

ACKNOWLEDGMENTS

First of all, I would like to acknowledge my advisor, Prof. Ravi V. Bellamkonda, for his guidance over the years. He encouraged me to continue my research career, provided a great environment, and always will be a good mentor. I feel lucky to have a chance to work with him.

I also would like to acknowledge my thesis committee members, Prof. Andreas Bommarius, Prof. Andrés J. García, Prof. Niren Murthy and Prof. Robert J. McKeon. I am thankful for their guidance and insight for this study.

I was fortunate to meet my great labmates. I would like to express my appreciation to all members of the Neurological Biomaterials and Cancer Therapeutics Laboratory. The memories of the times we have shared will be in my mind forever and I will wish the best of luck for all of you in your career and beyond.

I also like to express my appreciation to my sincere friends: Sungmoon, Moon and Shannon who always emotionally supported me, listen to me and were there for me whenever I needed them.

My parents and my brother always provide me unconditional love and any supports and prayed for me every morning. I know they are always with me and in my mind wherever I stay.

Without any of you, I could not get though this journey.

TABLE OF CONTENTS

LIST OF TABLES

LIST OF FIGURES

SUMMARY

Chondroitin sulfate proteoglycans (CSPGs) are one major class of axon growth inhibitors that are upregulated and accumulated around the lesion site after spinal cord injury (SCI), and result in regenerative failure. To overcome CSPG-mediated inhibition, digestion of CSPGs with chondroitinase ABC (chABC) has been explored and it has shown promising results. chABC digests glycosaminoglycan chains on CSPGs and can thereby enhance axonal regeneration and promote functional recovery when delivered at the site of injury. However, chABC has a crucial limitation; it is thermally unstable and loses its enzymatic activity rapidly at 37 ℃. Therefore, it necessitates the use of repeated injections or local infusions with a pump for days to weeks to provide fresh chABC to retain its enzymatic activity. Maintaining these infusion systems is invasive and clinically problematic.

In this dissertation, three studies are reported that demonstrate our strategy to overcome current limitations of using chABC and develop a delivery system for facilitating chABC treatment after SCI: First, we enhanced the thermostability of chABC by adding trehalose, a protein stabilizer, and developed a system for its sustained local delivery *in vivo*. Enzymatic activity was assayed by sodium dodecyl sulfate-polyacrylamide gel electrophoresis (SDS-PAGE) and dimethylmethylene blue (DMMB), and conformational change of the enzyme was measured via circular dichroism (CD) with and without trehalose. When stabilized with trehalose, chABC remained enzymatically active at 37 ℃ for up to 4 weeks *in vitro*. We developed a lipid microtube-agarose hydrogel delivery system for a sustained release and showed that chABC released from the delivery system is still functionally active and slowly released over 2 weeks *in vitro*. Second, the hydrogel-

microtube system was used to locally deliver chABC over two weeks at the lesion site following a dorsal over hemisection injury at T10. The scaffold consisting of hydrogel and chABC loaded lipid microtubes was implanted at the top of the lesion site immediately following injury. To determine effectiveness of topical delivery of thermostabilized chABC, animal groups treated with single injection or gel scaffold implantation of chABC and penicillinase (P'ase) were included as controls. Two weeks after surgery, the functionality of released chABC and the cellular responses were examined by immunohistological analysis with 3B3, CS-56, GFAP and Wisteria floribunda agglutinin (WFA). The results demonstrated that thermostabilized chABC was successfully delivered slowly and locally without the need for an indwelling catheter by using the hydrogel-microtube delivery system *in vivo*. The results demonstrated that released chABC from the gel scaffold effectively digested CSPGs, and therefore, there were significant differences in CSPG digestion at the lesion site between groups treated with chABC loaded microtube-hydrogel scaffolds and controls. Third, a long term *in vivo* study (45 days) was conducted to examine axonal sprouting/regeneration and functional recovery with both a single treatment each of microtube loaded chABC or Neurotrophin-3 (NT-3), and a combination of them by using the hydrogel-microtube delivery system. Over the long term study period, the treated animals showed significant improvement in locomotor function and more sprouting of cholera toxin B subunit (CTB)-positive ascending dorsal column fibers and 5-HT serotonergic fibers around the lesion site.

We demonstrated that this significant improvement of chABC thermostability facilitates the development of a minimally invasive method for sustained, local delivery of chABC that is potentially a useful and effective approach for treating SCI. In addition to that,

we demonstrated that combinatorial therapy with chABC and neurotrophic factors could

provide a synergistic effect on axonal regrowth and functional recovery after SCI.

CHAPTER 1

INTRODUCTION

1.1. STATEMENT OF PROBLEM

Unlike in the peripheral nervous system (PNS) or embryonic nervous system, in the central nervous system (CNS) the severed axons fail to regrow through the lesion site, even though the spared neurons survive for years.

There are approximately 255,000 people living with SCI in the United States and there are 12,000 new cases added each year. After injury to the central nervous system, the lesioned axons fail to re-grow and recover function (Schwab and Bartholdi, 1996). The extent of sensory and motor function loss after spinal cord injury (SCI) varies depending on the level of injury, and often results in permanent functional loss. Complete neurological recovery after SCI is experienced by less than 1% of patients. Since 2000, the most frequent category of spinal cord injury is incomplete tetraplegia (34.1%), followed by complete paraplegia (23.0%), complete tetraplegia (18.3%), and incomplete paraplegia (18.5%). The cost for treatment is up to $ 0.7 million per patient in the first year, and the lifetime cost is up to $ 3 million (National Spinal Cord Injury Statistical Center, 2008). The cellular and molecular mechanisms of the inflammation process, cell death, the mechanism of axon growth failure and receptor/targeting relationships are all active areas of research. While many groups are investigating a number of strategies to encourage axonal regeneration, a breakthrough clinical therapy has yet to be developed.

A challenge in the environment of the injured spinal cord is that the inhibitory molecules create a non-permissive environment for axonal regrowth and it results in a failure of axonal regeneration and complete functional recovery. chABC, which digests CS-GAGs on CSPGs, has shown promise as a therapeutic agent for SCI treatment (Yick et al., 2000; Krekoski et al., 2001; Bradbury et al., 2002) and CNS regeneration (Moon et al., 2001; Fox and Caterson, 2002; Pizzorusso et al., 2002). However there are crucial limitations and difficulties to be applied for clinical treatment; chABC is thermally very unstable and it loses its enzymatic activity quickly at body temperature. Therefore, multiple injection of chABC or mini-pump/catheter-mediated delivery system has been used to provide fresh chABC *in vivo* for long periods. However, these infusion systems are invasive and require much effort to maintain. In this study, an alternative strategy for chABC delivery *in vivo* is developed and tested alone or in combination with neurtophin-3 (NT-3) to enhance axonal regeneration after SCI.

1.2. HYPOTHESIS

The central hypothesis of this dissertation is that the digestion of CSPG by chondroitinase ABC will promote axonal regeneration and functional recovery after SCI. The chABC digestion will remove the inhibitory effect of CSPGs limiting axonal regeneration after CNS injury and provide a permissive substrate for axonal outgrowth. We hypothesized that delivery of thermostabilized chABC using our slow and local delivery system will provide a sufficient amount of bioactive chABC to effectively digest CSPGs at the lesion site. Also, the delivery method will be more efficient than single injection of an equal amount of chABC to digest CSPGs, and it will enhance axonal sprouting/regeneration and induce

behavioral recovery. Therefore, our slow local delivery system could be an alternative method to current mini-pump/catheter delivery methods, which are invasive and infection-prone because they are chronically implanted. We believe that a combination strategy of chABC and neurtophin-3 using the slow release delivery system will encourage even more axonal regeneration and functional recovery.

It is important to achieve following design criteria to demonstrate our hypothesis: 1) thermostabilized chABC; 2) a delivery vehicle for slow release in a temporally controlled manner; and 3) a non-pump/single administration method in a spatially controlled manner. Strategies to solve these challenges are: 1) protein stabilizers; 2) lipid microtube and hydrogel mediated delivery system; and 3) a topical delivery model to the dorsal over hemisection injury.

1.3. OBJECTIVES

The overall purpose of the work described in this thesis is to develop an approach to successfully use chABC as a therapeutic agent. To overcome limitations of chABC treatment for SCI, it is necessary to improve thermostability of chABC and develop a delivery strategy for thermostabilized chABC *in vivo*.

To meet this goal, the following objectives were set:

1. To improve the thermal stability of chABC and develop a minimally invasive and slow delivery system.

    a. Determine ability of trehalose to improve thermostability of chABC *in vitro*.

    b. Develop a hydrogel and lipid microtube mediated delivery scaffold and evaluate functionality of post-released chABC *in vitro*.

2. To supply thermostabilized chABC *in vivo* by implanting a hydrogel-lipid microtube delivery system with a topical delivery model and examine the functionality of released chABC and the cellular responses after SCI.

    a. Examine delivery efficiency of chABC by evaluating CSPG digestion two after implantation.

3. To apply a combinatorial strategy using chABC and NT-3 to enhance therapeutic effects and examine axonal sprouting/regeneration and functional recovery after SCI.

1.4. REFERENCES

Barritt AW, Davies M, Marchand F, Hartley R, Grist J, Yip P, McMahon SB, Bradbury EJ (2006) Chondroitinase ABC promotes sprouting of intact and injured spinal systems after spinal cord injury. J Neurosci 26:10856-10867.

Bradbury EJ, Moon LD, Popat RJ, King VR, Bennett GS, Patel PN, Fawcett JW, McMahon SB (2002) Chondroitinase ABC promotes functional recovery after spinal cord injury. Nature 416:636-640.

Fox K, Caterson B (2002) Neuroscience. Freeing the brain from the perineuronal net. Science 298:1187-1189.

Krekoski CA, Neubauer D, Zuo J, Muir D (2001) Axonal regeneration into acellular nerve grafts is enhanced by degradation of chondroitin sulfate proteoglycan. J Neurosci 21:6206-6213.

Moon LD, Asher RA, Rhodes KE, Fawcett JW (2001) Regeneration of CNS axons back to their target following treatment of adult rat brain with chondroitinase ABC. Nat Neurosci 4:465-466.

Pizzorusso T, Medini P, Berardi N, Chierzi S, Fawcett JW, Maffei L (2002) Reactivation of ocular dominance plasticity in the adult visual cortex. Science 298:1248-1251.

Schwab ME, Bartholdi D (1996) Degeneration and regeneration of axons in the lesioned spinal cord. Physiol Rev 76:319-370.

Yick LW, Wu W, So KF, Yip HK, Shum DK (2000) Chondroitinase ABC promotes axonal regeneration of Clarke's neurons after spinal cord injury. Neuroreport 11:1063-1067.

CHAPTER 2

RELEVANT BACKGROUND

Injuries trigger cellular and molecular signal cascades which upregulate inhibitors to axonal outgrowth and result in regenerative failure. Inhibition could be caused by myelin-associated inhibitors, immune-response molecules, glial scars, inhibitory extracellular matrix (ECM) molecules, and the lack of trophic factors. One major class of growth inhibitors are chondroitin sulfate proteoglycans (CSPGs) that accumulate around lesion site after SCI.

Studies have investigated CSPG-mediated inhibition to axonal regeneration. Chondroitinase ABC (chABC) digests glycosaminoglycan chains on CSPGs and can potentially overcome CSPG mediated inhibition and promote axonal sprouting/regeneration when delivered into lesion sites. However, chABC loses its enzymatic activity rapidly at 37 ºC, necessitating the use of repeated injections or local infusions with a catheter and pump for days to weeks to digest the CSPGs being produced continuously. Maintaining these infusion systems is invasive and clinically problematic.

To overcome the limitations of chABC therapy for clinical application, the following technical achievements must be met; stable bioactivity of chABC, a delivery system for sustained local delivery *in vivo*, and a non-pump/catheter administration. In this chapter, limitations that need to be overcome are described, and alternative methods and strategies to solve these challenges are discussed.

2.1 CELLULAR AND MOLECULAR RESPONSES AFTER SCI

After injury to the central nervous system (CNS), the inflammation process is triggered, a series of cellular and molecular responses are cascaded and eventually glial scars are formed around the lesioned tissue (Fawcett and Asher, 1999). The failure of neurite regrowth and permanent functional loss result from these cellular events. To begin, macrophages and microglia, oligodendrocyte precursors, meningeal cells and astrocytes migrate into the lesion site. These cells produce inhibitory molecules, such as myelin-associated glycoprotein (MAG), CSPGs and other proteoglycans, free radicals, nitric oxide, etc. The final form is a tightly interwoven glial scar formed around the lesioned site (Rudge and Silver, 1990). Macrophages from the bloodstream and microglia from the surrounding tissues are the first cells to arrive at the site, usually within a few hours after injury. They remove myelin debris, produce and release cytokines, recruit oligodendrocyte precursors and initiate reactive astrocytes. Inhibitory molecules are up-regulated and the injury site is exposed to non-permissive environment for axonal regeneration. Myelin-derived growth inhibitory proteins, such as NOGO, myelin associated glycoprotein (MAG), and oligodendrocyte-myelin glycoprotein (OMgp), contribute to the failure of optic nerve regeneration and spinal cord regeneration (Selles-Navarro et al., 2001). Oligodendrocyte precursors migrate from the surrounding tissue after 3-5 days and myelin debris contains myelin-associated inhibitory molecules: NOGO is present on the myelin surface and collapses the neuronal growth cone (Bandtlow et al., 1993); MAG is produced by and present in oligodendrocytes (Kastin and Pan, 2005); and OMgp is most recently identified and inhibits neurite outgrowth (Kottis et al., 2002).

If meningeal layers, which cover the CNS, are penetrated, meningeal cells migrate to cover the exposed area of CNS and form a barrier to axon regeneration. Astrocytes are the predominant and final structure of the astro-glial scar with ECM and ECM molecules. These cells divide in reactive form, slowly migrate into the injured area, fill the space caused by injury, and produce inhibitory molecules, such as chondroitin sulfate proteoglycans (CSPGs). This astro-glial scar acts as a barrier that prevents axons from passing through and inhibits axonal regeneration. CSPGs are over-expressed in extracellular matrix at the lesion site where reactive astrocytes are present, and ultimately form astro-glial scars that act as barriers to axonal outgrowth. CSPGs are generally accepted as potent inhibitory molecules of axon growth in the adult CNS. Therefore, recent studies focus on alleviating CSPG-mediated inhibition by delivering the enzyme chABC *in vivo* and to encourage axonal regeneration and functional recovery (Moon et al., 2001; Bradbury et al., 2002; Barritt et al., 2006).

2.2 CSPG-MEDIATED INHIBITION AFTER SCI AND CURRENT TREATMENTS

It is known that axons of the CNS cannot regenerate to form functional connections after injuries. However in the mid-1980s studies demonstrated that CNS neurons can regenerate their axons over long distances when a favorable environment is provided (So and Cho, 1989). Currently, many studies are investigating CSPG-mediated inhibition by removing the inhibitory nature of CSPGs through enzyme-mediated modification. These studies suggest that attenuating inhibitory effects of CSPG by chABC digestion enhances axonal growth and functional recovery. chABC is a bacterial lyase produced from the bactreum *Proteus vulgaris* that is able to digest CSPGs. The therapeutic significance of chABC has been demonstrated in studies that delivered this enzyme to enhance nerve

regeneration (Bradbury et al., 2002; Barritt et al., 2006). However there are several limitations to clinical treatment before implementation can occur.

2.2.1   CHONDROTIN SULFATE PROTEOGLYCANS

CSPGs consist of a core protein and glycosaminoglycan (GAG) chain that are covalently linked to form a brush-like structure (Fig. 2.1). The GAGs are linked to the core protein by a trisaccharide composed of two galactose and one xylose residue. GAG is made of repeating disaccharides containing either two modifier sugars, glucuronic acid (GlcNAc) or galactosamine (GalNAc) and an uronic acid (glucuronate or iduronate). These chondroitin sugars can have over 100 individual sugar molecules and each can be sulfated in various positions and quantities. Figure 2.2 shows that chondroitin sulfate glycosaminoglycans (CSPG) have structural diversity (e.g. chondroitin-4-sulfate (ΔglcA-β1,3-4S-galNAc), chondroitin-6-sulfate (ΔglcA-β1,3-6S-galNAc), chondroitin-2,6-sulfate (Δ2S-glcA-β1,3-6S-galNAc), dermatan-4-sulfate (ΔiduA-α1,3-4S-galNAc), etc.) (Gilbert et al., 2005).

CSPGs are upregulated after injury in the CNS and become a major contributor to the failure of axonal regeneration (Pindzola et al., 1993; McKeon et al., 1995; Fitch and Silver, 1997; Asher et al., 2000; Asher et al., 2002; Jones et al., 2003; Tang et al., 2003). CSPGs also regulate neurons during development by defining barriers in CNS structures: perineuronal nets (PNNs) (Matthews et al., 2002) in the brain and spinal cord, the roof plate, a putative axon barrier, of the spinal cord and optic tectum (Snow et al., 1990a), and the hippocampus (Wilson and Snow, 2000). Studies have shown that neurite outgrowth is inhibited by CSPGs *in vitro* (Snow et al., 1990b; McKeon et al., 1991; Snow and Letourneau, 1992; Condic et al., 1999; Hynds and Snow, 1999; Snow et al., 2001; Johnson et al., 2002)

and *in vivo* after injury of optic nerve (Selles-Navarro et al., 2001) or the dorsal root entry zone (Zhang et al., 2001). However, the precise contribution of different CSPGs to CSPG-mediated inhibition in the CNS and the mechanism of cellular transduction of the inhibitory signal mediated by CSPGs are not clear. Because CSPGs have a significant structural diversity, the nature and profile of CSPG deposition patterns have been recently investigated (Jones et al., 2003; Properzi et al., 2005). Specific CSPGs are differentially over-expressed in astro-glial scar after injury and CSPGs have varying degrees of inhibition (Gilbert et al., 2005).

After spinal cord injury, glial scars present a physical barrier and also produce repulsive molecules such as CSPGs. This effect of CSPG-mediated inhibition can be attenuated by applying chABC, which is an enzyme degrading CS-GAG (Snow and Letourneau, 1992; Zuo et al., 1998; Krekoski et al., 2001). Therefore, enhanced axonal regeneration can be achieved by removing CSPGs or the GAG side chains of CSPGs with enzymes, such as chABC.

2.2.2   CHONDROITINASE ABC

chABC is one of a class chondroitinases and has a molecular weight of 120 to 145 kDa as determined by gel filtration (100 k Da in the SDS-PAGE). It is produced from bacterium *Proteus vulgarism* and there is no mammalian equivalent (Ryan MJ, 1994). chABC cleaves chondroitin, chondroitin-4-sulfate (C-4-S), chondroitin-6-sulfate (C-6-S), dermatan sulfate (DS) and hyaluronan GAGs by β-elimination of 1,4-hexosaminidic bonds into disaccharides and tetrasaccharides, yielding protein enriched core molecules with a linkage of oligosaccharides (Oike et al., 1982).
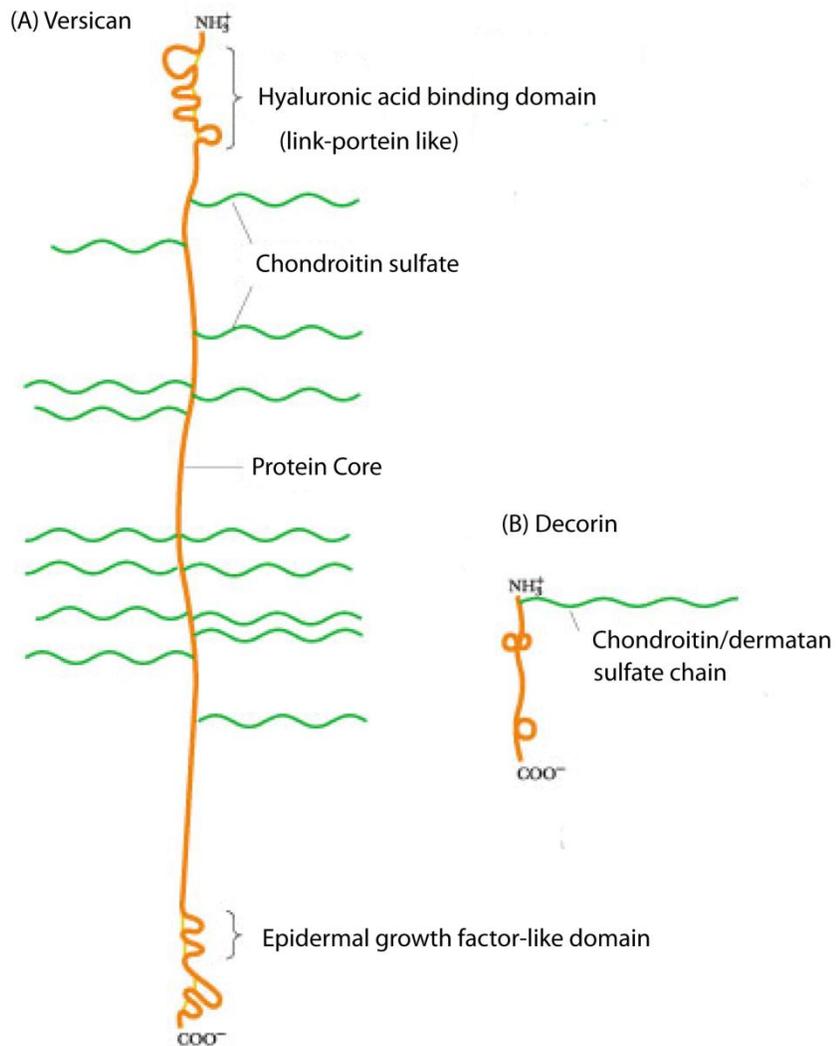
Figure 2.1. Structure of chondroitin sulfate proteoglycan (CSPG). (A) versican, a large CSPG belonging to the lectican family and (B) decorin, a small CSPG of extracellular matrix.
(Figure modified from http://web.virginia.edu/Heidi/chapter9/chp9.htm)
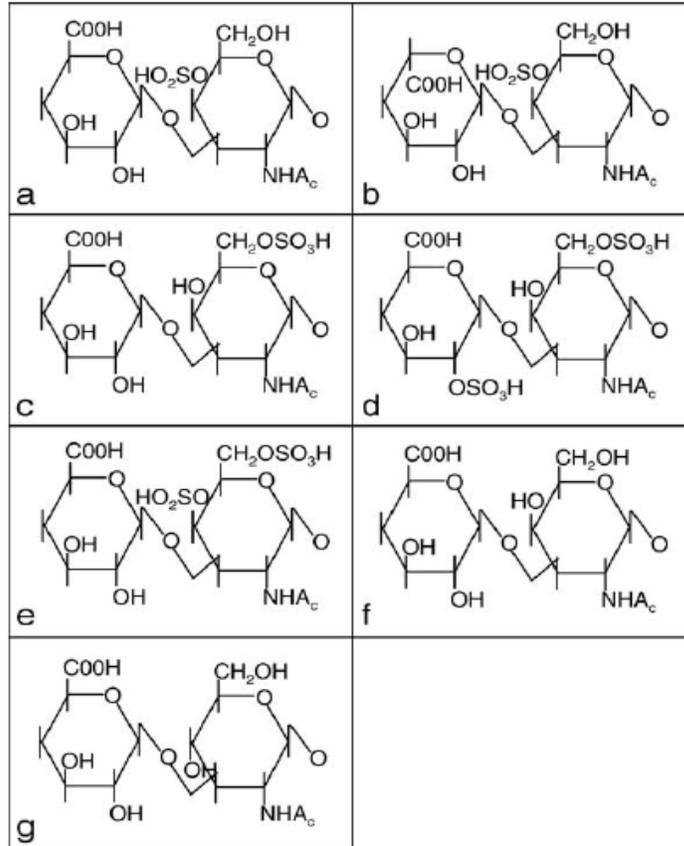
Figure 2.2. Schematic structure of various CSPGs and hyaluronan. Figure from Gilbert et al., 2005.

The chABC is isolated from *Proteus vulgaris* contain two distinct eliminases, endolytic (chABC I) and exolytic (chABC II) lyases (Hamai et al., 1997). chABC is commercially available and the commonly used chondroitinase enzymes are provided by Seikagaku Corporation (Japan) as "chondroitinase ABC (chABC I + chABC II)" and "chondroitinase ABC, protease-free (chABC I)". Usually the highly purified chABC, "chondroitinase ABC, protease-free", has been used for *in vivo* study and is used in this study.

chABC I is a 997 amino acid residue monomeric protein that degrades its substrates to tetrasaccharides and disaccharides. The complete crystal structure of chABC I has been

determined to contain three domains: the N terminal, central, and C terminal domains. The overall dimensions of chABC I is 115 Å × 70 Å × 55 Å and is folded into the three distinct domains (Huang et al., 2003). This structure shows overall similarity to other GAG lyases with additional domains on the N terminal. About 400 amino acid residues are in the C terminal domain also shows a homology to chondroitinase AC (cAC; two domain) (Fethiere et al., 1999) and bacterial hyaluronidases (Li et al., 2000). The role of this C-domain is not clear, however, one loop in this domain acts as a substrate-binding site. The N terminal domain consists of residues 25-234 and is the most flexible in chABC I compared to others. The N-domain has a common topology to other ligand-binding domains, particularly the carbohydrate-binding domains of xylanases and glucanases (Lo Conte et al., 2000). The central domain (residues 235-617) contains 15 α-helices and is most likely the catalytic site. The α-helix domain shows very similar sequence identity to the catalytic domains of cAC and hyaluronidase. The active site of chABC I, as informed by superimposition with cAC structure, has been investigated (Prabhakar et al., 2005a; Prabhakar et al., 2005b). However, the active site has not been clearly defined and it is still unknown as to why chABC quickly loses its enzymatic function at body temperature. In addition, a strategy has not been developed to increase the enzymatic lifetime of chABC.
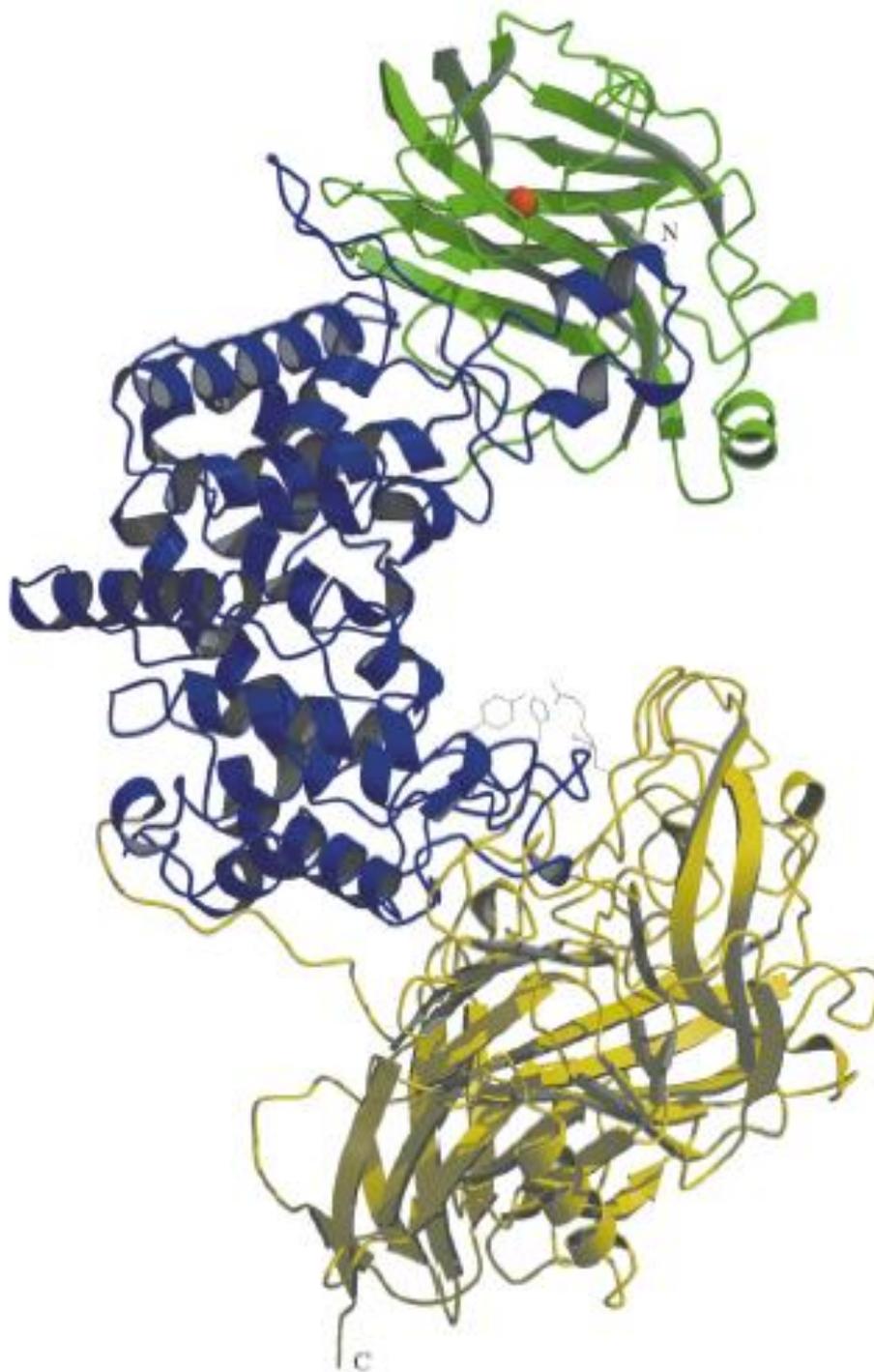
Figure 2.3. Ribbon drawing of chondroitinase ABC I (figure from (Huang et al., 2003)); the N-terminal (green), middle catalytic (blue) and C-terminal domain (yellow), from top to bottom.

chABC has the widest substrate specificity; therefore, it has been used widely, including as a therapeutic agent for SCI. Treatment with chABC has shown promising results with various CNS applications, such as regeneration of ascending sensory neurons and descending corticospinal tract axons in the spinal cord (Bradbury et al., 2002), sensory neurons in the dorsal root entry zone (Steinmetz et al., 2005), and retinal ganglian cell axons in the tectum (Tropea et al., 2003). Therefore, chABC offers a potential treatment strategy for neural injury.

2.2.3 DELIVERY OF CHONDROITIANSE ABC FOR AXONAL REGENERATION AND LIMITATIONS

chABC promotes axonal regeneration and functional recovery after CNS injury (Yick et al., 2000; Moon et al., 2001; Bradbury et al., 2002; Yick et al., 2003; Chau et al., 2004) and developmental disease (Pizzorusso et al., 2006). It promotes neurite sprouting in intact and injured spinal cords (Barritt et al., 2006). Most groups deliver chABC via intrathecal injection varying the infusion frequency from every other day to every other week, for time periods ranging from 2 weeks up to 6 weeks (Chau et al., 2004; Caggiano et al., 2005; Houle et al., 2006; Huang et al., 2006). Some groups inject chABC in combination with other therapeutic agents (Tropea et al., 2003) or with transplantation, such as that of E14 fetal spinal cords (Kim et al., 2006) or autologous peripheral nervous grafts (Houle et al., 2006), to obtain a synergistic effect.

However, there are several limitations and difficulties to these methods. chABC is thermally very sensitive at body temperatures, so after 1 hour of incubation at 37 ℃ it quickly loses 50% of its enzymatic activity (by Morgan-Elson reaction). It loses most of its

enzymatic function after a day. In addition, CSPGs are upregulated and accumulate in the extracellular matrix around the injured site up to at least 2 weeks after the primary injury. Therefore, most researchers continuously infuse chABC intrathecally through mini-pumps/catheters to maintain a supply of fresh enzyme. Another limitation is the diffusion of chABC. Most of these deliveries are performed intrathecally with a catheter, so it is hard for chABC to diffuse into deep regions of the tissue. Because intrathecal delivery allows the drug to flow through intrathecal space, the drug washes away quickly and does not last a long time in the target area. Also, because of this drug diffusion, the concentration immediately dilutes to significantly low concentrations, so high concentrations (from 2U/ml to 1000U/ml) are needed to compensate. This is a problem for chABC. Because this enzyme is very expensive, it is costly to apply therapeutically in high concentrations. As we can see, there are several problems to overcome; specifically there is a compelling need to control chABC delivery both spatially and temporally.

2.3 THERAPEUTIC STRATEGIES TO IMPROVE THERMAL STABILITY OF PROTEINS

Thermal stabilization of protein has many practical applications in research and industry. Since chemical reactions are generally faster at higher temperatures, enzymes, which are stable at higher temperature, would yield a more efficient process (Schoemaker et al., 2003; Unsworth et al., 2007). Also in the laboratory, thermally stable proteins/enzymes are easier to store or handle. Many studies have been conducted to engineer thermostability of proteins and there are two general strategies for protein engineering to improve the thermal stability of proteins or enzymes (Bae et al., 2008): rational design and directed

evolution. Another strategy is to add cosolvents for modifying solvent environment (Cleland and Wang, 1990).

2.3.1 PROTEIN ENGINEERING

In rational design, precise changes on amino acid sequence are designed from detailed knowledge of the structure and function of the protein by using site-directed mutation (Chen, 1999; Eijsink et al., 2004). It is generally inexpensive and easy, however the detailed structure of a protein is often not available and even with the detailed information it is difficult to predict the effect of mutation on protein functions. The other strategy, directed evolution, involves generation of random mutations in the protein sequence, and does not require information as to how the structure is related to function (Kuchner and Arnold, 1997; Eijsink et al., 2005). This mimics natural evolution; random mutation is applied to a protein, selected to pick desirable variants, and further rounds of mutation and selection are applied. This directed evolution approach is hard to predict the results of stability and functionality, and it requires an effort to narrow down best candidate. Random or rational engineered/directed mutation is generated by screening a library of variants to produce a stable variant. Many mutations that result in the most stable variant would have been difficult to predict by rational design and the results of directed evolution are often better than rational results. However these two techniques are not mutually exclusive and recently researchers engineer proteins in combination of these methods to render desired changes (Eijsink et al., 2004).

Enzyme stability can be improved by rational design, directed evolution or in combination. Surface position is good candidate for optimizing protein stability (Martin et al.,

2002). Surface or near-surface interactions are important for protein stability. However, very limited number of mutants can lead to an increase of stability and do not affect functionality. Random method has been used to generate mutation and it can lead high stability, but some of which are not easy to define rationally. Therefore, recently semi-rational method is frequently used. To apply for our case, chABC, several charged residues could be selected from the surface of the 3D structure (Prabhakar et al., 2005a; Prabhakar et al., 2005b), except active residues, and randomly mutate these residues and find optimized mutants. The stability of mutated chABC can be determined by 2D structure (circular dichroism) or 3D (X-ray crystal structure), and the functionality by enzymatic activity assays, such as, SDS-PAGE, western blotting, DMMB and HPLC method.

2.3.2 USAGE OF COSOLVENTS IN AQUEOUS SYSTEM

The other approach to stabilize protein is through addition of cosolvents. Cosolvents can be broadly categorized into the following: sugars and polyols (sugar alcohol), amino acid, amines, salts, polymers and surfactants. The level of stabilization by different cosolvents varies for particular proteins. Therefore, a cosolvent that stabilizes one protein/enzyme may not stabilize another (Hatti-Kaul and Mattiasson). Sugars (Carninci et al., 1998) and polyols (Xie and Timasheff, 1997a) are the more commonly used nonspecific protein stabilizers. Amino acids are also commonly used as stabilizer or osmolytes (Taneja and Ahmad, 1994; Remmele et al., 1998). The cosolvent may affect both the structural stability and activity of protein. Sugars and polyols always have been shown to enhance the thermal stability of proteins, but some amino acids have been found to destabilize the protein. The effects of salts also depend on pH of the medium and their chemical nature (Rishi et al., 1998). Therefore,

sugar or polyol are safe candidates as cosolvents. Often higher concentration of protein increases its own stability, however high concentration could lead a chance of protein aggregation. Surfactant is often used to reduce protein aggregation or protein surface adsorption, however the concentration of surfactants need to be carefully decide to avoid side effects (Faustino et al., 2009).

2.3.2.1   TREHALOSE AS A PROTEIN STABILIZER

Among various cosolvents, trehalose shows an exceptional improvement of thermal stability of protein (Kaushik and Bhat, 2003). Trehalose accumulates dramatically during heat shock and stationary phase in many organisms, then enhances thermo-tolerance and reduces aggregation of denatured proteins. Therefore, trehalose is a good candidate as a stabilizer for chABC. It has not been found in mammals, however this improves the tolerance of mammalian cells to desiccation and cryopreservation *in vitro*. This approach would be more convenient than the engineering protein.

Trehalose is found in nature as a disaccharide, two α-D-glucose molecules with the alpha bond in a 1α→1 glycosidic linkage (α-D-glucopyranosyl(1→1)-α-D-glucopyranoside). It is commonly used as a sweetener in food and as a cryopreservation additive. It is also known as an exceptional protein stabilizer, providing protection to biological materials during dehydration and desiccation (Sampedro et al., 1998). It promotes survival under extreme heat by stabilizing proteins in order to retain their conformation and suppresses the aggregation of denatured proteins (Singer and Lindquist, 1998). Further, trehalose stabilizes labile proteins during lyophilization (Zhang et al., 2009), protects enzymatic activity, such as

with RNase A, lysozyme, cytochromes during exposure to high temperatures in solution, and in a freeze-dried state (Kaushik and Bhat, 2003).
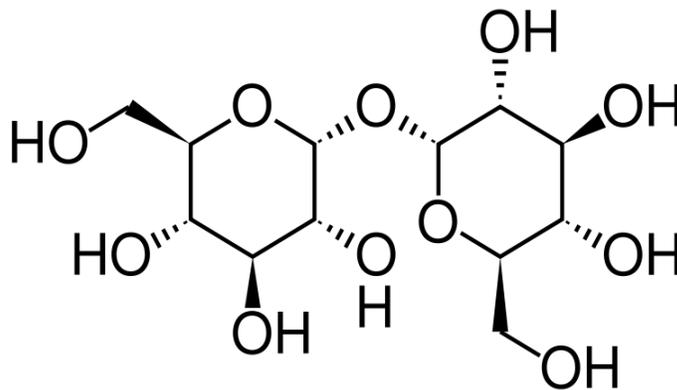
Figure 2.4. Structure of trehalose.

2.3.2.2 THE POSSIBLE MECHANISMS OF TREHALOSE STABILIZATION OF CHABC

As described previously, trehalose has unique properties with exceptional ability to protect biological materials under extreme conditions (Cottone et al., 2005; Hedoux et al., 2006). Many studies have been conducted to understand the mechanism of trehalose and possible mechanisms have been proposed, however the molecular mechanism of trehalose stabilization is poorly understood (Hedoux et al., 2009). There are several hypotheses to explain the mechanism of trehalose efficiency: 1) water replacement model (Crowe et al., 1984), 2) preferential hydration hypothesis (Arakawa and Timasheff, 1983), 3) vitrification of solutions (Green et al., 1989) and 4) the influence on the water tetrahedral hydrogen-bond network (Branca et al., 1999). However, the molecular mechanism probably depends on the nature of applied stresses.

The preferential interaction theory was proposed by Arakawa and Timasheff in 1983. They observed that bovine serum albumin and lysozyme were preferentially hydrated in amino acids. Preferential interaction is also stated as preferential binding of the cosolvent or preferential exclusion (preferential hydration). The cosolvent chemical potential perturbation by the protein is the driving force of preferential interaction, which causes change of the amount of water in contact with protein (Timasheff, 2002). Studies showed that trehalose stabilizes the folded structure of proteins in solution due to greater preferential hydration of the unfolded state compared to the native state (Xie and Timasheff, 1997b). Therefore, the mechanism seems to be opposite from the stabilization mechanism in the dried state, which is water replacement. Sugars generally protect proteins from dehydration by preventing the decrease of spacing through hydrogen bonding to the dried protein surface, serving as a water substitute (Carpenter et al., 1993). Like this, the mechanism of stabilization can be different under different applied stress conditions.

The primary mechanism by which trehalose is likely to affect the stability of the proteins is by increasing the surface tension of water around the proteins due to hydrogen bond formation between the hydroxyl groups of trehalose and water. In solution, trehalose stabilizes RNase A by increasing the surface tension of the trehalose solution, leading to the preferential hydration of the protein (Xie and Timasheff, 1997a). Surface tension of trehalose solutions increases linearly with increasing trehalose concentration (Kita et al., 1994), and there is a strong correlation between surface tension and increase in T_m (Jai et al., 2003). Increasing solvent surface tension necessitates more energy to form a cavity in order to increase the surface area of proteins upon denaturation. In fact, other protein stabilizers, such as polyols and carboxylic salts (Kaushik and Bhat, 1999) show a correlation between surface

tension increase and enhanced protein thermal stability. Studies also have shown that the dynamic fluctuation of polar side chains at the solvent-protein interface is reduced in the presence of trehalose (Hedoux et al., 2009). The increased surface tension or the limited exposure of hydrophobic groups to the water molecules leads to preferential hydration, resulting in the stabilization of the tertiary structure of protein (Timasheff, 2002).

2.3.3 PROTEIN STABILIZATION BY PEGYLATION

PEGylation describes a process of covalent conjugation with polyethylene glycol (PEG) polymer chains to biological molecules. PEG (Figure 2.5) manufactured by polymerization of ethylene oxide with water, ethylene glycol or ethylene glycol oligomers and various molecular weights of PEG can be prepared by modulation of the polymerization reaction. In 1970s, Aluchowski et al. studied a pioneering method of PEG conjugation (Abuchowski et al., 1977). In the study, methoxypolyethylene glycol was covalently attached to bovine serum albumin and it lost its immunogenicity and the potential of PEG conjugation. After this successful study, a number of studies followed and PEG has been applied to several biological therapies and success have been achieved in parallel with improvements of the PEG properties (Veronese and Mero, 2008). PEG is a biologically favorable molecule, a non-toxic and non-immunogenic molecules approved by the US FDA for internal use. PEGylation has been well established in the clinic and there are many PEGylated pharmaceuticals on the market, such as Pegasys (PEGylated interferon alpha), Oncaspar (PEGyleated L-asparaginase), Neulasta (PEGylated granulocyte colony-stimulating factor), Doxil/Caelyx (PEGylated liposome containing doxorubicin), etc (Veronese and Mero, 2008).

Figure 2.5 Poly(ethylene glycol)

Proteins/enzymes are delicate molecules and easily denatured or deactivated. PEGylation is can be applied to these therapeutic agents to modify or improve their stability, degradation by proteases or immunogenicity, and degree of renal excertion. The covalently attached PEG chains change the physical and chemical properties of the agents. Several PEG chains are attached on the surface of agents and result in increasing the molecular weight and creating water cloud surrounding the PEGylated agents by hydrogen bond formation between ether-oxygen in PEG (Figure 2.6). The modification improves pharmacokinetics of drugs: shielding the PEGylated agents from the host's immune system reduces immunogenicity and antigenicity and increases stability. It also provides high solubility in both aqueous and organic solvent, high mobility in solution, high hydration increasing hydrodynamic size in solution, and increases of the retention time in blood (Israelachvili, 1997). Due to the pharmacokinetic benefits of PEGylation, therapeutic proteins, peptides and antibody fragments have been PEGylated for several drug delivery applications (Harris and Chess, 2003).
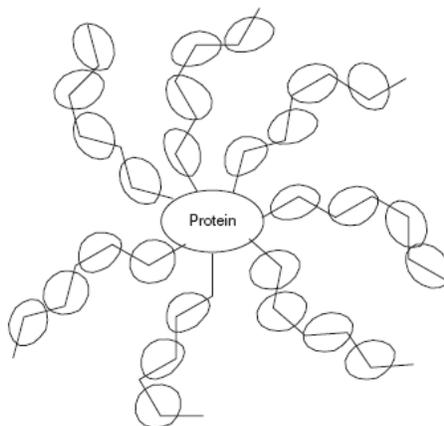
Figure 2.6 Schematic of PEGylated protein. The circles represent the water cloud recruited by the ether-oxygen groups of the PEG polymer. Figure from Veronese and Mero, 2008.

Hydroxyl group of the PEG terminal can react with the various protein amino acid residues. Since amino groups are present in every protein, generally at the surface and exposed to the solvent, it is the most exploited residue for PEGylation by alkylation or acylation. Amino group modification can negatively affect surface properties of the protein and in some cases the modification decreases enzymatic/biological activity (Banci et al., 1990; Greenwald et al., 2003). Modifying cysteine thiol residue by formation of thio-ethers or disulfides allows site-specific conjugation. Generally cysteine residues are involved in catalysis or disulfide bridges, so available free cysteine residues are rarely present. Therefore, sometimes this residue is genetically introduced in a desirable position for convenient applications (Kopchick et al., 2002). Disulfide-linked PEG conjugation can be a reversible modification and it allows a releasable PEGylation under mild reducing conditions (Woghiren et al., 1993). Similarly customized triggering moiety by enzymatic reaction, hydrolysis, or linker self-immolation cleaves the link and releases PEGylation, regenerating native agents and preserving its bioactivity. Recent reports demonstrate that the customized linkers of cytokines, peptide hormones, enzymes or receptor proteins are released under

physiological conditions and at specific and therapeutically useful rates (Filpula and Zhao, 2008).

Other amino acid residues, such as arginine (Veronese and Mero, 2008), glutamine, the alcohol group of serine and threonine, and the phenolic group of tyrosine (Orsatti and Veronese, 1999) are usable sites for PEG conjugation. For glutamine residue conjugation, the enzyme, transglutaminase, is used because there is no chemical method (Sato et al., 1996) and this glutamine-PEGylation is very specific (Fontana et al., 2008). However, because of a lack of specificity (arginine) and harsh reaction conditions (serine and theronine) other methods still need to be improved for therapeutic applications.

Since covalent binding is involved in PEGylation, and several PEG chains are usually linked on the surface, the size and conformation of the agents are changed. Also, there is a possibility that conjugated PEG polymers can block the binding sites and active sites resulting in loss or damage of the agent's bioactivity. Therefore, the mass, number of chains and link positions need to be investigated for each case to maintain its bioactivity. To avoid these complications, genetically engineered proteins can be used: a genetic variant of amino acids is inserted at a site far from biologically active site and used for a residue to PEG conjugation (Kopchick et al., 2002).

PEGylation has many advantages and some disadvantages to be used as a protein stabilizer. In our case with chABC, it would not be an ideal method for several reasons. Linked PEG chains can mask catalytic site of chABC, however exact positions of the site are still not clear and the mechanism of deactivation of chABC enzymatic activity is also unknown. Therefore, it is not easy to design a relevant PEG polymer conjugation for chABC to thermostabilize its enzymatic activity. Additionally, chABC is a relatively large molecule

and the increased size of chABC with PEGylation will result in limited diffusion through the nerve tissue. Therefore, we decided to use cosolvent in this study.

2.4 THERAPEUTIC STRATEGIES FOR CONTROLLED RELEASE OF AGENTS BY DELIVERY CARRIERS

The formulation of macromolecular agents, such as proteins, enzymes, and DNA in drug delivery systems is widely investigated due to the increased needs as therapeutics. Various carriers have been used for the efficient delivery of agents for different therapeutic purposes. For slow and local delivery of chABC after SCI, it is important to control temporally and spatially the amount of protein delivered over a period of time. Also, the delivery vehicle is able to maintain bioactivity of the agents over the period of time. The implanted vehicle itself and by-product of degraded vehicle should not induce significantly increase of inflammation response or aggravation of immune responses. Currently major delivery method of chABC for clinical and *in vivo* application to treat SCI is intrathecal injection through the implanted catheter with mini-pump or syringe (Bradbury et al., 2002; Barritt et al., 2006). This delivery system consists of two parts: 1) an infusion pump or an external catheter end implanted under the skin on the back of the animal, and 2) catheter inserted in the lesion site. However the internal catheter end is chronically implanted, and human cases have reported that intrathecal catheter-tip causes inflammatory mass (Peng and Massicotte, 2004), and surgical site infection (Burgher et al., 2007). Also an insoluble gelatin sponge and gelfoam containing chABC was used to treat SCI (Yick et al., 2003). In this study, we investigated a carrier-based drug delivery.

2.4.1 POLYMER NANOPARTICLE

Various delivery vehicles are used to deliver drugs into the CNS and PNS, such as liposomes, polymer nanoparticles and lipid microtubules. In order to locally deliver drugs for spinal cord treatment, PLGA nanoparticles and lipid microtubules could be considered for sustained delivery. Our laboratory has used both vehicles for in vivo sustained drug delivery. PLGA is a biocompatible and biodegradable polymer and is approved by US Food and Drug Administration for human use. PLGA nanoparticle have been used for sustain release of encapsulated agents (Shive and Anderson, 1997). The double emulsion method is used to make PLGA nanoparticles and is simple and takes a relatively short time, a total of 3 days. Additionally, it is easy to store in nanoparticle powder form at -80 ºC after lyophilizing. However during the double emulsion procedure, the releasing agent, such as protein, can be exposed to organic solvents (ex. Dichloromethane) and high temperatures. Without co-encapsulation of acid-neutralizing base, the pH is predominantly below pH 5.8 (detection limit in this paper) (Li et al., 2005). Therefore proteins undergo physical denaturation and chemical degradation during fabrication (Sah et al., 1999; Kim et al., 1999) and unpredictable release profiles often occur, such as a burst effect or incomplete release (Kim et al., 1999). Only a few proteins have shown the ability of controlled delivery from PLGA spheres (Kim et al., 2005).

2.4.2 LIPID MICROTUBES

Lipid microtubes are also capable of the slow release of protein or bio-agents for *in vivo* application. It spontaneously forms hollow and open-ended cylinders (Schnur, 1993) with 0.5 μm of the average inner diameter and the lengths of the cylinders depend on the

cooling rate (Thomas et al., 1995; Meilander et al., 2001). Microtubes have a high aspect ratio and it allows for a large storage volume and they are stable in physiological medium at 37 ℃ (Spargo et al., 1995) for prolonged a period of time. The fabrication process takes a relatively long time, a total of 15 days, and microtubes need to be prepared freshly. However, there is no toxic procedure for proteins, which could cause denaturation or degradation, during the fabrication process. Microtubes show a stable and continuous release profile and could be used as sustained delivery vehicles for proteins, such as neurotrophic factors (Jain et al., 2006), and even nucleic acids (Meilander et al., 2003). It is also easy to combine with hydrogels to support a scaffold for *in vivo* application and non-inflammatory (Rudolph et al., 1992; Meilander et al., 2001). Lipid microtubes are injectable either by themselves, or when embedded in thermo-reversible hydrogels as reported in Jain et al. (2006) for localization. The study showed that an agarose hydrogel scaffold embedded by BDNF loading lipid microtubes was implanted into a spinal cord cavity and led to the reduction of the inflammatory response and enhanced axonal infiltration into the scaffold.

The molecules are released through the ends of microtubes, and a mathematical model of release profile of proteins has been developed previously in our laboratory (Meilander et al., 2004). The release of proteins can be predicted with the molecular weight and protein concentration. The slow release of agents can be modified by controlling the length of microtube, type of gel, and gel concentration for desire delivered amount of agent for different application.

2.5   PHARMACOLOGICAL STRATEGIES FOR SCI

2.5.1 NEUROPROTECTIVE THERAPY TO TREAT ACUTE SCI

There are limited therapies for SCI and no effective treatment to reduce damage and to promote functional recovery (Martinon and Ibarra, 2008). Methylprednisolone (MP), which is a synthetic cortico-steroid and typically used for anti-inflammatory effect, has been used as a drug for acute SCI in humans for three decades with limited clinical support, and it is the only available drug for acute SCI in human. However it is based in large part on physiological hypotheses and its beneficial effect on the neurological recovery of patients has not been clearly proven (Hugenholtz, 2003). The effect of MP administration in patients with acute spinal cord injury was clinically examined by National Acute Spinal Cord Injury Study I, II and III (NASCIS) (Bracken et al., 1984; Bracken et al., 1985; Bracken et al., 1990; Bracken et al., 1992; Bracken et al., 1997; Bracken et al., 1998). In NASCIS II, a patient sub-group received a 24 hour high-dose infusion of MP within 8 hours following acute SCI showed improved neurological recovery (Bracken et al., 1990). Therefore within 8 hours after injury and high-dose infusion (typically 30 mg/kg bolus injection and 5.4 mg/kg/h following injection over 23 hours) has been an implied standard for clinical treatment. The high-dose of MP causes several side effects, such as impaired lung capacity and the higher incidence of sepsis and pneumonia. Compelling evidence of its efficacy is not yet conclusive (Gerndt et al., 1997).   To minimize the side effects related to systemic delivery, localized delivery methods have been developed: previously, our group developed a sustained and local delivery method. MP was delivered on the top of the lesion site by agarose hydrogel delivery system embedded with biodegradable polymer nanoparticles and showed effective diffusion through the spinal nerve tissue and significantly reduced early inflammation

(Chvatal et al., 2008; Kim et al., 2009). However, still there is the confusion with MP utility for acute SCI and MP should be used with caution, particularly if infusion goes longer than 24 hours.

A wide range of other pharmacological treatments have also been evaluated and in some cases have shown potential with promising results. Cyclooxygenase (COX) is an enzyme that is involved in prostanoids formation. Pharmacological COX inhibitor acts as an anti-inflammatory agent reducing inflammation and pain, and some selective (indomethacin; (Pantovic et al., 2005)) or non-selective (NS-398 to COX-2; (Hains et al., 2001)) COX inhibitors promoted neuroprotection. Immunophilins (IPs) are peptidyl-prolyl *cis-trans* isomerases and some IPs are receptor for immunosuppressive drugs such as cyclosporine A and FK506 (Sosa et al., 2005). Drugs inhibits the activity of calcineurin, which is a protein phosphatase and activates the T cells of the immune system, and the drug binding can promote neuroprotective effect and results in inducing neuroregeneration (Ibarra and Diaz-Ruiz, 2006).

Oxygen radical-induced lipid peroxidation (LP) plays an important detrimental role in acute CNS injury. Therefore, several therapeutic strategies have been applied to diminish its effects (Hall et al., 1992). As previously mentioned, MP has been used for human SCI and lazaroids, 21-aminosteroids, also show significant antioxidant effects without the same side effects of MP (Hall and Springer, 2004). Tirilazad, one of lazaroids, was also examined in the NACIS III and tirilazad treated patients showed slightly better neurological recovery, but not significantly higher than those treated with MP (Bracken et al., 1997). Therefore, there is a possibility for the use of tirilazad in humans bearing FDA approval.

Calpains are a family of calcium-dependent, non-lysosomal cysteine proteases. Hyperactivation of calpains follows traumatic brain injury or spinal cord injury due to Ca2+ influx and it leads irreversible cell damages such as breakdown of cytoskeleton and plasma membrane and damage of ion channels, cell adhesion molecules and surface receptors. Therefore, calpain can cause neural cell apoptosis after SCI (Ray et al., 2003). Highly specific inhibitor to calpain for therapeutic use has been investigated such as E-64-d (Zhang et al., 2003) and leupeptin (Momeni and Kanje, 2006), and these inhibitors demonstrated neuprotective ability in models of SCI.

Besides those therapeutic strategies, there are a number of pharmacological therapy targets, such as apoptosis inhibitors, steroid hormone and soldium channel blockers, and NMDA and AMPA-Kainate receptor antagonists (Martinon and Ibarra, 2008).

2.5.2   NERVE GROWTH FACTORS: NEW POSSIBLE THERAPEUTIC STRATEGY

Several neurotrophic factors induce neuroprotection and promote axonal outgrowth and functional recovery in traumatic injuries to the CNS. Neurotrophic factors that play an important role in the survival, development and function of neurons, include brain-derived neurotrophic factor (BDNF), nerve growth factor (NGF), neurotrophin three (NT-3) and neurotrophin-4/5 (NT-4/5). They belong to a class of growth factors and secreted proteins.

BDNF was originally found in the brain, but is also found in the peripheral nervous system. It helps to support the survival of existing neurons and encourages the regrowth and the differentiation of neurons and synapses (Waterhouse and Xu, 2009). Therefore, BDNF has been used for treatment after CNS injuries to improve motor and sensory neuronal survival and outgrowth (Schmidt and Leach, 2003).

NT-3 is in the NGF-family of neurotrophins and binds three receptors: the receptor tyrosine kinase neurotrophin receptors (TrkC and TrkB) and low affinity nerve growth factor receptor (LNGFR). It helps to support the survival and differentiation of existing neurons, and encourages the growth and differentiation of new neurons and synapses. NT-3 leads to branching and elaboration of sensory endings (Krimm et al., 2004), promotes nerve regeneration and sensory improvement (Sahenk et al., 2005) and acts as a survival factor for adult sensory neurons (Ljungberg et al., 1999). Since the sensory pathway runs along the dorsal column of spinal cord and a dorsal over hemisection was used in this study, NT-3 was chosen for delivery into spinal cord to encourage nerve survival and outgrowth after the injury.

For axonal regeneration through the lesion site after SCI, a balance between a permissive and favorable environment for the axons in the lesioned area is important. Therefore, in this study, a more permissive environment was achieved by degrading the inhibitory molecules CSPGs with chABC, while an improvement of regeneration ability was achieved by the supporting neurotrophic factor, NT-3.

2.6 CONCLUSIONS

Many researchers have shown that strategies delivering chABC alone or in combination with other therapeutic agents give promising results after SCI, although there are some limitations and difficulties. Therefore, there is a need to develop an alternative method to control the release of chABC temporally and spatially *in vivo*. In this study, we improved the thermal stability of chABC and developed a sustained delivery scaffold for topical delivery model combining 1) the chABC improved thermal stability by introducing

trehalose; 2) a temporal control method using lipid microtubules for long-term and continuous slow release; and 3) a spatial control method utilizing agarose gel to fabricate a scaffold for local delivery to the lesion site via implantation.

This chapter briefly summarizes the background to design and develop strategies for chABC or neurotrophic factor mediated treatment for SCI, as described above.

2.7 REFERENCES

Abuchowski A, van Es T, Palczuk NC, Davis FF (1977) Alteration of immunological properties of bovine serum albumin by covalent attachment of polyethylene glycol. J Biol Chem 252:3578-3581.

Arakawa T, Timasheff SN (1983) Preferential interactions of proteins with solvent components in aqueous amino acid solutions. Arch Biochem Biophys 224:169-177.

Asher RA, Morgenstern DA, Shearer MC, Adcock KH, Pesheva P, Fawcett JW (2002) Versican is upregulated in CNS injury and is a product of oligodendrocyte lineage cells. J Neurosci 22:2225-2236.

Asher RA, Morgenstern DA, Fidler PS, Adcock KH, Oohira A, Braistead JE, Levine JM, Margolis RU, Rogers JH, Fawcett JW (2000) Neurocan is upregulated in injured brain and in cytokine-treated astrocytes. J Neurosci 20:2427-2438.

Bae E, Bannen RM, Phillips GN, Jr. (2008) Bioinformatic method for protein thermal stabilization by structural entropy optimization. Proc Natl Acad Sci U S A 105:9594-9597.

Banci L, Bertini I, Caliceti P, Monsu Scolaro L, Schiavon O, Veronese FM (1990) Spectroscopic characterization of polyethyleneglycol modified superoxide dismutase: 1H NMR studies on its Cu2Co2 derivative. J Inorg Biochem 39:149-159.

Bandtlow CE, Schmidt MF, Hassinger TD, Schwab ME, Kater SB (1993) Role of intracellular calcium in NI-35-evoked collapse of neuronal growth cones. Science 259:80-83.

Bracken MB, Collins WF, Freeman DF, Shepard MJ, Wagner FW, Silten RM, Hellenbrand KG, Ransohoff J, Hunt WE, Perot PL, Jr., et al. (1984) Efficacy of methylprednisolone in acute spinal cord injury. JAMA 251:45-52.

Bracken MB, Shepard MJ, Hellenbrand KG, Collins WF, Leo LS, Freeman DF, Wagner FC, Flamm ES, Eisenberg HM, Goodman JH, et al. (1985) Methylprednisolone and neurological function 1 year after spinal cord injury. Results of the National Acute Spinal Cord Injury Study. J Neurosurg 63:704-713.

Bracken MB, Shepard MJ, Collins WF, Holford TR, Young W, Baskin DS, Eisenberg HM, Flamm E, Leo-Summers L, Maroon J, et al. (1990) A randomized, controlled trial of methylprednisolone or naloxone in the treatment of acute spinal-cord injury. Results of the Second National Acute Spinal Cord Injury Study. N Engl J Med 322:1405-1411.

Bracken MB, Shepard MJ, Collins WF, Jr., Holford TR, Baskin DS, Eisenberg HM, Flamm E, Leo-Summers L, Maroon JC, Marshall LF, et al. (1992) Methylprednisolone or naloxone treatment after acute spinal cord injury: 1-year follow-up data. Results of the second National Acute Spinal Cord Injury Study. J Neurosurg 76:23-31.

Bracken MB, Shepard MJ, Holford TR, Leo-Summers L, Aldrich EF, Fazl M, Fehlings M, Herr DL, Hitchon PW, Marshall LF, Nockels RP, Pascale V, Perot PL, Jr., Piepmeier J, Sonntag VK, Wagner F, Wilberger JE, Winn HR, Young W (1997) Administration of methylprednisolone for 24 or 48 hours or tirilazad mesylate for 48 hours in the treatment of acute spinal cord injury. Results of the Third National Acute Spinal Cord Injury Randomized Controlled Trial. National Acute Spinal Cord Injury Study. JAMA 277:1597-1604.

Bracken MB, Shepard MJ, Holford TR, Leo-Summers L, Aldrich EF, Fazl M, Fehlings MG, Herr DL, Hitchon PW, Marshall LF, Nockels RP, Pascale V, Perot PL, Jr., Piepmeier J, Sonntag VK, Wagner F, Wilberger JE, Winn HR, Young W (1998) Methylprednisolone or tirilazad mesylate administration after acute spinal cord injury: 1-year follow up. Results of the third National Acute Spinal Cord Injury randomized controlled trial. J Neurosurg 89:699-706.

Branca C, Magazu S, Maisano G, Migliardo P (1999) Anomalous cryoprotective effectiveness of trehalose: Raman scattering evidences. J Chem Phys 111 (1): 281-287.

Barritt AW, Davies M, Marchand F, Hartley R, Grist J, Yip P, McMahon SB, Bradbury EJ (2006) Chondroitinase ABC promotes sprouting of intact and injured spinal systems after spinal cord injury. J Neurosci 26:10856-10867.

Bradbury EJ, Moon LD, Popat RJ, King VR, Bennett GS, Patel PN, Fawcett JW, McMahon SB (2002) Chondroitinase ABC promotes functional recovery after spinal cord injury. Nature 416:636-640.

Burgher AH, Barnett CF, Obray JB, Mauck WD (2007) Introduction of infection control measures to reduce infection associated with implantable pain therapy devices. Pain Pract 7:279-284.

Caggiano AO, Zimber MP, Ganguly A, Blight AR, Gruskin EA (2005) Chondroitinase ABCI improves locomotion and bladder function following contusion injury of the rat spinal cord. J Neurotrauma 22:226-239.

Carninci P, Nishiyama Y, Westover A, Itoh M, Nagaoka S, Sasaki N, Okazaki Y, Muramatsu M, Hayashizaki Y (1998) Thermostabilization and thermoactivation of thermolabile

enzymes by trehalose and its application for the synthesis of full length cDNA. Proc Natl Acad Sci U S A 95:520-524.

Carpenter JF, Prestrelski SJ, Arakawa T (1993) Separation of freezing- and drying-induced denaturation of lyophilized proteins using stress-specific stabilization. I. Enzyme activity and calorimetric studies. Arch Biochem Biophys 303:456-464.

Chau CH, Shum DK, Li H, Pei J, Lui YY, Wirthlin L, Chan YS, Xu XM (2004) Chondroitinase ABC enhances axonal regrowth through Schwann cell-seeded guidance channels after spinal cord injury. FASEB J 18:194-196.

Chen R (1999) A general strategy for enzyme engineering. Trends Biotechnol 17:344-345.

Chvatal SA, Kim YT, Bratt-Leal AM, Lee H, Bellamkonda RV (2008) Spatial distribution and acute anti-inflammatory effects of Methylprednisolone after sustained local delivery to the contused spinal cord. Biomaterials 29:1967-1975.

Cleland JL, Wang DI (1990) Cosolvent assisted protein refolding. Biotechnology (N Y) 8:1274-1278.

Condic ML, Snow DM, Letourneau PC (1999) Embryonic neurons adapt to the inhibitory proteoglycan aggrecan by increasing integrin expression. J Neurosci 19:10036-10043.

Cottone G, Giuffrida S, Ciccotti G, Cordone L (2005) Molecular dynamics simulation of sucrose- and trehalose-coated carboxy-myoglobin. Proteins 59:291-302.

Crowe LM, Mouradian R, Crowe JH, Jackson SA, Womersley C (1984) Effects of carbohydrates on membrane stability at low water activities. Biochim Biophys Acta 769:141-150.

Faustino CM, Calado AR, Garcia-Rio L (2009) Gemini Surfactant-Protein Interactions: Effect of pH, Temperature, and Surfactant Stereochemistry. Biomacromolecules.

Fawcett JW, Asher RA (1999) The glial scar and central nervous system repair. Brain Res Bull 49:377-391.

Fethiere J, Eggimann B, Cygler M (1999) Crystal structure of chondroitin AC lyase, a representative of a family of glycosaminoglycan degrading enzymes. J Mol Biol 288:635-647.

Filpula D, Zhao H (2008) Releasable PEGylation of proteins with customized linkers. Adv Drug Deliv Rev 60:29-49.

Fitch MT, Silver J (1997) Activated macrophages and the blood-brain barrier: inflammation after CNS injury leads to increases in putative inhibitory molecules. Exp Neurol 148:587-603.

Fontana A, Spolaore B, Mero A, Veronese FM (2008) Site-specific modification and PEGylation of pharmaceutical proteins mediated by transglutaminase. Adv Drug Deliv Rev 60:13-28.

Gerndt SJ, Rodriguez JL, Pawlik JW, Taheri PA, Wahl WL, Micheals AJ, Papadopoulos SM (1997) Consequences of high-dose steroid therapy for acute spinal cord injury. J Trauma 42:279-284.

Gilbert RJ, McKeon RJ, Darr A, Calabro A, Hascall VC, Bellamkonda RV (2005) CS-4,6 is differentially upregulated in glial scar and is a potent inhibitor of neurite extension. Mol Cell Neurosci 29:545-558.

Green JL, Angell CA (1989) Phase relations and vitrification in saccharide-water solutions and the trehalose anomaly. J Phys Chem 93:2880-2882.

Greenwald RB, Choe YH, McGuire J, Conover CD (2003) Effective drug delivery by PEGylated drug conjugates. Adv Drug Deliv Rev 55:217-250.

Hains BC, Yucra JA, Hulsebosch CE (2001) Reduction of pathological and behavioral deficits following spinal cord contusion injury with the selective cyclooxygenase-2 inhibitor NS-398. J Neurotrauma 18:409-423.

Hall ED, Springer JE (2004) Neuroprotection and acute spinal cord injury: a reappraisal. NeuroRx 1:80-100.

Hall ED, Yonkers PA, Andrus PK, Cox JW, Anderson DK (1992) Biochemistry and pharmacology of lipid antioxidants in acute brain and spinal cord injury. J Neurotrauma 9 Suppl 2:S425-442.

Hamai A, Hashimoto N, Mochizuki H, Kato F, Makiguchi Y, Horie K, Suzuki S (1997) Two distinct chondroitin sulfate ABC lyases. An endoeliminase yielding tetrasaccharides and an exoeliminase preferentially acting on oligosaccharides. J Biol Chem 272:9123-9130.

Harris JM, Chess RB (2003) Effect of pegylation on pharmaceuticals. Nat Rev Drug Discov 2:214-221.

Hatti-Kaul and Mattiasson, (2003) Isolation and purification of proteins. CRC

Hedoux A, Willart JF, Paccou L, Guinet Y, Affouard F, Lerbret A, Descamps M (2009) Thermostabilization mechanism of bovine serum albumin by trehalose. J Phys Chem B 113:6119-6126.

Hedoux A, Willart JF, Ionov R, Affouard F, Guinet Y, Paccou L, Lerbret A, Descamps M (2006) Analysis of sugar bioprotective mechanisms on the thermal denaturation of lysozyme from Raman scattering and differential scanning calorimetry investigations. J Phys Chem B 110:22886-22893.

Houle JD, Tom VJ, Mayes D, Wagoner G, Phillips N, Silver J (2006) Combining an autologous peripheral nervous system "bridge" and matrix modification by chondroitinase allows robust, functional regeneration beyond a hemisection lesion of the adult rat spinal cord. J Neurosci 26:7405-7415.

Huang W, Lunin VV, Li Y, Suzuki S, Sugiura N, Miyazono H, Cygler M (2003) Crystal structure of Proteus vulgaris chondroitin sulfate ABC lyase I at 1.9A resolution. J Mol Biol 328:623-634.

Huang WC, Kuo WC, Cherng JH, Hsu SH, Chen PR, Huang SH, Huang MC, Liu JC, Cheng H (2006) Chondroitinase ABC promotes axonal re-growth and behavior recovery in spinal cord injury. Biochem Biophys Res Commun 349:963-968.

Hugenholtz H (2003) Methylprednisolone for acute spinal cord injury: not a standard of care. CMAJ 168:1145-1146.

Hynds DL, Snow DM (1999) Neurite outgrowth inhibition by chondroitin sulfate proteoglycan: stalling/stopping exceeds turning in human neuroblastoma growth cones. Exp Neurol 160:244-255.

Ibarra A, Diaz-Ruiz A (2006) Protective effect of cyclosporin-A in spinal cord injury: an overview. Curr Med Chem 13:2703-2710.

Israelachvili J (1997) The different faces of poly(ethylene glycol). Proc Natl Acad Sci U S A 94:8378-8379.

Jain A, Kim YT, McKeon RJ, Bellamkonda RV (2006) In situ gelling hydrogels for conformal repair of spinal cord defects, and local delivery of BDNF after spinal cord injury. Biomaterials 27:497-504.

Johnson WE, Caterson B, Eisenstein SM, Hynds DL, Snow DM, Roberts S (2002) Human intervertebral disc aggrecan inhibits nerve growth in vitro. Arthritis Rheum 46:2658-2664.

Jones LL, Margolis RU, Tuszynski MH (2003) The chondroitin sulfate proteoglycans neurocan, brevican, phosphacan, and versican are differentially regulated following spinal cord injury. Exp Neurol 182:399-411.

Kastin AJ, Pan W (2005) Targeting neurite growth inhibitors to induce CNS regeneration. Curr Pharm Des 11:1247-1253.

Kaushik JK, Bhat R (2003) Why is trehalose an exceptional protein stabilizer? An analysis of the thermal stability of proteins in the presence of the compatible osmolyte trehalose. J Biol Chem 278:26458-26465.

Kim BG, Dai HN, Lynskey JV, McAtee M, Bregman BS (2006) Degradation of chondroitin sulfate proteoglycans potentiates transplant-mediated axonal remodeling and functional recovery after spinal cord injury in adult rats. J Comp Neurol 497:182-198.

Kim YT, Caldwell JM, Bellamkonda RV (2009) Nanoparticle-mediated local delivery of Methylprednisolone after spinal cord injury. Biomaterials 30:2582-2590.

Kopchick JJ, Parkinson C, Stevens EC, Trainer PJ (2002) Growth hormone receptor antagonists: discovery, development, and use in patients with acromegaly. Endocr Rev 23:623-646.

Krekoski CA, Neubauer D, Zuo J, Muir D (2001) Axonal regeneration into acellular nerve grafts is enhanced by degradation of chondroitin sulfate proteoglycan. J Neurosci 21:6206-6213.

Krimm RF, Davis BM, Woodbury CJ, Albers KM (2004) NT3 expressed in skin causes enhancement of SA1 sensory neurons that leads to postnatal enhancement of Merkel cells. J Comp Neurol 471:352-360.

Kuchner O, Arnold FH (1997) Directed evolution of enzyme catalysts. Trends Biotechnol 15:523-530.

Ljungberg C, Novikov L, Kellerth JO, Ebendal T, Wiberg M (1999) The neurotrophins NGF and NT-3 reduce sensory neuronal loss in adult rat after peripheral nerve lesion. Neurosci Lett 262:29-32.

Lo Conte L, Ailey B, Hubbard TJ, Brenner SE, Murzin AG, Chothia C (2000) SCOP: a structural classification of proteins database. Nucleic Acids Res 28:257-259.

Martinon S, Ibarra A (2008) Pharmacological neuroprotective therapy for acute spinal cord injury: state of the art. Mini Rev Med Chem 8:222-230.

Matthews RT, Kelly GM, Zerillo CA, Gray G, Tiemeyer M, Hockfield S (2002) Aggrecan glycoforms contribute to the molecular heterogeneity of perineuronal nets. J Neurosci 22:7536-7547.

McKeon RJ, Hoke A, Silver J (1995) Injury-induced proteoglycans inhibit the potential for laminin-mediated axon growth on astrocytic scars. Exp Neurol 136:32-43.

McKeon RJ, Schreiber RC, Rudge JS, Silver J (1991) Reduction of neurite outgrowth in a model of glial scarring following CNS injury is correlated with the expression of inhibitory molecules on reactive astrocytes. J Neurosci 11:3398-3411.

Meilander NJ, Yu X, Ziats NP, Bellamkonda RV (2001) Lipid-based microtubular drug delivery vehicles. J Control Release 71:141-152.

Meilander NJ, Pasumarthy MK, Kowalczyk TH, Cooper MJ, Bellamkonda RV (2003) Sustained release of plasmid DNA using lipid microtubules and agarose hydrogel. J Control Release 88:321-331.

Momeni HR, Kanje M (2006) Calpain inhibitors delay injury-induced apoptosis in adult mouse spinal cord motor neurons. Neuroreport 17:761-765.

Moon LD, Asher RA, Rhodes KE, Fawcett JW (2001) Regeneration of CNS axons back to their target following treatment of adult rat brain with chondroitinase ABC. Nat Neurosci 4:465-466.

Oike Y, Kimata K, Shinomura T, Suzuki S, Takahashi N, Tanabe K (1982) A mapping technique for probing the structure of proteoglycan core molecules. J Biol Chem 257:9751-9758.

Orsatti L, Veronese FM (1999) An unusual coupling of poly(ethylene glycol) to tyrosine residues in epidermal growth factor. Journal of Bioactive and Compatible Polymers 14:429-436.

Pantovic R, Draganic P, Erakovic V, Blagovic B, Milin C, Simonic A (2005) Effect of indomethacin on motor activity and spinal cord free fatty acid content after experimental spinal cord injury in rabbits. Spinal Cord 43:519-526.

Peng P, Massicotte EM (2004) Spinal cord compression from intrathecal catheter-tip inflammatory mass: case report and a review of etiology. Reg Anesth Pain Med 29:237-242.

Pindzola RR, Doller C, Silver J (1993) Putative inhibitory extracellular matrix molecules at the dorsal root entry zone of the spinal cord during development and after root and sciatic nerve lesions. Dev Biol 156:34-48.

Pizzorusso T, Medini P, Landi S, Baldini S, Berardi N, Maffei L (2006) Structural and functional recovery from early monocular deprivation in adult rats. Proc Natl Acad Sci U S A 103:8517-8522.

Prabhakar V, Capila I, Bosques CJ, Pojasek K, Sasisekharan R (2005a) Chondroitinase ABC I from Proteus vulgaris: cloning, recombinant expression and active site identification. Biochem J 386:103-112.

Prabhakar V, Raman R, Capila I, Bosques CJ, Pojasek K, Sasisekharan R (2005b) Biochemical characterization of the chondroitinase ABC I active site. Biochem J 390:395-405.

Properzi F, Carulli D, Asher RA, Muir E, Camargo LM, van Kuppevelt TH, ten Dam GB, Furukawa Y, Mikami T, Sugahara K, Toida T, Geller HM, Fawcett JW (2005) Chondroitin 6-sulphate synthesis is up-regulated in injured CNS, induced by injury-related cytokines and enhanced in axon-growth inhibitory glia. Eur J Neurosci 21:378-390.

Ray SK, Hogan EL, Banik NL (2003) Calpain in the pathophysiology of spinal cord injury: neuroprotection with calpain inhibitors. Brain Res Brain Res Rev 42:169-185.

Remmele RL, Jr., Nightlinger NS, Srinivasan S, Gombotz WR (1998) Interleukin-1 receptor (IL-1R) liquid formulation development using differential scanning calorimetry. Pharm Res 15:200-208.

Rishi V, Anjum F, Ahmad F, Pfeil W (1998) Role of non-compatible osmolytes in the stabilization of proteins during heat stress. Biochem J 329 (Pt 1):137-143.

Rudge JS, Silver J (1990) Inhibition of neurite outgrowth on astroglial scars in vitro. J Neurosci 10:3594-3603.

Rudolph AS, Stilwell G, Cliff RO, Kahn B, Spargo BJ, Rollwagen F, Monroy RL (1992) Biocompatibility of lipid microcylinders: effect on cell growth and antigen presentation in culture. Biomaterials 13:1085-1092.

Ryan MJ KK, Tilley BC, Lotvin JA (1994) Cloning and expression of the chondroitinase I and II genes from Proteus vugaris. Patent WO.

Sahenk Z, Nagaraja HN, McCracken BS, King WM, Freimer ML, Cedarbaum JM, Mendell JR (2005) NT-3 promotes nerve regeneration and sensory improvement in CMT1A mouse models and in patients. Neurology 65:681-689.

Sampedro JG, Guerra G, Pardo JP, Uribe S (1998) Trehalose-mediated protection of the plasma membrane H+-ATPase from Kluyveromyces lactis during freeze-drying and rehydration. Cryobiology 37:131-138.

Sato H, Ikeda M, Suzuki K, Hirayama K (1996) Site-specific modification of interleukin-2 by the combined use of genetic engineering techniques and transglutaminase. Biochemistry 35:13072-13080.Schnur JM (1993) Lipid Tubules: A Paradigm for Molecularly Engineered Structures. Science 262:1669-1676.

Schoemaker HE, Mink D, Wubbolts MG (2003) Dispelling the myths--biocatalysis in industrial synthesis. Science 299:1694-1697.

Selles-Navarro I, Ellezam B, Fajardo R, Latour M, McKerracher L (2001) Retinal ganglion cell and nonneuronal cell responses to a microcrush lesion of adult rat optic nerve. Exp Neurol 167:282-289.

Shive MS, Anderson JM (1997) Biodegradation and biocompatibility of PLA and PLGA microspheres. Adv Drug Deliv Rev 28:5-24.

Singer MA, Lindquist S (1998) Thermotolerance in Saccharomyces cerevisiae: the Yin and Yang of trehalose. Trends Biotechnol 16:460-468.

Snow DM, Letourneau PC (1992) Neurite outgrowth on a step gradient of chondroitin sulfate proteoglycan (CS-PG). J Neurobiol 23:322-336.

Snow DM, Steindler DA, Silver J (1990a) Molecular and cellular characterization of the glial roof plate of the spinal cord and optic tectum: a possible role for a proteoglycan in the development of an axon barrier. Dev Biol 138:359-376.

Snow DM, Mullins N, Hynds DL (2001) Nervous system-derived chondroitin sulfate proteoglycans regulate growth cone morphology and inhibit neurite outgrowth: a light, epifluorescence, and electron microscopy study. Microsc Res Tech 54:273-286.

Snow DM, Lemmon V, Carrino DA, Caplan AI, Silver J (1990b) Sulfated proteoglycans in astroglial barriers inhibit neurite outgrowth in vitro. Exp Neurol 109:111-130.

So KF, Cho EY. (1989) Advances in neural regeneration. Ann R Australas Coll Dent Surg 10:53-61.

Sosa I, Reyes O, Kuffler DP (2005) Immunosuppressants: neuroprotection and promoting neurological recovery following peripheral nerve and spinal cord lesions. Exp Neurol 195:7-15.

Spargo BJ, Cliff RO, Rollwagen FM, Rudolph AS (1995) Controlled release of transforming growth factor-beta from lipid-based microcylinders. J Microencapsul 12:247-254.

Steinmetz MP, Horn KP, Tom VJ, Miller JH, Busch SA, Nair D, Silver DJ, Silver J (2005) Chronic enhancement of the intrinsic growth capacity of sensory neurons combined with the degradation of inhibitory proteoglycans allows functional regeneration of sensory axons through the dorsal root entry zone in the mammalian spinal cord. J Neurosci 25:8066-8076.

Taneja S, Ahmad F (1994) Increased thermal stability of proteins in the presence of amino acids. Biochem J 303 (Pt 1):147-153.

Tang X, Davies JE, Davies SJ (2003) Changes in distribution, cell associations, and protein expression levels of NG2, neurocan, phosphacan, brevican, versican V2, and tenascin-C during acute to chronic maturation of spinal cord scar tissue. J Neurosci Res 71:427-444.

Thomas BN, Safinya CR, Plano RJ, Clark NA (1995) Lipid Tubule Self-Assembly: Length Dependence on Cooling Rate Through a First-Order Phase Transition. Science 267:1635-1638.

Timasheff SN (2002) Protein-solvent preferential interactions, protein hydration, and the modulation of biochemical reactions by solvent components. Proc Natl Acad Sci U S A 99:9721-9726.

Tropea D, Caleo M, Maffei L (2003) Synergistic effects of brain-derived neurotrophic factor and chondroitinase ABC on retinal fiber sprouting after denervation of the superior colliculus in adult rats. J Neurosci 23:7034-7044.

Unsworth LD, van der Oost J, Koutsopoulos S (2007) Hyperthermophilic enzymes--stability, activity and implementation strategies for high temperature applications. FEBS J 274:4044-4056.

Veronese FM, Mero A (2008) The impact of PEGylation on biological therapies. BioDrugs 22:315-329.

Wilson MT, Snow DM (2000) Chondroitin sulfate proteoglycan expression pattern in hippocampal development: potential regulation of axon tract formation. J Comp Neurol 424:532-546.

Woghiren C, Sharma B, Stein S (1993) Protected thiol-polyethylene glycol: a new activated polymer for reversible protein modification. Bioconjug Chem 4:314-318.

Xie G, Timasheff SN (1997a) The thermodynamic mechanism of protein stabilization by trehalose. Biophys Chem 64:25-43.

Xie G, Timasheff SN (1997b) Mechanism of the stabilization of ribonuclease A by sorbitol: preferential hydration is greater for the denatured then for the native protein. Protein Sci 6:211-221.

Yick LW, Cheung PT, So KF, Wu W (2003) Axonal regeneration of Clarke's neurons beyond the spinal cord injury scar after treatment with chondroitinase ABC. Exp Neurol 182:160-168.

Yick LW, Wu W, So KF, Yip HK, Shum DK (2000) Chondroitinase ABC promotes axonal regeneration of Clarke's neurons after spinal cord injury. Neuroreport 11:1063-1067.

Zhang Y, Deng Y, Wang X, Xu J, Li Z (2009) Conformational and bioactivity analysis of insulin: freeze-drying TBA/water co-solvent system in the presence of surfactant and sugar. Int J Pharm 371:71-81.

Zhang SX, Bondada V, Geddes JW (2003) Evaluation of conditions for calpain inhibition in the rat spinal cord: effective postinjury inhibition with intraspinal MDL28170 microinjection. J Neurotrauma 20:59-

Zhang Y, Tohyama K, Winterbottom JK, Haque NS, Schachner M, Lieberman AR, Anderson PN (2001) Correlation between putative inhibitory molecules at the dorsal root entry zone and failure of dorsal root axonal regeneration. Mol Cell Neurosci 17:444-459.

Zuo J, Neubauer D, Dyess K, Ferguson TA, Muir D (1998) Degradation of chondroitin sulfate proteoglycan enhances the neurite-promoting potential of spinal cord tissue. Exp Neurol 154:654-662.

CHAPTER 3

IMPROVEMENT OF THERMOSTABILITY OF CHONDROITINASE ABC ENZYMATIC ACTIVITY AND DEVELOPMENT OF LIPID MICROTUBE AND HYDROGEL MEDIATED DELIVERY SYSTEM

(Partially published with R.J. McKeon and R.V. Bellamkonda, Proceedings of the National Academy of Sciences, 2009)

Spinal cord injury (SCI) triggers cellular and molecular signal cascades which, amongst other things, induce growth cone inhibitors and result in regenerative failure. Chondroitin sulfate proteoglycans (CSPGs) are upregulated and accumulate around lesion sites after SCI and are major inhibitors of axonal regeneration. To overcome the inhibitory effect of CSPGs, modification or digestion of CSPGs has been explored. It has been reported that chondroitinase ABC (chABC) can digest glycosaminoglycan chains on CSPGs and enhance regeneration when delivered into lesion sites (Bradbury et al., 2002). However, chABC has a crucial limitation; it is thermally sensitive and at body temperature, 37ºC, its enzymatic activity is significantly attenuated within 72 hours (Tester et al., 2007). This necessitates the use of multiple or continuous infusions with a pump to maintain enzymatic functionality for periods as long as two weeks. However, maintaining these infusion systems is invasive and clinically problematic. Here, to overcome the current limitations, we report: 1) improvement of the thermal stability of chABC, and 2) development of a minimally invasive strategy for delivery of chABC *in vivo* over a period of 2 weeks or longer. By adding a protein stabilizer, trehalose, the thermostability of chABC was improved and chABC

maintained its enzymatic activity for 4 weeks. Enzymatic activity and conformational change were assayed by functional and structural tests such as dimethylmethylene blue staining of digested CSPGs, sodium dodecyl sulfate-polyacrylamide gel electrophoresis and circular dichroism. A scaffold consisting of lipid microtubules and agarose gel was used for sustained and spatially controlled release of thermally stabilized chABC *in vitro*. chABC released from the gel-microtubule scaffold showed enzymatic activity for 2 weeks. These results have important implications for strategies that aim to digest CSPGs as a means of reducing growth cone inhibition after SCI.

3.1   INTRODUCTION

Physical damage to the adult central nervous system (CNS) often leads to permanent functional loss due to the inability of mature axons to regenerate. A major impediment to regeneration is the formation of astro-glial scar tissue at the lesion site along with a number of myelin associated inhibitory moieties. After injury to the CNS, an inflammation process is triggered that includes a cascade of cellular and molecular responses occurs and a glial scar is formed around the lesioned tissue (Fawcett and Asher, 1999). Macrophages, microglia, oligodendrocyte precursors, meningeal cells and astrocytes migrate into the lesion site and produce inhibitory molecules, such as myelin-associated glycoprotein (MAG), CSPGs, free radicals, nitric oxide, etc. The final 'product' is a tightly interwoven glial scar formed around the lesioned site composed primarily of CSPGs and reactive astrocytes.

chABC has been shown to promote axonal growth and functional recovery in a number of models including spinal cord injury (Bradbury et al., 2002) and monocular deprivation (Pizzorusso et al., 2006). It promotes axonal sprouting in both intact and injured

46

spinal cords (Barritt et al., 2006), perhaps via its action on perineural nets. Currently, chABC is typically delivered via intrathecal injection, with infusion frequency varying from every other day to every other week, and for time periods ranging from 2 weeks up to 6 weeks (Chau et al., 2004; Caggiano et al., 2005; Houle et al., 2006; Huang et al., 2006). Some groups inject chABC in combination with other therapeutic agents (Tropea et al., 2003) or in combination with cell transplantation, such as cells from E14 fetal spinal cords (Kim et al., 2006) or autologous peripheral nerve grafts (Houle et al., 2006), to obtain a synergistic effect.

However, there are several limitations to using chABC *in vivo*. ChABC is thermally sensitive at body temperature, and loses 50% of its enzymatic activity after 1 hour of incubation at 37 ℃ (by Morgan-Elson reaction; Seikagaku, Japan). Most of its enzymatic function is lost within 3-5 days (Tester et al., 2007). Generally, CSPGs are upregulated and accumulate in the lesion site for at least 2 weeks after the primary injury. Therefore for chABC to remove CSPGs, it would need to be delivered for at least two weeks intrathecally through pumps to provide a 'fresh' supply of enzyme. Another limitation is that the diffusion of chABC into deep regions of the cord is limited when delivered intrathecally. Because of this delivery method the drug flows through intrathecal space and washes away quickly, necessitating high concentrations (from 2U/ml to 1000U/ml) compensate. Therefore, there is a compelling need to control chABC delivery both spatially and temporally.

To overcome these limitations, trehalose was introduced as a stabilizer to retain the enzymatic functionality of chABC. Trehalose is a superior stabilizer among sugars or polyols and trehalose could give a longer lifetime to chABC. The concentration of trehalose was decided after *in vitro* experiments with various concentrations of trehalose. Second, to develop a sustained and local delivery system for providing bioactive agents, an agarose

hydrogel and lipid microtube was used. With the agarose hydrogel and lipid microtube mediated delivery system, the release of the drug can be temporally and spatially controlled by the combination of the concentration or type of agarose gel and the length of the lipid microtube (Meilander et al., 2001). Agarose gel was used to construct an implantable delivery carrier *in vivo* embedded with either lipid microtubes (Jain et al., 2006) or polymer nanoparticles (Chvatal et al., 2008; Kim et al., 2009). This is referred to as the 'hydrogel-microtube delivery system'. Using both trehalose and the hydrogel-microtube delivery system, a sustained and local release of chABC and neurotrophine three (NT-3) was achieved.

In this study, we improved the thermal stability of chABC and developed agarose gel scaffolds for spatio-temporal controlled delivery. The *in vitro* experiments performed determined whether trehalose can be used as a protein stabilizer to improve the thermal stability of chABC, and ultimately increase the lifetime of enzymatic activity at body temperature. In addition, lipid microtubes and an agarose hydrogel were introduced to a develop delivery scaffold and subsequently examined as a drug delivery system for spatio-temporally controlled release *in vitro*. Last, we showed an alternative approach that will allow us to apply chABC as a therapeutic agent *in vivo*, as described later in chapter 4 and 5.

3.2 MATERIALS AND METHODS

3.2.1 ENZYMATIC ACTIVITY ASSAY WITH SDS-PAGE

Because of its exceptional ability to stabilize and maintain the enzymatic activity of a number of proteins, trehalose was used to stabilize chABC at body temperature (37 ºC) (Kaushik and Bhat, 2003). To determine the proper concentration of trehalose for stabilizing the enzymatic function of chABC, various concentrations of trehalose, from 20 mM to 1 M,

were tested for their ability to digest the GAG chains of a specific CSPG, decorin, which consists of a core protein and a CS-GAG chain. Various concentrations of trehalose (20, 50, 100, 250, 500 mM and 1 M) were prepared in 1X phosphate buffered saline (PBS). chABC (2U/0.5ml; 250ng) was mixed with these trehalose concentrations and each mixture was incubated for 1, 2, 3 or 4 weeks in a 37 ℃ water bath. After co-incubating for different time durations of trehalose and chABC at 37 ℃, 10 µl of decorin (5 µg) was added, incubated at 37 ℃ for 4 additional hours and the resultant products were analyzed with sodium dodecyl sulfate-polyacrylamide gel electrophoresis (SDS-PAGE). Penicillinase (P'ase; 250 ng) was used as a control enzyme.

When intact, decorin appears as a large molecular weight smear on an SDS-PAGE gel. A tighter and lower molecular weight decorin band after incubation with chABC would indicate preservation of chABC enzymatic activity. chABC without trehalose was used as a negative control and was incubated at 37 ℃ for the same incubation durations, mixed with decorin, and incubated at 37 ℃ for an additional 4 hours. After incubating, the mixtures were diluted 1:1 with Tris-SDS sample buffer containing 5% β-mercaptoethanol and were further incubated for 4 minutes at 95 ℃ to denature the protein. The gel electrode assembly was placed in an electrophoresis chamber (BIORAD) and the chamber was filled with Tris running buffer. 20 µl of the prepared samples was loaded into each lane of SDS gradient gel (4% - 15%; BIORAD) and run at 200 volts for 1 hour.

Silver staining was conducted to visualize separated proteins. Because the enzymatic thermostability of chABC depends on lot and time (Tester et al., 2007), all experiments in this study were performed with chABC from the same lot.

3.2.2 SILVER STAINING PROCEDURE

After running on SDS-PAGE, the gel was fixed in a solution containing methanol, acetic acid, and water in a 45:5:50 ratio for 90 min and washed with water for 20 min twice. The gel was washed with 0.02 sodium thiosulfate ($Na_2S_2O_3 \cdot 5H_2O$) for 3 min and with water for 30 sec twice, then washed with 0.1 % silver nitrate for 30 min and with water for 30 sec. A developing solution containing 2.5 % sodium carbonate/ 0.02% formaldehyde was added. The gel was developed for 2-4 min and protein bands generally appeared within 30 sec. The developing solution was removed before overdevelopment and a solution containing 1 % acetic acid was added to quench the reaction. After rinsing with water, the gel was imaged on the BIORAD ChemiDoc XRS HQ in the epi-white mode.

3.2.3 ENZYMATIC ACTIVITY ASSAY WITH DMMB

To further characterize stability of chABC, a dimethylmethylene blue (DMMB) assay was used to quantify CS-GAGs that remained after digestion of decorin with chABC. Diluted chABC (40mU) in 1X PBS (200µl) was mixed with 1 M of trehalose and incubated at 37 ℃ to subject it to thermal stress. 10 µl of incubated chABC solution was sampled for analysis on day 1, 3, 7 and 14. The sampled chABC/trehalose was then mixed with 10µg of decorin and incubated at 37 ℃ for 10 minutes. Next, the DMMB reagent was added and absorbance was measured on a Microplate Reader (BIO-TEK Instruments, Inc.). The same concentration of chABC/trehalose without added decorin was measured as the background on the same plate and the measured background absorbance was subtracted from absorbance of the other samples. chABC in 1X PBS without trehalose was prepared to determine the degree to which the enzymatic activity of chABC is improved by adding trehalose. The absorbance of decorin

digested by fresh chABC was considered to represent 100% of enzymatic activity. The percentage of sample absorbance relative to this standard was calculated and a deactivation curve was plotted. The absorbance of trehalose in 1X PBS at the same concentration as above was measured to make sure that trehalose does not interfere DMMB results.

3.2.4   FABRICATION OF LIPID MICROTUBES

Hollow and open-ended lipid microtubes (Fig. 3.1.) were fabricated using 1,2-bis-(triscosa-10,12-diynoyl)-sn-glycero-3-phosphocholine (DC8,9PC, Avanti Polar Lipids, Alabaster, AL) as previously described (Meilander et al., 2001; Meilander et al., 2003). Briefly, the lipid was dissolved in 70% ethanol at a concentration of 1 mg/ml. The solution was slowly cooled from 55 ℃ to 21 ℃, heated to 33 ℃ and cooled again to 20 ℃ by a programmed water bath (Thermo NESLAB, Portsmouth, NH) for 48 hours. During this cooling procedure, the microtubes self-assembled into hollow structures (Spargo et al., 1995; Meilander et al., 2001). The average length of microtube can be controlled by modifying the cooling process (Lando et al., 1990; Thomas et al., 1995). After 2 weeks of incubation at room temperature, 50 mM (18.9 mg/ml) of trehalose was added to the microtube solution, mixed gently and incubated overnight to support the stability of the lipid microtube structure. The microtube solution was centrifuged for 5 min at 3000 rpm, dried overnight in a biological hood for complete lyophilization. Microtubes were loaded with chABC, NT-3 or P'ase in buffer, 1 M trehalose in 1X PBS, and incubated overnight at 4 ℃ to allow for full rehydration. Microtubes were transferred to a new tube and extra buffer, 1 X PBS, was added to wash out left-over agents outside.
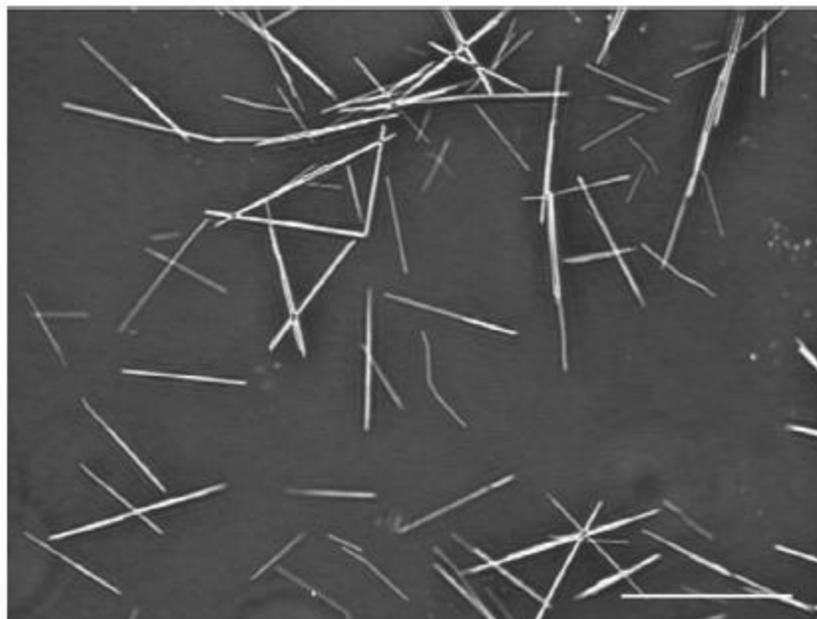
Figure 3.1. Micrograph of lipid microtubes formed from $DC_{8,9}PC$ lipid in bright field microscopy, scale bar is 50 µm. Figure from Meilander et al., 2001.

3.2.5 PREPARATION OF AGENT-LOADED LIPID MICROTUBES

The loading concentration of the drug was calculated based on the loading efficiency. The loading efficiency was defined as the ratio of the entire internal volume of the microtubes to the volume of the drug solution added to lyophilized microtubes (Meilander et al., 2001). Figure 3.2 shows a histogram of the lengths of microtubes used in this study. The average length was about 37 µm (0.5 µm of inner diameter) and the total number of microtubes from 1 mg of lipid was approximately 1×10^8. Therefore, the total inside volume of microtubes yielded from 1 mg of lipid was 0.75 µl. To increase the loading efficiency, we tried to increase the internal volume of lipid microtubes by using more lipid solution,

increasing the surface area of lyophilized microtubes for more efficient rehydrating with the solution of interest, and decreasing the loaded volume of solution of interest.
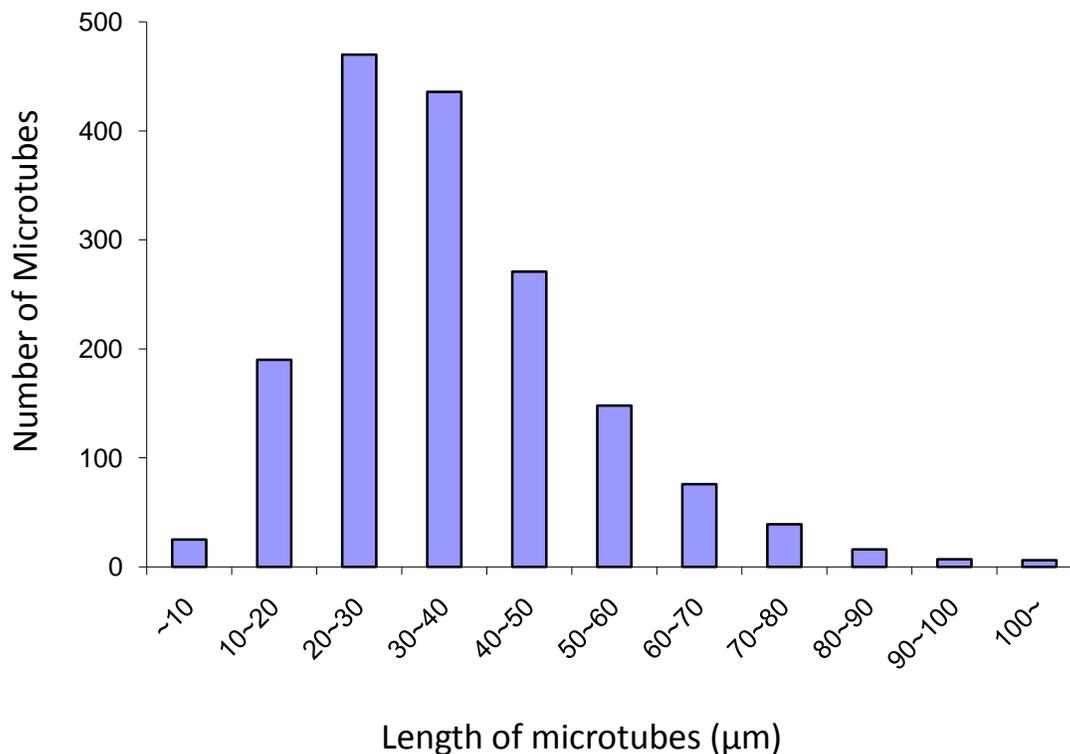
Figure 3.2. Histogram of microtube length distribution. The average length is about 37 μm, total number of microtubes from 1 mg of lipid is approximately 1×10^8 and total inside volume of microtubes from 1 mg of lipid is 0.75 μl.

3.2.6 ENZYAMTIC ACTIVITY ASSAY OF POST-RELEASED CHONDROTINASE ABC FROM LIPID MICROTUBES/HYDROGEL-MICROTUBE DELIVERY SCAFFOLD

SDS-PAGE was used to examine any potential adverse effects of the lipid microtubes on chABC as a carrier for sustained release, such as loss of enzymatic activity. The DMMB

assay was used to characterize the release profile of chABC from microtubes. After preparing microtubes loaded with chABC (~20 mU) and 1 M trehalose, the microtubes were co-incubated with decorin (5 µg/200 µl). After 4 hours at 37 ºC, the co-incubated samples were centrifuged and the supernatant was analyzed by SDS-PAGE as described in the section 3.2.1.

The enzymatic activity of released chABC from the hydrogel-microtube delivery system was characterized via DMMB assay. In order to physically maintain chABC/trehalose/microtubes in place *in vivo*, SeaPlaque® agarose (Cambrex), an agarose hydrogel, was dissolved in 1X PBS at a concentration of 1.2% (w/v) (Jain et al., 2006; Dodla and Bellamkonda, 2008). After it was cooled below 37 ºC, the gel was mixed with an equal volume of microtubes loaded with chABC/ 1M trehalose, placed in a 96-well plate, and gelled at 4 ºC. The final working concentration of the gel was 0.6% (w/v). After the mixture gelled, 1X PBS was added above the mixture and incubated in a 37 ºC incubator for up to 2 weeks. During this incubation, the supernatant was collected and replaced with fresh 1X PBS every other day. The collected supernatant was mixed with decorin, incubated at 37 ºC and analyzed with DMMB assay as described in the section 3.2.3. The same measurement was conducted with microtubes loaded with P'ase (50 ng; same amount as chABC) and trehalose as an enzyme control.

3.2.7   CHABC RELEASE PROFILES FROM LIPID MICROTUBES

The delivered amount can be determined by calculating the loading efficiency, which is the ratio between the loaded volume of therapeutic agent and the entire internal volume of the microtubes. After the release profile of the agent loaded microtubes is measured *in vitro*, the daily delivered amount of agent *in vivo* can be predicted. Currently, there is no

commercially available kit for quantifying chABC levels or antibody to chABC, therefore, the release profile of chABC was determined via SDS-PAGE and silver staining. The samples of chABC released from the hydrogel-microtube mixture were prepared as described in section 3.2.6, and the amount of chABC was determined via SDS-PAGE as described in section 3.2.1 and silver staining as described in the section 3.2.2. Various different amounts of chABC were prepared as a standard and run on SDS-PAGE at the same time with the collected samples. Intensity measurements of the collected samples and chABC standards were detected using a Microplate Reader (BIO-TEK Instruments, Inc.). The amount of the released chABC was determined by the standard curve and the release profile was obtained.

3.2.8   NT-3 RELEASE PROFILES FROM LIPID MICROTUBES

NT-3 was loaded into lipid microtubes and the release profile of NT-3 was determined by using methods similar to those previously published (Jain et al., 2006). An NT-3 Sandwich ELISA Kit (Chemicon) was used to quantify the NT-3 release profile. NT-3 (PeproTech Inc.) containing microtubes were mixed with SeaPlaque® agarose gel, placed in a 96-well plate, and cooled for gelation (30 ng per plate). The final working concentration of the gel was 0.6 % (w/v). During incubation in a 37 ℃ incubator for 2 weeks, the supernatant was collected and replaced with fresh PBS every other day after sampling at day 1 and stored at -80 ℃. The retrieved supernatants were pooled for the NT-3 ELISA and absorbance measurements of the samples were taken at 450 nm using a Microplate Reader (BIO-TEK Instruments, Inc.). The amount of the NT-3 was determined by the standard curve and the release profile was obtained.

3.2.9 ANALYSIS OF TEMPERATURE DEPENDENT CONFORMATION OF CHABC

To investigate the potential of conformational changes contributing to the thermal destabilization of chABC, we conducted circular dichroism (CD) studies with and without trehalose stabilization. chABC was dissolved into 50 mM sodium phosphate (pH 7.4) and placed in 10 mm light path length quartz cells. Scans collected measurements from between 195 and 300 nm with a 1nm bandwidth. For the denaturation curve, scans collected measurements from between 5 and 85 °C at a wavelength of 222 nm with a scan rate of 2.5 °C/min. Four scans were averaged for each running condition. The transient temperatures between fresh chABC in buffer and chABC in trehalose solution were compared.

3.3 RESULTS

3.3.1 FUNCTIONAL STABILITY OF CHABC AT BODY TEMPERATURE (37 °C) WITHOUT THERMAL STABILIZATION

We investigated the enzymatic activity of unstabilized versus trehalose-stabilized chABC by evaluating its ability to digest the CSPG decorin followed by SDS-PAGE. Decorin, our model CSPG, has a simple molecular structure consisting of one chondroitin or dermatan sulfate GAG chain on its core protein. Intact decorin migrates as a larger molecular weight broad smear on an SDS-PAGE gel (Fig. 3.3, Lane 3). A tighter and lower molecular weight decorin band after digestion by chABC indicates preservation of chABC activity. When the CS-GAG chain of decorin was digested by chABC, the core protein migrates at ~40-45 kDa (Fig. 3.3, Lane 1), and chABC alone migrates between 97 kDa and 116 kDa (Fig. 3.3, Lane 4). chABC pre-incubated for 24 hours at 37 °C retained its ability to degrade decorin (Fig. 3.3, Lane 2), but chABC lost the ability to completely degrade decorin GAG

chains after 1 week of pre-incubation at 37 ° (Fig. 3.3, Lane 5). In contrast, following incubation with 1 M trehalose at 37 ℃ for one week, chABC retained its ability to degrade decorin (Fig. 3.3, Lane 6).
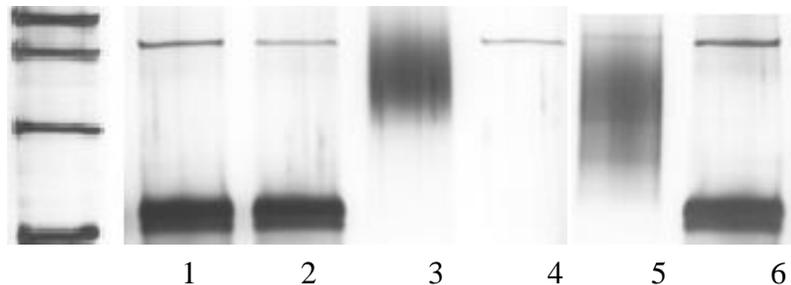
Figure 3.3. SDS-PAGE assay for chABC enzymatic activity after 1 day pre-incubation and 1 week of pre-incubation at 37 ℃ with and without trehalose. Lane 1: fresh chABC + decorin, Lane 2: 1 day pre-incubated chABC + decorin, Lane 3: intact decorin, Lane 4: chABC, Lane 5: 1 week pre-incubated chABC + decorin, and Lane 6: 1 week pre-incubated chABC with trehalose + decorin. Thermostability of chABC was enhanced with trehalose and trehalose-chABC still retained the ability to digest decorin after 1 week incubation at body temperature.

3.3.2 TREHALOSE SIGNIFICANTLY ENHANCES THERMOSTABILITY OF CHABC ENZYMATIC ACTIVITY

To improve the thermal stability of chABC, trehalose was introduced as a protein stabilizer. To determine the proper concentration of trehalose, different concentrations of trehalose, from 20 mM to 1 M, were evaluated for their ability to preserve chABC enzymatic activity. Trehalose concentrations above 500 mM successfully preserve chABC enzyme activity after 2 weeks of incubation at 37 ℃ (Fig. 3.4).
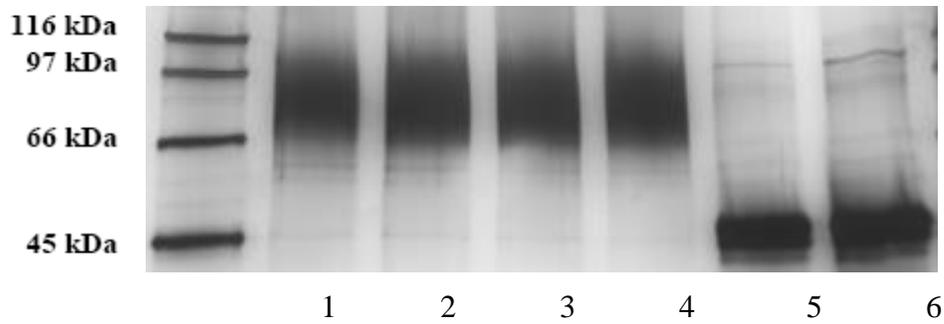
Figure 3.4. chABC enzymatic activity assay with different concentrations of trehalose by SDS-PAGE. Each lane represents 1) 20 mM, 2) 50 mM, 3) 100 mM, 4) 250 mM, 5) 500 mM and 6) 1M of trehalose-chABC with decorin after 2 weeks of pre-incubation at 37 ℃.
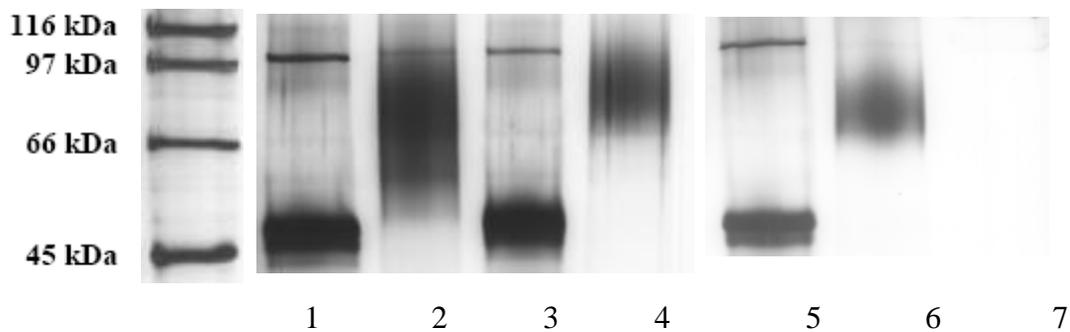
Figure 3.5. chABC enzymatic activity test after 4 weeks of pre-incubation with and without trehalose at 37 ℃ by SDS-PAGE. Lane 1: 4 weeks pre-incubated chABC with trehalose + decorin, Lane 2: 4 weeks pre-incubated chABC + decorin, Lane 3: fresh chABC + decorin, Lane 4: decorin, Lane 5: fresh chABC + decorin, Lane 6: fresh P'ase + decorin, and Lane 7: fresh P'ase (out of molecular weight range from gel; ~28 kDa). The trehalose-thermostabilized chABC still retained its activity to degrade CS-GAG of decorin after 4 weeks of pre-incubation at body temperature and P'ase had no effect on decorin CS-GAG.

To investigate whether trehalose can preserve chABC activity at 37 ºC for longer periods, 1M trehalose-chABC solutions were pre-incubated for 4 weeks at 37 ºC, and then added to decorin for digestion. In figure 3.5, Lane 1 demonstrates that after 4 weeks of pre-incubation with 1 M trehalose, chABC digested decorin, and confirms the ability of trehalose to preserve chABC activity at 37 ºC. In comparison, after 4 weeks of incubation in PBS at 37 ºC without trehalose, chABC lost its enzymatic activity (Fig. 3.5, Lane 2). Decorin incubated with fresh chABC (Fig. 3.5, Lane 3) and intact decorin (incubated for 4 hours at 37 ºC; Fig. 3.5, Lane 4) were run as controls at the same time. P'ase was used as a control enzyme, and when decorin was incubated with P'ase at 37 ºC (Fig. 3.5, Lane 6), no decorin digestion was observed as expected. P'ase was not shown (P'ase alone; Fig. 3.5, Lane 7) because molecular weight of P'ase (28 kDa) is out of range of this molecular standard weight.

3.3.3 TEMPERATURE STABILIZATION OF CHABC BY TREHALOSE IS DUE TO CONFORMATIONAL STABILITY

Deactivation profiles of chABC enzymatic activity with and without trehalose over time were evaluated with by the DMMB assay (Fig 3.6). At every time point except day 1, there was a statistically significant difference between control and trehalose treated samples. The enzymatic activity of chABC was maintained up to day 15 with trehalose. In comparison however, without trehalose, chABC quickly lost its enzymatic activity after day 3 and was completely inactive by day 5. Based on this deactivation study, a kinetic deactivation constant k_d was evaluated by assuming a two-state transition between native state (N), to unfolded state (D):

$$N \rightarrow D$$
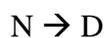
$$dN/dt = -k_bN; \quad N = N_0\exp(-k_bt)$$

where N_0 represents initial N and the first-order kinetics was adapted (the dotted line in figure 3.6). The deactivation rate constant of chABC was computed to be 0.27 [day^{-1}; R^2=0.98]. The slope of the decline in chABC activity when it is thermostabilized by trehalose is gentle and not precipitous and the kinetic deactivation constant of trehalose-chABC was 0.017 [day^{-1}; R^2=0.74].

To investigate whether increased thermal stability of chABC in the presence of trehalose is due to conformational stabilization of the enzyme, conformational changes in chABC as a function of temperature with and without trehalose were quantified by CD (Fig. 3.7). Ellipticity change measured by CD is directly proportional to the change in concentration of native and unfolded forms; therefore CD has been applied to protein folding study. The thermodynamics of protein conformational stability can be described by following equations (Greenfield et al., 1999):

$$K = \alpha / (1-\alpha) \tag{1}$$

$$\Delta G = nRT\ln K; \quad \Delta G = \Delta H - T\Delta S \tag{2}$$

$$\theta_{obs} = (a_1 - a_2)\,\alpha + a_2 \tag{3}$$

where K is the equilibrium constant of folding, α is the friction folded, ΔG is the free energy of folding, R is the gas constant, T is temperature (Kelvin), ΔH is the enthalpy of folding and ΔS is the entropy of folding. θ_{obs} represents the observed ellipticity, a_1 is fully folded (maximum) θ_{obs} and a_2 is fully native (minimum) θ_{obs}. Based on these equations, ΔH and the midpoint transition temperature, T_m, were calculated by fitting the best curve to θ_{obs}.
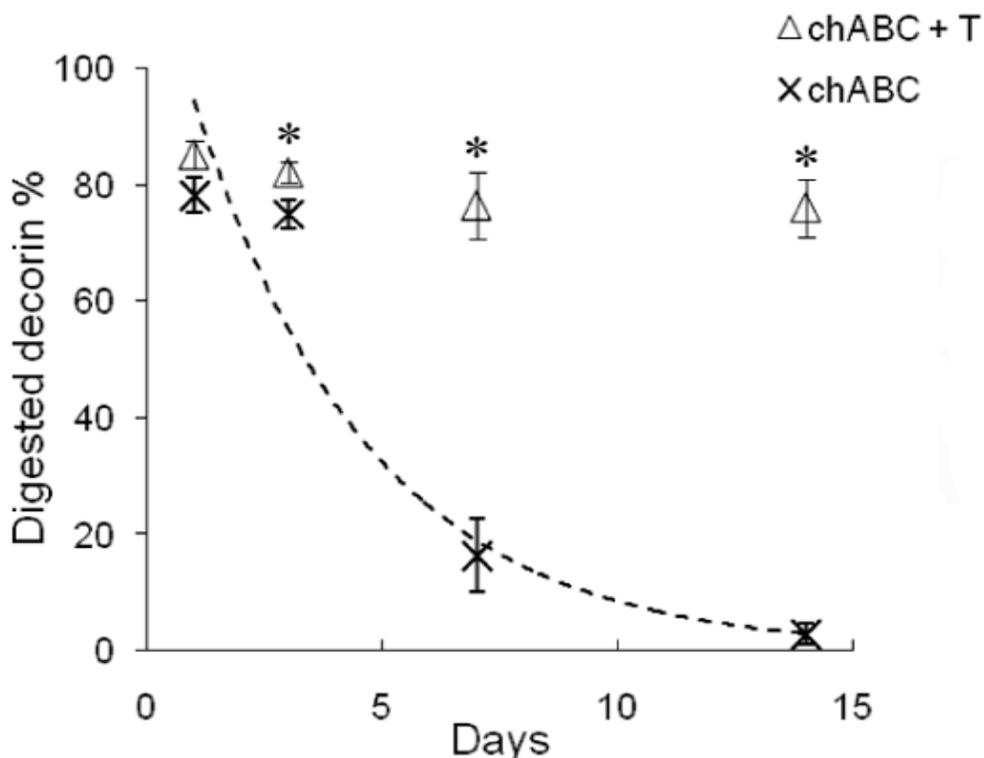
Figure 3.6. Kinetic analysis of chABC deactivation by DMMB assay. The X axis represents days and the Y axis represents percentage of digested decorin. Asterisks denote a significant difference from chABC in 1X PBS ($P < 0.05$) and data represent mean ± SEM. The dotted line represents the calculated deactivation curve of chABC in 1x PBS. Data are mean ± SEM. chABC in 1X PBS (×) loses most activity within 5 days, and in contrast, chABC in 1 M trehalose (Δ) retains its activity to degrade decorin CS-GAG up to 15 days.

Initial values of ΔH, T_m, a_1 and a_2 were estimated, and calculated θ was fitted to the $θ_{obs}$ by curve fitting routine. The spectrum was measured at 222 nm and from 20 °C to 90 °C at the rate of 2.5 °C/min and 1 min of delay. The T_m, $ΔH_m$ and $ΔS_m$ of chABC in 1 M trehalose solution were 64.2 °C, 171 kJ·mol^{-1} and 506 J K^{-1} mol^{-1} respectively, versus the T_m, $ΔH_m$ and $ΔS_m$ of chABC dissolved in sodium phosphate buffer were 56.2 °C, 176 kJ·mol^{-1} and 533 J

61

K^{-1} mol^{-1}. Therefore, the increment in the midpoint of transition, ΔT_m, between the two conditions is 8 °C, indicating that chABC's conformation is thermally more stable in the presence of 1 M trehalose.
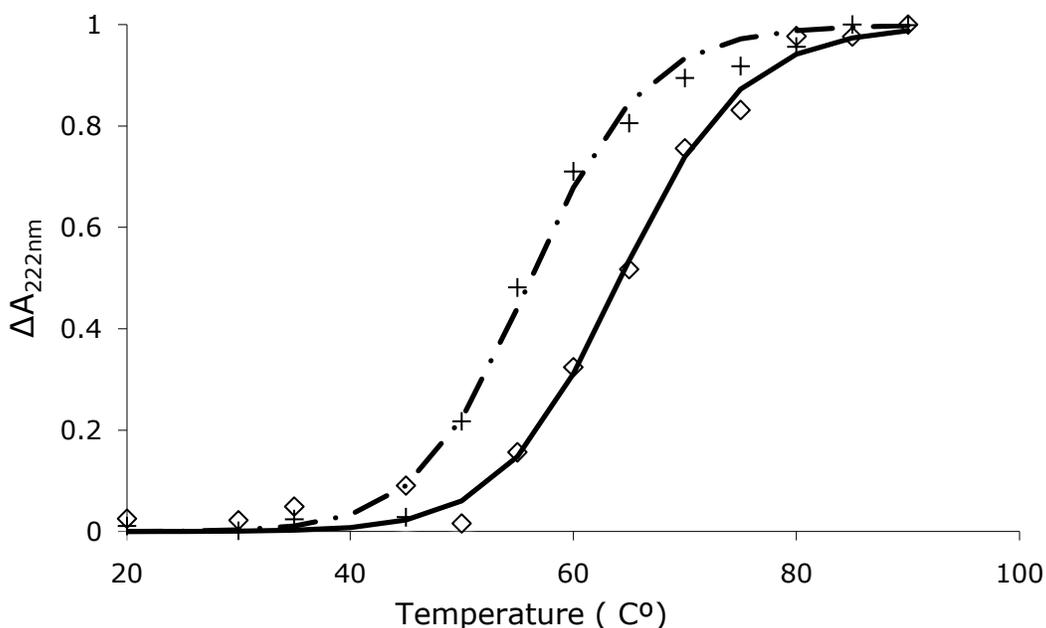
Figure 3.7. The normalized thermal denaturation curves (fraction unfolded) of chABC in pH 7.4 were measured by the changes of the absorbance at 222nm. The dashed line represents chABC in 50 mM sodium phosphate buffer and the solid line represents chABC in 1M trehalose solution. T_m of chABC in 1 M trehalose solution was 64.2 °C and the T_m of chABC dissolved in buffer solution was 56.2 °C. Therefore, the increment in the midpoint of transition, ΔT_m, between the two conditions is 8 °C and can be attributed to the presence of trehalose.

3.3.4 LIPID MICROTUBE ENCAPSULATED CHABC IS BIOLOGICALLY ACTIVE FOR 2 WEEKS

To verify that self-assembled, hollow lipid microtubes (0.5 microns x 40 microns in dimensions) can be loaded with chABC without compromising its enzymatic activity, chABC released from fresh microtubes (without pre-incubation at 37 °C) was tested with SDS-PAGE (Fig. 3.8B) for its ability to digest decorin. As indicated by the digested decorin band, microtube loading does not negatively impact chABC activity.

After confirming that lipid microtubes can be used for chABC delivery, post-release activity of chABC or P'ase from microtubes was plotted (Fig. 3.8A) as a function of time, and their relative enzymatic activity was measured by DMMB assay (Melrose and Ghosh, 1988; de Jong et al., 1989). 100% of digested decorin on the Y-axis represents 1X PBS with no decorin. This release profile showed that, when combined with trehalose, chABC released from microtubes retained its enzymatic activity up to 15 days *in vitro*. As expected, the combination of the control enzyme P'ase with trehalose did not digest of decorin.
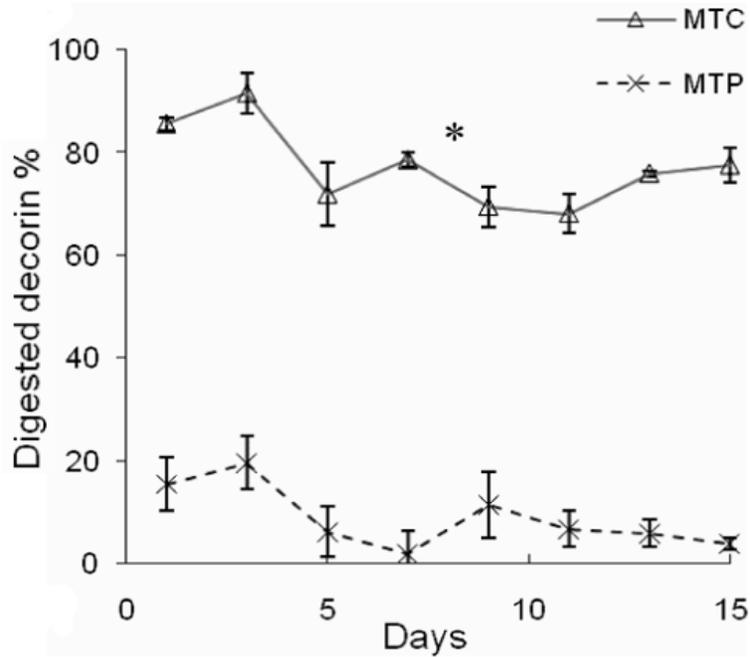
(A)
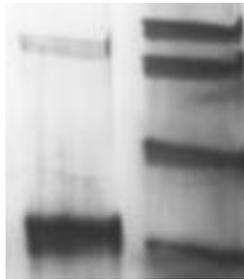
(B)

Figure 3.8. Enzymatic activity of post-released chABC from lipid microtubes. (A) Quantification of the amount of CS-GAGs that remained after digestion of decorin with the released enzymes by DMMB assay. chABC (Δ) and P'ase ($\times$) with trehalose/microtubes. The Y-axis represents percentage of digested decorin and the X-axis represents time. All data points are significantly different ($P < 0.05$; mean $\pm$ SEM). (B) SDS-PAGE assay of chABC released from trehalose/microtube + decorin.

3.3.5. RELEASE PROFILE OF MICROTUBE ENCAPSULATED NT-3 CONFIRMS A SUSTAINED DELIVERY FOR 2 WEEK

To characterize the release profile of NT-3, NT-3 released from microtubes was tested with NT-3 sandwich ELISA kit to measure released amount (Fig. 3.9).
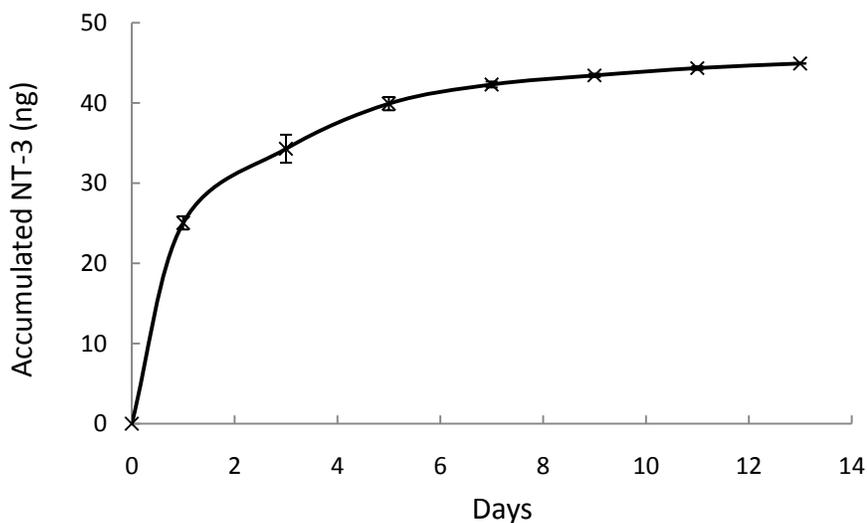
Figure 3.9. Release profile of NT-3 from the hydrogel-microtube delivery scaffold.

3.4 DISCUSSION

The purpose of this study was to develop an approach that allows the application of chABC as a therapeutic agent *in vivo*. chABC is one of the more promising therapeutic interventions for SCI, however, the thermal instability of chABC compromises its potential for *in vivo* application (Tester et al., 2007). In this study, we demonstrate that the enzymatic activity of chABC could be maintained at body temperature over time and that thermostabilized chABC delivered by a hydrogel-lipid microtube scaffold system over two

weeks remains enzymatically active *in vitro*. In this chapter, it is shown that this hydrogel-microtube delivery scaffold has a potential to provide an alternative delivery method to chronically implanted, invasive pumps, which is minimally invasive and effectively delivers chABC *in vivo*.

After 24 hour incubation at 37 ℃, the enzymatic activity of chABC, which is used in this study, was still preserved. However after 1 week of incubation at 37 ℃, a broaden decorin band appeared (Fig. 3.3, Lane 5), indicating that enzymatic activity was weakened leading to incomplete digestion of CS-GAGs on decorin even after sufficient reaction time. At body temperature chABC quickly loses most of its enzymatic activity within 5 days (the DMMB assay; Fig. 3.6; ×-dashed line) and the retained enzymatic activity is not enough to completely digest CS-GAG chains, though partial digestion is still possible (seen as a broaden band in SDS-PAGE assay; Fig. 3.3). chABC typically lost most of its enzymatic function within one week at body temperature, however the rate of enzymatic activity loss and the amount of enzymatic activity retained depend on several factors. The SDS-PAGE assay showed different retained activities of chABC from different lots. Other studies also showed that enzymatic thermostability of chABC depends on lot and time (Tester et al., 2007). Large differences exist between lots, since function can be lost anywhere from 1 day to 2 weeks, so all experiments in this study were performed with chABC from the same lot.

Biodegradable polymer nanoparticles also could be considered as a carrier for sustained delivery of chABC (Cohen et al., 1991; Genta et al., 2001; Kim and Burgess, 2002; Singh et al., 2009). Before using the lipid microtube, poly(lactic-co-glycolic acid) (PLGA) nanoparticles were examined as drug carriers for chABC in a preliminary. The double emulsion method was used to make PLGA nanoparticles, and is simple, takes a relatively

66

short time and is easy to store in powder form at -80 ºC after lyophilizing comparing to the fabrication procedure of lipid microtubes. After fabricating powder form of PLGA nanoparticle encapsulating chABC, the enzymatic activity of chABC released from the PLGA particles was characterized with the same assessment described in the section 3.2.1. However the mark band (Fig. 3.3, Lane 1) presenting core protein due to GAG chain digestion by chABC was not observed and a broad band of decorin, similar to the one in Lane 5 of figure 3.3, was seen in the gel. chABC lost its enzymatic activity after the fabrication procedure of PLGA nanoparticles. It is possible that proteins undergo physical denaturation and chemical degradation during fabrication. The acidification of the internal PLGA microenvironment and the water-in-oil-in-water (w/o/w) encapsulation procedure are considered major protein stresses inducing inactivation and aggregation (van de Weert et al., 2000; Perez-Rodriguez et al., 2003; Estey et al., 2006). During the double emulsion procedure, chABC is exposed to organic solvents, dichloromethane, and the pH of inside particles is predominantly below pH 5.8 (detection limit in this paper, Li and Schwendeman, 2005).

Our laboratory has previously reported the use of lipid microtubes for the slow delivery of a variety of proteins (Meilander et al., 2001), DNA (Meilander et al., 2003; Yu and Bellamkonda, 2003; Meilander-Lin et al., 2005) and neurotrophic factors (Yu and Bellamkonda, 2003; Jain et al., 2006) *in vivo*. Relative to other delivery systems such as polyester based PLGA nanoparticles, lipid microtubes have the advantage that there is no exposure to heat or organic solvents that might cause denaturation or degradation, during the fabrication process. As is evident from figure 3.8B, release from lipid microtubes does not adversely affect the enzymatic activity of chABC. In addition to that, lipid microtubes are

injectable either by themselves, or when embedded in thermo-reversible hydrogels as reported in Jain et al. (2006), Dodla et al. (2008) and Chvatal et al. (2008).

Here, the lipid microtube-gel delivery system provides sustained delivery of thermostabilized chABC over a period of 2 weeks, with the microtubes enabling slow release while the hydrogel localizes the tubes to the lesion site. We have developed a mathematical model (Meilander et al., 2001), to predict the release profile of compounds with a range of molecular weights such as myoglobin (17.8 kDa), albumin (66.4 kDa) and thyroglobulin (660 kDa). These studies suggest that an initial burst release of protein from day 1 to day 3 is followed by a slow and continuous release, leading to a cumulative percentage of released agents of 80-100% by day 14. Further, microtubes show a stable and continuous release profile with delivery of BDNF (Brain derived neurotrophic factor) (Jain et al., 2006), and NT-3 (neurotrophin-3) (Dodla and Bellamkonda, 2008).As the molecular weight of chABC (120 kDa) is within the protein molecular weight range previously tested, most of the chABC loaded into microtubes is likely released by day 14.

In this study, we chose to stabilize chABC by adding trehalose since it is known as an exceptional stabilizer and widely used with proteins (Carninci et al., 1998; Kreilgaard et al., 1998). The molecular mechanism of trehalose-mediated thermostabilization is still poorly understood (Hedoux et al., 2009). There are several hypotheses outlining the mechanisms of protein stabilization by trehalose − water replacement (Crowe et al., 1984), preferential hydration (Timasheff, 2002), vitrification of solutions (Green et al., 1989) and the influence of trehalose on the water tetrahedral hydrogen bond network (Branca et al., 1999). Previous works have shown that surface tension of trehalose solutions increases linearly with increase in trehalose concentration (Kita et al., 1994), and there is a strong correlation between

surface tension and increase in T_m (Kaushik and Bhat, 2003). Studies have shown that the dynamic fluctuation of polar side chains at the solvent-protein interface was reduced in the presence of trehalose (Hedoux et al., 2009). The increased surface tension or the limited exposure of hydrophobic groups to the water molecules leads to preferential hydration, resulting in the stabilization of the tertiary structure of protein (Timasheff, 2002). In this study, the Δ T_m of chABC (8 °C) with 1M trehalose addition is similar in range to its effects on other enzymes such as RNase A (5.5 °C) and lysozyme (8.4 °C) (Kaushik and Bhat, 2003), where increased conformational thermostabilization (increase of T_m) induces an increase in enzymatic activity. These enzymes also show an increase of ΔT_m when concentration of trehalose increases, and it describes the observation that only high concentration (500 mM and 1 M) of trehalose preserved the enzymatic activity of chABC in this study. Therefore, trehalose's ability to thermally stabilize chABC is consistent with its effects on other enzymes.

3.5   CONCLUSIONS

In this study, improvement of thermostability of chABC enzymatic activity was attained by adding trehalose up to 4 weeks. We demonstrated that thermostabilized chABC can be slowly delivered by the lipid microtube-hydrogel delivery system and the released chABC retains its enzymatically activity over two weeks *in vitro*. Therefore, these achievements of thermostabilization and development of the sustained delivery system provide an alternative and novel application for chABC treatment after SCI.

3.6 REFERENCES

Barritt AW, Davies M, Marchand F, Hartley R, Grist J, Yip P, McMahon SB, Bradbury EJ (2006) Chondroitinase ABC promotes sprouting of intact and injured spinal systems after spinal cord injury. J Neurosci 26:10856-10867.

Bradbury EJ, Moon LD, Popat RJ, King VR, Bennett GS, Patel PN, Fawcett JW, McMahon SB (2002) Chondroitinase ABC promotes functional recovery after spinal cord injury. Nature 416:636-640.

Branca C, Magazu S, Maisano G, Migliardo P (1999) Anomalous cryoprotective effectiveness of trehalose: Raman scattering evidences. J Chem Phys 111 (1): 281-287.

Caggiano AO, Zimber MP, Ganguly A, Blight AR, Gruskin EA (2005) Chondroitinase ABCI improves locomotion and bladder function following contusion injury of the rat spinal cord. J Neurotrauma 22:226-239.

Carninci P, Nishiyama Y, Westover A, Itoh M, Nagaoka S, Sasaki N, Okazaki Y, Muramatsu M, Hayashizaki Y (1998) Thermostabilization and thermoactivation of thermolabile enzymes by trehalose and its application for the synthesis of full length cDNA. Proc Natl Acad Sci U S A 95:520-524.

Chau CH, Shum DK, Li H, Pei J, Lui YY, Wirthlin L, Chan YS, Xu XM (2004) Chondroitinase ABC enhances axonal regrowth through Schwann cell-seeded guidance channels after spinal cord injury. FASEB J 18:194-196.

Chvatal SA, Kim YT, Bratt-Leal AM, Lee H, Bellamkonda RV (2008) Spatial distribution and acute anti-inflammatory effects of Methylprednisolone after sustained local delivery to the contused spinal cord. Biomaterials 29:1967-1975.

Cohen S, Yoshioka T, Lucarelli M, Hwang LH, Langer R (1991) Controlled delivery systems for proteins based on poly(lactic/glycolic acid) microspheres. Pharm Res 8:713-720.

Crowe LM, Mouradian R, Crowe JH, Jackson SA, Womersley C (1984) Effects of carbohydrates on membrane stability at low water activities. Biochim Biophys Acta 769:141-150.

de Jong JG, Wevers RA, Laarakkers C, Poorthuis BJ (1989) Dimethylmethylene blue-based spectrophotometry of glycosaminoglycans in untreated urine: a rapid screening procedure for mucopolysaccharidoses. Clin Chem 35:1472-1477.

Dodla MC, Bellamkonda RV (2008) Differences between the effect of anisotropic and isotropic laminin and nerve growth factor presenting scaffolds on nerve regeneration across long peripheral nerve gaps. Biomaterials 29:33-46.

Estey T, Kang J, Schwendeman SP, Carpenter JF (2006) BSA degradation under acidic conditions: a model for protein instability during release from PLGA delivery systems. J Pharm Sci 95:1626-1639.

Fawcett JW, Asher RA (1999) The glial scar and central nervous system repair. Brain Res Bull 49:377-391.

Genta I, Perugini P, Pavanetto F, Maculotti K, Modena T, Casado B, Lupi A, Iadarola P, Conti B (2001) Enzyme loaded biodegradable microspheres in vitro ex vivo evaluation. J Control Release 77:287-295.

Green JL, Angell CA (1989) Phase relations and vitrification in saccharide-water solutions and the trehalose anomaly. *J Phys Chem* 93:2880-2882.

Greenfield NJ (1999) Applications of circular dichroism in protein and peptide analysis. Trends Analyt Chem 18(4):236-244.

Hedoux A, Willart JF, Paccou L, Guinet Y, Affouard F, Lerbret A, Descamps M (2009) Thermostabilization mechanism of bovine serum albumin by trehalose. J Phys Chem B 113:6119-6126.

Houle JD, Tom VJ, Mayes D, Wagoner G, Phillips N, Silver J (2006) Combining an autologous peripheral nervous system "bridge" and matrix modification by chondroitinase allows robust, functional regeneration beyond a hemisection lesion of the adult rat spinal cord. J Neurosci 26:7405-7415.

Huang WC, Kuo WC, Cherng JH, Hsu SH, Chen PR, Huang SH, Huang MC, Liu JC, Cheng H (2006) Chondroitinase ABC promotes axonal re-growth and behavior recovery in spinal cord injury. Biochem Biophys Res Commun 349:963-968.

Jain A, Kim YT, McKeon RJ, Bellamkonda RV (2006) In situ gelling hydrogels for conformal repair of spinal cord defects, and local delivery of BDNF after spinal cord injury. Biomaterials 27:497-504.

Kaushik, J. K., and Bhat, R. (1998) Thermal stability of proteins in aqueous polyol solutions. J. Phys. Chem. B 102, 7058–7066

Kaushik, J. K., and Bhat, R. (1999) A mechanistic analysis of the increase in the thermal stability of proteins in aqueous carboxylic acid salt solutions. Protein Sci. 8, 222–233

Kaushik JK, Bhat R (2003) Why is trehalose an exceptional protein stabilizer? An analysis of the thermal stability of proteins in the presence of the compatible osmolyte trehalose. J Biol Chem 278:26458-26465.

Kim BG, Dai HN, Lynskey JV, McAtee M, Bregman BS (2006) Degradation of chondroitin sulfate proteoglycans potentiates transplant-mediated axonal remodeling and functional recovery after spinal cord injury in adult rats. J Comp Neurol 497:182-198.

Kim H, Burgess DJ (2002) Effect of drug stability on the analysis of release data from controlled release microspheres. J Microencapsul 19:631-640.

Kim YT, Caldwell JM, Bellamkonda RV (2009) Nanoparticle-mediated local delivery of Methylprednisolone after spinal cord injury. Biomaterials 30:2582-2590.

Kita Y, Arakawa T, Lin TY, Timasheff SN (1994) Contribution of the surface free energy perturbation to protein-solvent interactions. Biochemistry 33:15178-15189.

Kreilgaard L, Frokjaer S, Flink JM, Randolph TW, Carpenter JF (1998) Effects of additives on the stability of recombinant human factor XIII during freeze-drying and storage in the dried solid. Arch Biochem Biophys 360:121-134.

Li L, Schwendeman SP (2005) Mapping neutral microclimate pH in PLGA microspheres. J Control Release 101:163-173.

Lando JB, Hansen JE, Sudiwala RV, Rickert SE (1990) The formation of polymerizable tubules. Polym Adv Technol 1:27-32.

Meilander-Lin NJ, Cheung PJ, Wilson DL, Bellamkonda RV (2005) Sustained in vivo gene delivery from agarose hydrogel prolongs nonviral gene expression in skin. Tissue Eng 11:546-555.

Meilander NJ, Yu X, Ziats NP, Bellamkonda RV (2001) Lipid-based microtubular drug delivery vehicles. J Control Release 71:141-152.

Meilander NJ, Pasumarthy MK, Kowalczyk TH, Cooper MJ, Bellamkonda RV (2003) Sustained release of plasmid DNA using lipid microtubules and agarose hydrogel. J Control Release 88:321-331.

Melrose J, Ghosh P (1988) The quantitative discrimination of corneal type I, but not skeletal type II, keratan sulfate in glycosaminoglycan mixtures by using a combination of dimethylmethylene blue and endo-beta-D-galactosidase digestion. Anal Biochem 170:293-300.

Perez-Rodriguez C, Montano N, Gonzalez K, Griebenow K (2003) Stabilization of alpha-chymotrypsin at the CH2Cl2/water interface and upon water-in-oil-in-water encapsulation in PLGA microspheres. J Control Release 89:71-85.

Pizzorusso T, Medini P, Landi S, Baldini S, Berardi N, Maffei L (2006) Structural and functional recovery from early monocular deprivation in adult rats. Proc Natl Acad Sci U S A 103:8517-8522.

Singh D, Dixit VK, Saraf S (2009) Formulation optimization of serratiopeptidase-loaded PLGA microspheres using selected variables. PDA J Pharm Sci Technol 63:103-112.

Spargo BJ, Cliff RO, Rollwagen FM, Rudolph AS (1995) Controlled release of transforming growth factor-beta from lipid-based microcylinders. J Microencapsul 12:247-254.

Tester NJ, Plaas AH, Howland DR (2007) Effect of body temperature on chondroitinase ABC's ability to cleave chondroitin sulfate glycosaminoglycans. J Neurosci Res 85:1110-1118.

Timasheff SN (2002) Protein-solvent preferential interactions, protein hydration, and the modulation of biochemical reactions by solvent components. Proc Natl Acad Sci U S A 99:9721-9726.

Tropea D, Caleo M, Maffei L (2003) Synergistic effects of brain-derived neurotrophic factor and chondroitinase ABC on retinal fiber sprouting after denervation of the superior colliculus in adult rats. J Neurosci 23:7034-7044.

van de Weert M, Hoechstetter J, Hennink WE, Crommelin DJ (2000) The effect of a water/organic solvent interface on the structural stability of lysozyme. J Control Release 68:351-359.

Yu X, Bellamkonda RV (2003) Tissue-engineered scaffolds are effective alternatives to autografts for bridging peripheral nerve gaps. Tissue Eng 9:421-430.

CHAPTER 4

DELIVERY OF THERMOSTABILIZED CHABC BY IMPLANTING HYDROGEL-MICROTUBE SCAFFOLDS AFTER SPINAL CORD INJURY AND EXAMINATION OF CELLULAR AND MOLECULAR RESPONSES: SHORT TERM STUDY

(Partially as published with R.J. McKeon and R.V. Bellamkonda, Proceedings of the National Academy of Science, 2009)

Chondroitin sulfate proteoglycans (CSPGs) are upregulated and accumulate around the lesion site after spinal cord injury (SCI), and are major inhibitors of regeneration. To overcome CSPG-mediated inhibition, modification or digestion of CSPGs with chondroitinase ABC (chABC) has been explored. chABC digests glycosaminoglycan (GAG) chains on CSPGs and enhances sprouting and regeneration when delivered to the lesion site. However, chABC has a crucial limitation; it is thermally unstable at body temperature (37ºC) and its enzymatic activity is significantly attenuated within 3 days. Therefore, multiple or continuous infusions with an indwelling catheter are necessary to maintain enzymatic functionality for periods of 2 weeks or longer and such devices are invasive and clinically problematic. To overcome these limitations, we enhanced the thermal stability of chABC by adding a protein stabilizer, trehalose, and demonstrated that chABC maintained its enzymatic activity for 4 weeks at 37 ºC *in vitro*. Also, we developed a delivery scaffold for chABC *in vivo* application in the temporally and spatially controlled manner.

In this chapter, a dorsal over hemisection injury was made at thoracic vertebrae T10 in adult rats, and thermally stabilized chABC was delivered to the lesion site by a minimally

invasive hydrogel-microtube scaffold carrying chABC-loaded lipid microtubules at the lesion site immediately following injury. To determine the effectiveness of topical delivery of thermostabilized chABC, animal groups treated with single injection or hydrogel scaffold implantation of chABC, chABC/trehalose and P'ase were included as controls. Two weeks after surgery, the enzymatic functionality of released chABC *in vivo* was examined by CS-56, WFA and 3B3 immunostaining.

The results demonstrated that thermally stabilized chABC was successfully delivered slowly and locally without a catheter/mini-pump and the released chABC effectively digested CSPGs *in vivo* and significant differences of CSPG digestion were observed in 3B3-IR and CS-56-IR between groups. We suggest that chABC could be combined with other therapies or agents, such as neurotrophic factors to treat SCI.

4.1 INTRODUCTION

After injury, a series of cellular and molecular events occur, and results in the formation of astro-glial scar tissue consisting of interwoven reactive astrocytes and chondroitin sulfate proteoglycan (CSPGs). The CSPG-astroglial scar provides a non-permissive environment for axon regeneration. Studies have shown that CSPGs are upregulated after injury in the CNS and neurite regrowth is inhibited by CSPGs (McKeon et al., 1995; Stichel et al., 1995; Lemons et al., 1999; Jones et al., 2002). It has been shown that growth cone stall or change growth orientation at the CSPG-rich region *in vitro* and *in vivo*. Therefore, it is important to remove or attenuate the inhibitory nature of CSPGs by modifying CSPGs and to encourage axons to regrow through the inhibitory regions around the lesion site. Therefore, chABC has been used to treat SCI, based on the concept that

removing or attenuating inhibitory activity of CSPGs could promote axonal regeneration. After promising results for axonal outgrowth were reported *in vitro* (Snow and Letourneau, 1992; Zuo et al., 1998) and *in vivo* (Yick et al., 2000; Moon et al., 2001; Bradbury et al., 2002; Yick et al., 2003; Chau et al., 2004; Caggiano et al., 2005; Barritt et al., 2006; Houle et al., 2006), it has received a lot of attention as a potential therapy for spinal cord injury.

chABC shows the best enzymatic activity at 37 ℃ and the optimum pH is near 8.0. At physiological conditions, body temperature 37 ℃ and 7.4 pH, chABC should be suited for *in vivo* usage. However, as described in the previous chapters, there are crucial limitations when delivering chABC for SCI treatment, such as thermal stability of chABC and difficulties with spatio-temporal control. In general, CSPGs are upregulated and deposited around the lesion site for at least 2 weeks after the initial injury, and the CSPG-rich matrix surrounding the lesion site persists for up to 8 weeks following injury (Jones et al., 2003). Therefore, for chABC to degrade CSPG associated glycosaminoglycans (GAGs), a "fresh" supply would need to be delivered intrathecally for at least two weeks. Currently this is achieved via intrathecal injection, with the infusion frequency varying from days to weeks, and for time periods ranging from 2 to 6 weeks to compensate the rapid loss of enzymatic activity of chABC. A single administration of chABC containing gelfoam on lesion site of T11 hemisection promotes Clarke's nucleus neurons to regrow beyond the injury (Yick et al., 2000; Yick et al., 2003). Multiple or continuous infusions were also administrated, using an osmotic mini-pump (Chau et al., 2004; Houle et al., 2006; Huang et al., 2006) and catheters with externalized cannulas (Moon et al., 2001; Bradbury et al., 2002; Caggiano et al., 2005; Barritt et al., 2006).

Diffusion of chABC into deep regions of the cord, however, is limited when delivered intrathecally due to overflow into the intrathecal space, thereby diluting the enzyme rapidly and necessitating concentrated infusions (from 2 U/ml to 1000 U/ml) to compensate. With the exception of catheters with externalized cnnulas, the efficiency of CSPG digestion is dependent on the enzyme's stability at body temperature. Therefore, there is a compelling need to develop clinically viable methods for the spatially and temporally controlled delivery of 'fresh' chABC, preferably in a manner confining it to the lesion site. We demonstrated an alternative method using trehalose-thermostabilized chABC and a hydrogel and lipid microtube based minimally invasive system to deliver chABC in a temporally and spatially controlled manner *in vivo* in chapter 3.

Therefore, the study in chapter 4 was designed to investigate chABC's activity *in vivo* at the lesion site after SCI when delivered via our lipid microtube-hydrogel system and compare the CSPG digestion efficiency to a single injection of chABC. In this short term (two week) animal study, we locally delivered chABC to the lesion site by a topical delivery model and the dorsal over-hemisection injury was used. Thermostabilization of chABC and development of sustained delivery scaffold were achieved previously in the chapter 3. Two weeks after surgery, the animals were sacrificed, and the functionality of chABC released from the gel scaffold was examined. CS-56 and 3B3 immunostaining were used to examine the level of CSPGs and CSPG digestion by chABC's activity, and WFA was used to visualize perineuronal nets, which encapsulate synapses throughout the nervous system with CSPGs.

4.2 MATERIALS AND METHODS

4.2.1 FABRICATION OF MICROTUBE-HYDROGEL SCAFFOLDS

The fabrication procedure of the lipid microtube was previously published (Meilander et al., 2001; Meilander et al., 2003) and described in the Chapter 3, section 3.2.4. The hydrogel-microtube delivery scaffolds were fabricated by loading chABC/ 1M trehalose solution into the microtubes, and mixed with an equal amount of 2% (w/v) SeaPrep® agarose gel (Cambrex) in 1X PBS for 1% of final gel concentration. Before mixing SeaPrep agarose gel with the microtubes, the gel solution was filtered for sterilization and cooled to below 37 ºC to avoid deactivation of chABC or P'ase due to high temperature. After complete gelation at 4 ºC, each gel scaffold contained 10mU of chABC prior to being implanted in SCI animals, as described below, section 4.2.2.

4.2.2 TOPICAL DELIVERY OF HYDROGEL-MICROTUBE SCAFFOLDS IN A DORSAL OVER HEMISECTION INJURY MODEL

Adult male Spraque-Dawley rats (Charles River Laboratory) weighing between 235~260 g were anesthetized with 2% of isoflurane and maintained during surgery with 0.5% of isoflurane. The surgical area was shaved and the skin and muscles were opened to expose the thoracic vertebrae T9-T11. A single laminectomy was performed on T10 to expose the spinal cord by removing the bone with a micro-rongeur and the dura mater was excised. Using micro-scissors marked at 1.5 mm depth from the tip, a controlled dorsal hemisection injury (2 mm of width x 1.5 mm of depth) was made by cutting the dorsal columns at T10. Sustained topical delivery of thermostabilized chABC (MTC; n=8) was achieved using methods previously published (Chvatal et al., 2008). Briefly, the SeaPrep agarose hydrogel

embedded with lipid microtubes loaded with either chABC/1M trehalose or chABC alone was placed on top of the lesion site as shown schematically in figure 4.1. To stabilize the hydrogel embedded microtubes in place, a stiffer 0.7% of SeaKem agarose hydrogel solution was added on top. This denser gel was quickly gelled in situ by a stream of cooled air (Fig. 4.2) as described in a previous study (Jain et al., 2006). After ensuring complete gelation, the muscles were sutured together and the skin was closed with wound clips. Figure 4.3 demonstrates the topical delivery model applied into the spinal cord lesion site.

Table 1 describes experimental and control groups. As controls, 10 mU of chABC in 5 μL of 1X PBS (SC; n=6) or 1 M trehalose/1X PBS (STC; n=6) was injected as 'single injection' conditions that have local, but not sustained delivery. 100 ng of P'ase (Sigma) was delivered by single injection (STP; n=6) or hydrogel-microtube scaffold (MTP; n=6) with 1M trehalose as a negative enzymatic delivery control for chABC specificity. Sham (Sham; n=4) and trehalose loaded hydrogel scaffold conditions (MT; n=6) were also conducted. To avoid differences in the tissue reaction caused by absence of SeaKem agarose gel, after a single injection of agents, a pre-made SeaKem block was placed on top of the lesion site. After two weeks, the animals were anesthetized with a ketamine-xylazine-acepromazine cocktail (1:0.17:0.37 ml/kg) and transcardially perfused with 4% paraformaldehyde.
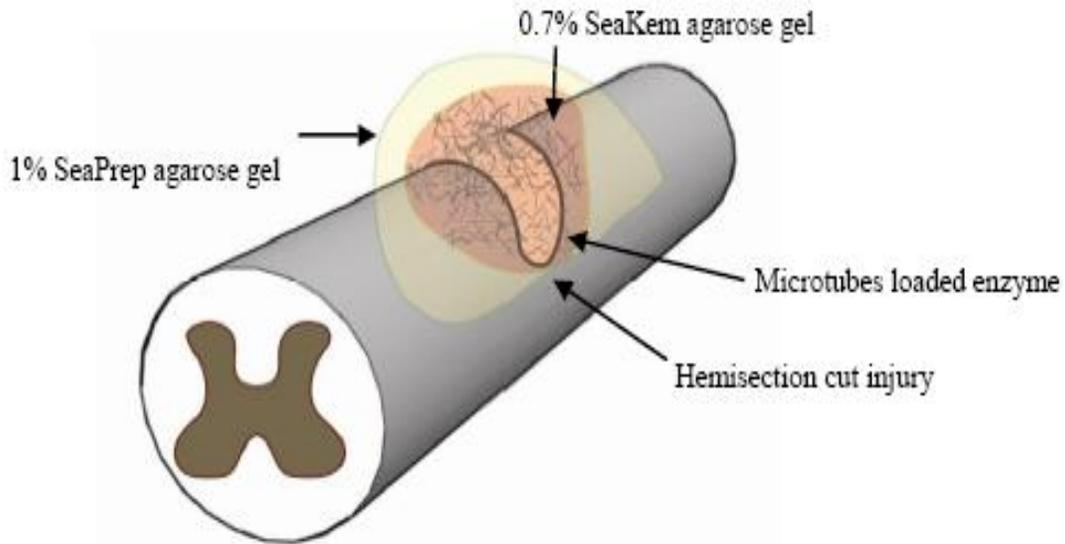
Figure 4.1. Schematic of spinal cord injury model and delivery of enzyme to lesion site. The 1 % SeaPrep agarose gel-microtube-scaffold is implanted on top of the lesion and covered with stiffer 0.7% SeaKem agarose gel to keep the scaffold in place.
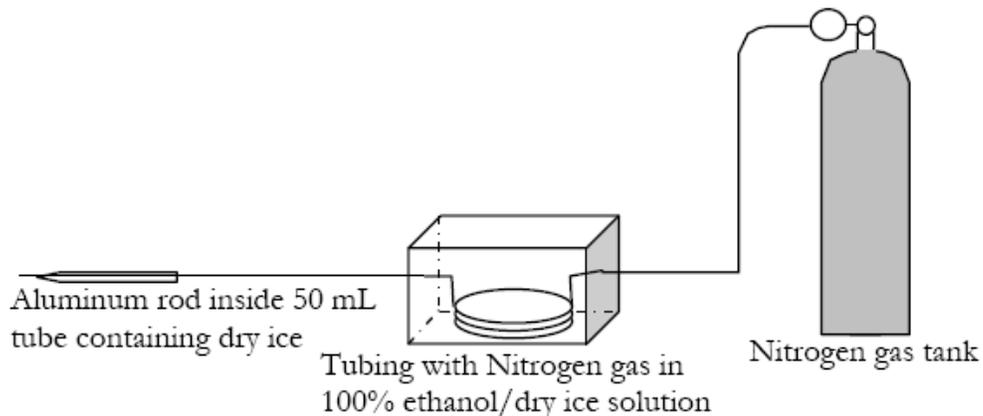
Figure 4.2. Schematic of gel cooling system. Tubing runs from the nitrogen gas tank to a Styrofoam box containing 100% ethanol and dry ice, and runs through an aluminum rod inside a tube containing dry ice to keep the nitrogen gas cool. The cooled nitrogen gas was applied over the stiffer agarose gel solution for *in situ* gelation, which covers the top of the gel-microtube delivery scaffold. Figure from Jain et al., 2006.
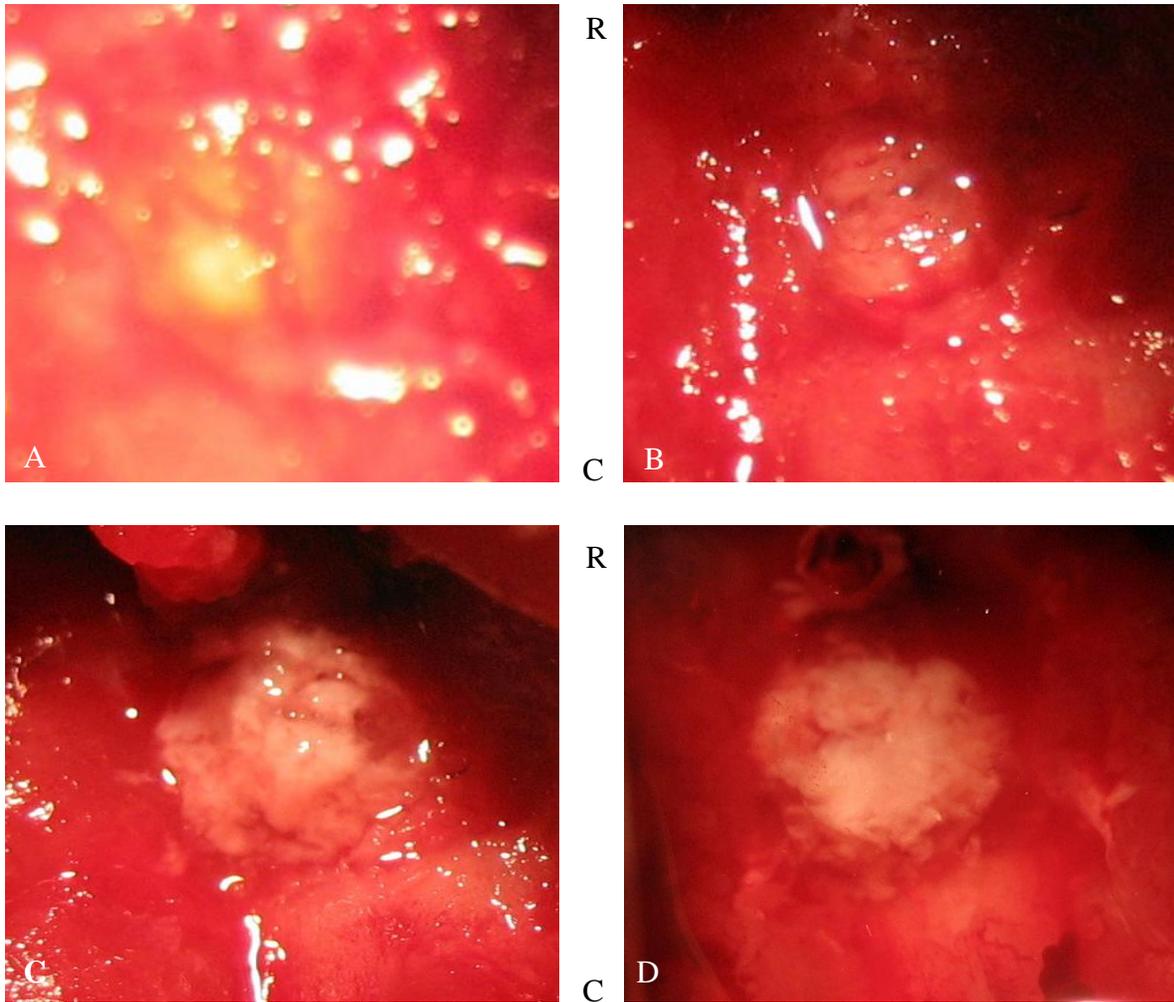
Figure 4.3. This figure demonstrates the topical delivery model applied into the spinal cord lesion site. A) Exposed intact spinal cord at T10 level after a single laminectomy. B) Dorsal over hemisection injury made with a single cut to the spinal cord column. C) Gel scaffold, embedded with chABC loaded microtubes, implanted on top of the lesion site. D) The implanted hydrogel-microtube delivery scaffold was covered with stiffer agarose gel to stabilize its location on top of the lesion site. (R = rostral, C = caudal)

Table 1. Experimental design of 2 week study with notation		
Notation of groups	**Components**	**# of rats**
MTC	Agarose gel scaffold embedded with microtubes loaded with chABC and trehalose	8
MT	Agarose gel scaffold embedded with microtubes loaded with trehalose	6
STC	Single injection of chABC with trehalose	8
SC	Single injection of chABC	6
MTP	Agarose gel scaffold embedded with microtubes loaded with penicillinase and trehalose	6
STP	Single injection of penicillinase with trehalose	6
NoT	Injury and no treatment	6
Sham	Conducted the same procedure except injury with other groups	4

M: lipid microtubes, S: single injection, T: trehalose, C: chABC and P: penicillinase

4.2.3 TISSUE PREPARATION AND IMMUNOHISTOCHEMISTRY OF SPINAL CORDS

At two weeks post-surgery, the animals were perfused transcardially with 1X PBS followed by 4% paraformaldehyde in 1X PBS. The T9-T11 spinal cord was removed, post-fixed in 4% paraformaldehyde and placed in 30% sucrose at 4 ºC until it sank to the bottom. Tissues were frozen in OCT and sagittal sections were cut with a cryostat (HM 560MV Cryostat) at 14 µm thickness. All sections were mounted in serial order onto charged microscope slides.

Sections were washed with 0.5% Triton X-100 PBS for 10 min and incubated with 4% of goat serum/0.5% Triton X-100 PBS (blocking solution) for 1 hour. The sections were incubated with primary antibodies diluted in blocking solution at 4 ℃ overnight. The following primary antibodies were applied: an antibody to the stub protein after chABC digestion (1:150, mouse IgM, clone 3-B-3; Seikagaku America) which recognizes unsaturated, C6-sulfated glycosaminoglycan stubs (Baker et al., 1991); chondroitin sulfate proteoglycan (1:250, mouse IgM, clone CS-56; Sigma) to identify CSPGs; glial fibrillary acidic protein (GFAP) (1:600, polyclonal rabbit IgG; Chemicon) for astrocytes; and Wisteria floribunda agglutinin (WFA) (5 µg/ml, biotin conjugate; Sigma) for perineuronal nets. After primary antibody incubation, sections were washed three times with 0.5% Triton X-100 PBS and incubated with the appropriate secondary antibodies conjugated to fluorophores for 1 hour at room temperature. The following secondary antibodies were used: goat anti-rabbit IgG(H+L) Alexa Fluor 488 (1:200 dilution in 0.5% Triton X-100 PBS; Invitrogen) for GFAP; goat anti-mouse IgM Alexa Fluor 594 (1:200) for 3B3 and CS-56; and streptavidin Alexa Flour 488 for WFA. Sections treated with secondary antibody but without primary antibody were used as staining controls. The sections were washed three times with 1X PBS and DAPI was applied to some of the sections for 15 min at room temperature to label the cell nuclei. The sections were washed twice with 1X PBS and then coverslipped using Fluoromount-G (Southern Biotechnology Associates, Inc.).

To examine the effectiveness and enzymatic functionality of chABC delivered by hydrogel-microtube delivery system and single injection treatments, triple staining was done with 3B3, GFAP and WFA, and adjacent sections were double stained with CS-56 and GFAP. GFAP labeling was used to delineate the border of the astroglial scar lining the lesion site

(Fig. 4.4A). Images were taken on the Zeiss Axioskop 2 Plus microscope (Zeiss, Thornwood, NY) with an Olympus Microfire digital camera.

4.2.4 QUANTITATIVE ANALYSIS OF CSPG DIGESTION AND ASTROCYTE RESPONSE

Quantification of CSPG digestion

To quantify the 3B3-immunoreactivity (IR) and CS-56-IR after chABC delivery around the lesion site, four or five micrographs were taken at 20x magnification along the lesion site as figure 4.4A. Relative to the lesion site, two caudal and two rostral images as well as one image underneath the lesion were used. At least four animals were chosen from each animal group and relative fluorescent intensity was measured using ImagePro software package (MediaCybernetics). The gross fluorescent intensity was measured for the region and a mean value was obtained and averaged for each animal. Background intensity was measured on each section and deducted from the measured 3B3-IR and CS-56-IR intensity.

Quantification of GFAP

To quantify the astrocyte responses, the spinal cord tissues were immunostained and imaged at 20x magnification along the lesion site with the same exposure time and conditions. The images were analyzed with a custom-built image analysis program (MATLAB; Mathworks) (Jain et al., 2006). This program generates line profiles radial to the defined interface and records the intensity of the fluorescent signal along the line profile, thus quantifying the relative value of intensity as a function of distance from the lesion interface (x=0) into the spinal cord (Fig. 4.4B). The number of line profiles (e.g. 30 lines), the color (one of RGB) to be read and the lesion interface can be selected by the user. With each run,

84

the relative intensity is averaged over all the line profiles. Four scans were performed for each staining image and the results were averaged again over all four scans. Four sections were chosen from each animal, four animals were chosen from each animal group and at least five images were captured. At least 80 images (five images X four spinal cord sections X four animals) were used and the relative intensity as a function of distance was averaged over 2400 (30 lines X 80 images) line profiles per experiment group. After this analysis, the relative intensity was compared between groups for different distances from the interface: 0-100, 100-300 and 300-500 µm.
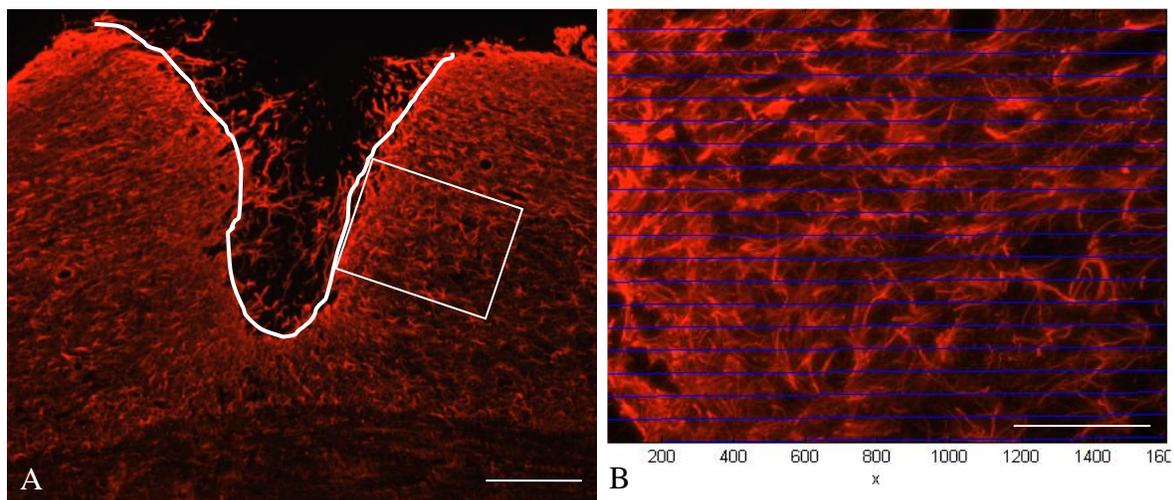
Figure 4.4. Micrographs of the GFAP immunostained tissue and method of image analysis with a custom developed MATLAB program. A) 4x immunostained image. The solid line represents the lesion boundary defined by GFAP immunoreactivity and the boxed areas denote regions selected for quantification. Scale bar is 500 µm. B) One of the boxes in figure A is expanded at 20x magnification to show analysis of fluorescent intensity using line profiles. The X axis represents distance from the lesion interface in pixel unit. The lines were generated from the lesion interface into the tissue, averaged and displayed as a function of distance from the interface to between experimental groups. Scale bar is 100 µm.

4.2.5 STATISTICAL ANALYSIS

Minitab software was used to determine the statistical differences existing between experimental conditions using analysis of variance (ANOVA). A p-value <0.05 was considered statistically different.

All animal protocols were approved by the Institutional Animal Care & Use Committee at Georgia Institute of Technology. Animal welfare, including pre-care, surgeries, pain management, post-care and monitoring was supervised by the Animal Research Committee of the Georgia Institute of Technology.

4.3 RESULTS

4.3.1 SUSTAINED DELIVERY OF ENCAPSULATED CHABC DIGESTS CSPGS EFFECTIVELY *IN VIVO*

The effectiveness and enzymatic activity of trehalose stabilized chABC when delivered *in vivo* after SIC using our lipid microtube-embedded hydrogel delivery system at the lesion site (Fig. 4.1) was examined by CS-56 and 3B3 immunostaining. The 3B3 antibody recognizes unsaturated, C6-sulfated glycosaminoglycan stubs (Baker et al., 1991) and therefore, can be used as a marker for CSPGs digested by chABC. The CS-56 antibody was used to identify intact CSPG deposition. GFAP immunoreactivity (GFAP-IR) was used to identify reactive astrocytes and in combination with either 3B3 or CS-56, to define the lesion boundary. Two weeks after hemisection SCI, tissue sections from the MTC (hydrogel-microtube delivery scaffold loaded with 1M trehalose/chABC; See Table 1 for notation of groups) treated animals showed significantly strong 3B3-IR near the lesion site (Fig. 4.5E)

while CS-56-IR in adjacent tissue sections was diminished (Fig. 4.5D). CS-56-IR was strong along the lesion interface in most of the tissue sections, however intensity of CS-56-IR was significantly reduced overall for the region near the lesion with sustained chABC delivery. In the no-treatment (NoT) group, the reverse IR was observed with strong CS-56 intensity and no 3B3-IR (Fig. 4.5A and B). Similar patterns were observed in the rest of the other control groups except the MTC group.

To determine if chABC delivery affected the integrity of PNNs in the vicinity of the lesion site, PNNs were labeled with Wisteria floribunda agglutinin (WFA) cytochemistry in the same tissue sections that were stained with 3B3. WFA is a lectin specific for N-aceylgalactosamine and results in visualizing net-like structures of PNNs. PNNs were observed near the lesion site in single injection-trehalose-chABC, no treatment (Fig. 4.5C) and other conditions except the MTC treated condition where significantly less WFA staining was observed (Fig. 4.5F). Immunostaining of WFA, 3B3, and CS-56 showed that WFA-PNNs were present in conditions when CS-56-IR intensity was strong and 3B3-IR was weak or absent around the lesion site. In the MTC treated group, the 3B3 positive region where CSPGs were degraded by chABC had no WFA-PNNs and low CS-56-IR.   Therefore sustained delivery of chABC resulted in significantly diminished PNNs close to the lesion interface implicating the potential for greater axonal sprouting.
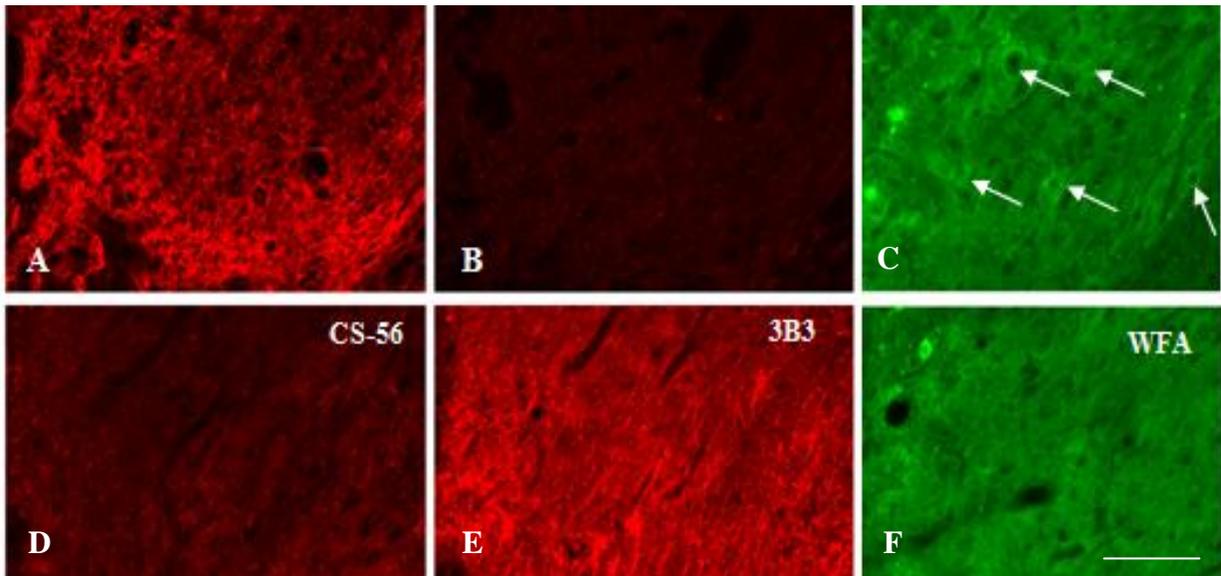
Figure 4.5. Immunohistological analysis of CSPG digestion *in vivo* (A-F). Images were taken right next to the lesion boundary of no treatment (A, B and C) and MTC treatment (hydrogel-microtube delivery scaffold loaded with chABC/ 1M trehalose; D, E, and F) animals. CS-56-IR for intact CSPGs (A and D). 3B3-IR for digested CSPGs (B and E). WFA staining for perineuronal nets (C and F). The intensity of CS-56-IR and WFA is inversely proportional to 3B3-IR. Arrows in (C) indicate WFA-PNNs. Scale bar is 100μm.

4.3.2   QUANTIFICATION OF 3B3, CS-56 AND GFAP IMMUNOSTAINING

Measurements of fluorescent pixel intensity were as used to quantify 3B3, CS-56 and GFAP immunostaining (Fig. 4.6) using an ImagePro software and a custom-built MATLAB routine. 3B3-IR is significantly higher in the MTC group as compared to all other groups (Fig.4.6A, $p < 0.05$). The average CS-56-IR is significantly lower in the MTC group than others and there is a statistical difference for CS-56-IR between MTC and no-treatment (NoT); MTC and STP (single injection-trehalose-P'ase) (Fig. 4.6B, $p < 0.05$).

GFAP-IR positive astrocytes were used to define the astro-glial scar region and the boundary of the lesion site (Fig. 4.4A). The fluorescent pixel intensity was quantified with a line profile image analysis program developed in MATLAB (Fig. 4.4B; Jain et al., 2006); the program measures intensity changes from the lesion interface into the spinal cord radially. The intensity of GFAP-IR decreased from the lesion site into the cord and the number of reactive astrocytes also decreased, and correlated positively with CS-56-IR intensity. Analyzed intensity was divided into three bins, 0-100, 100-300 and 300-500 μm away from the lesion interface. The GFAP-IR was lower in the MTC treated group than other groups, and there is a significant difference between the MTC treated group and other groups; NoT, STP and MT in 0-100 μm and 100-300 μm (Fig. 4.7, $p < 0.05$). This data confirm that our sustained delivery system using lipid microtubes embedded in agarose hydrogel does not negatively impact the astrogliotic response.
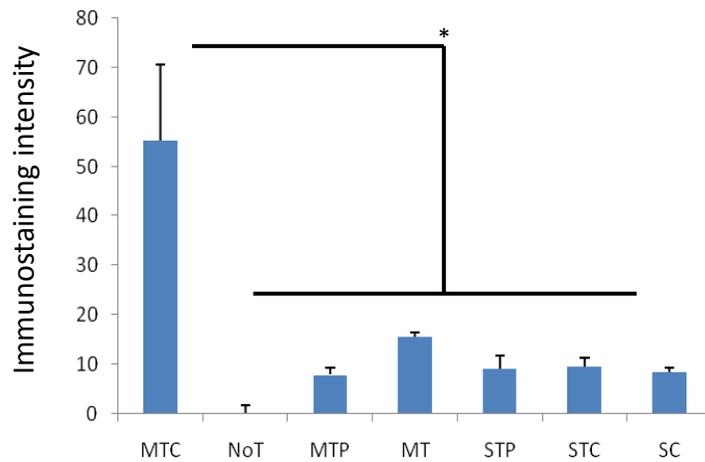
A   3B3
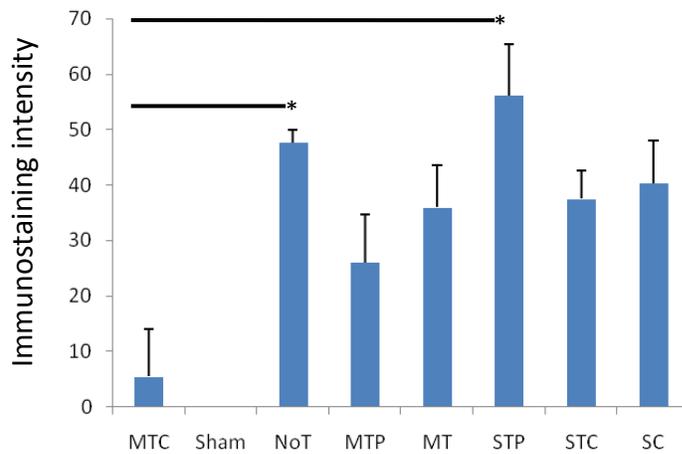
B   CS-56

Figure 4.6. Quantitative image analysis of 3B3-IR and CS-56-IR fluorescent intensity. The X axis represents each experimental condition treated for animal groups. The Y axis represents the relative fluorescent intensity of IR. The relative fluorescent intensity was measured alone the lesion boundary, and mean value was obtained and averaged for each animal. (A) 3B3-IR quantitative analysis. Asterisk denotes significant increase of 3B3-IR in MTC treatment compared to all other treatments (p<0.05). (B) CS-56-IR quantitative analysis. Asterisks denote significant decrease of CS-56-IR in MTC treatment when compared to NoT and STP treatments (p<0.05). No significant differences were observed among other treatments. The data represent the mean ± SEM.
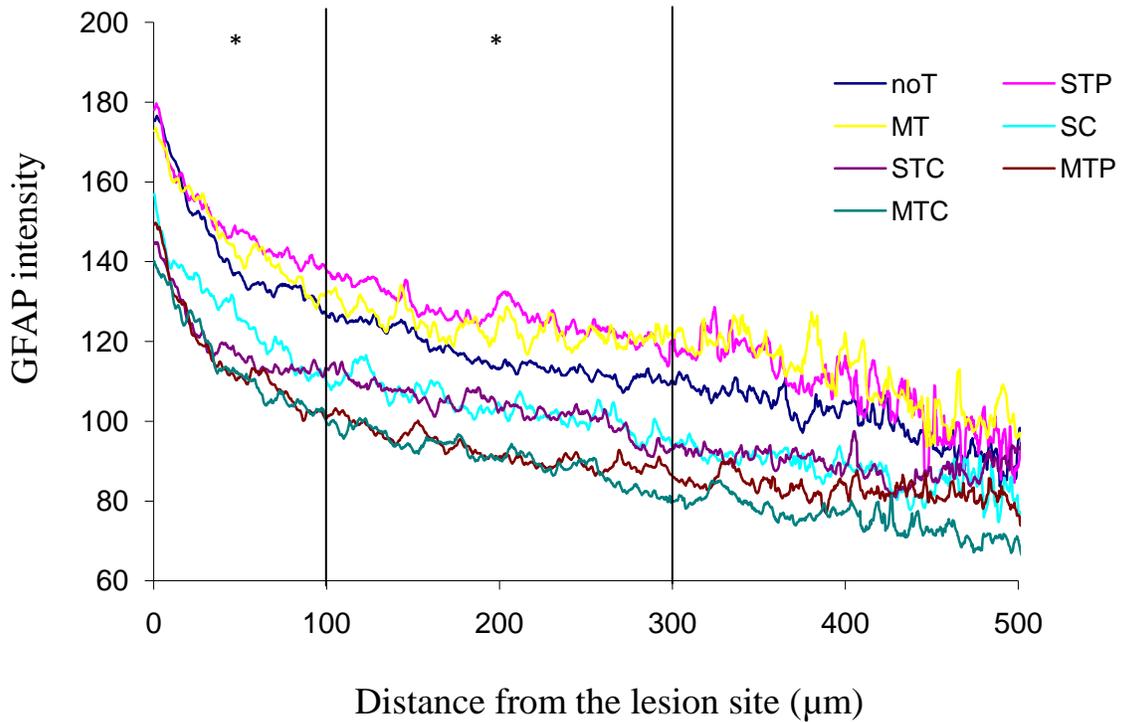
Figure 4.7. Quantitative image analysis of GFAP-IR fluorescent intensity by line profile. The X axis represents distance from the lesion interface into the spinal cord in µm and 0 represents the lesion interface delineate the border of the astroglial scar lining the lesion site. The Y axis represents the relative fluorescent intensity of GFAP-IR. Overall the intensity of GFAP-IR decreased from the lesion interface into the cord as a function of distance. The GFAP-IR was lower in the MTC treated group than other control groups. The IR intensity was analyzed by dividing into three bins, 0-100, 100-300 and 300-500. Asterisks denote a significant difference between the MTC treated group and other control groups; NoT, STP and MT in 0-100 µm and 100-300 µm (P <0.05). The data represent the mean.

4.4 DISCUSSION

The thermal instability of chABC represented a significant impediment to regeneration after SCI, as it limited drug delivery approaches and forced the use of infusion pumps or catheters for delivery. In this study, we demonstrate that the enzymatic activity of chABC could be maintained at 37 ºC by adding trehalose and that thermostabilized chABC delivered by a lipid microtube-hydrogel scaffold system remains enzymatically active for at least two weeks *in vivo*. This study therefore demonstrates that a single treatment with of the hydrogel-microtube system provides an effective and creative alternative to chronically implanted, invasive pumps/catheters that are typically used to deliver chABC *in vivo*.

Given that astro-glial scar deposition spans a period of 2 to 4 weeks post-injury, clinical application of chABC might require enzymatic activity over a period of weeks. Most studies to date have delivered chABC via multiple intrathecal injections to achieve prolonged action. The time required to reach peak deposition of CSPG at the lesion site is dependent on the type of CSPG (Jones et al., 2003). NG2 is the predominant CSPG expressed after SCI and reaches peak deposition between 1 and 2 weeks after injury, and the expression levels of neurocan, brevican, and versican are elevated after SCI, peak at 2 weeks and are maintained for 4 weeks or more. The production of several CSPGs and proteoglycan species is differently affected by degree and type of spinal cord injury. The main deposition pattern is that CSPG molecules are significantly elevated within 24 hours, slowly increase until they peak and then decrease, and overall CSPG-rich matrix persists up to 2 months. We chose a time point of 14 days after surgery to analyze the effectiveness of thermostabilized chABC and our delivery system because overall CSPG expression levels are highest at 14 ~ 18 days and decrease by 49 days (Iseda et al., 2008). Delivery of active agents during this period

92

would be expected to affect inflammation and cellular responses, modulate CSPGs deposition around lesion site, and promote axonal sprouting and outgrowth.

The sustained and local delivery of chABC was achieved over a 2 week time period using a previously characterized gel scaffold system in our laboratory. It has been demonstrated that agarose hydrogel-lipid microtube-based delivery acts as a sustained delivery system *in vitro* with various proteins and DNA (Meilander et al., 2001; Meilander et al., 2003). An *in situ* technique is used to quickly cool and set the liquid gel, and this gel cooling system (Fig. 4.2) allows the gel to mold into the shape of the injury site. A BDNF-loaded hydrogel-lipid microtube delivery scaffold was used to fill the lesion cavity on the dorsal column of the spinal cord (Jain et al., 2006), and methylprednisolone-loaded biodegradable PLGA nanoparticle-hydrogel was topically delivered to the contusion -injured spinal cord as described in figure 4.1 (Chvatal et al., 2008; Kim et al., 2009). This gel-microtube system also can be combined with a conduit to provide a bridge with neurotrophic factors for peripheral nerve regeneration (Dodla and Bellamkonda, 2008). The previous studies and this study demonstrate that our gel-microtube based delivery system does not aggravate inflammatory responses compared to control groups. By implanting the stabilized chABC sustained delivery scaffold on the top of the lesion site, we avoid a second surgery that could cause additional injury and stress to the animal. We also avoid a chronically inserted catheter/mini-pump that could induce inflammatory mass and increase infection risk (Penn, 2003; Peng and Massicotte, 2004).

In the MTC treated group, 3B3-IR is significantly higher compared to all other groups. As a control, to compare the effect of sustained delivery versus single administration, a dose of thermostabilized chABC (STC) equal to the total amount of chABC released from the

lipid-microtubes over 14 days was injected at the lesion site. This single injection had no effect as determined by a lack of 3B3 staining. This data indicates that indeed sustained release of chABC is critical either because chABC diffuses away and loses its enzymatic activity quickly after the single injection, or because CSPGs continue to be produced over time. In the MTC treated group, 3B3-IR is significantly higher compared to all other groups. It is interesting that in the STC group, small bright spots of 3B3-IR were observed around the lesion site (gray matter) possibly due to chABC digesting some CSPGs before being washed out. Once CSPGs are digested, the turn-over is relatively slow. PNNs were also degraded by the digestion of CSPGs following microtube-mediated release of chABC. In comparison, a single injection of chABC was not sufficient to break-down PNNs. In the MTC treated spinal cord, PNNs were not observed immediately around the lesion site, but PNNs were present approximately 1 mm away from the lesion site suggesting that thermostabilized chABC activity was localized to the region in the immediate vicinity of the lesion. Permissive environment

Another consequence of chABC treatment is the effects of the disaccharidic degradation products of CSPG generated by chABC digestion. The disaccharidic by-product protects neurons against inflammation-induced neurodegeneration by down-regulating T cell motility and decreasing cytokine secretion such as interferon-γ and tumor necrosis factor-α (Rolls et al., 2006). The by-product modulates intracellular signaling pathways such as PKCα and PYK2, and induces neuronal outgrowth and protects neurons against neuronal toxicity (Rolls et al., 2004). In this study, GFAP-IR quantification demonstrates that a) there is no elevation of inflammation response in gel scaffold treated groups, and b) GFAP-IR was significantly lower in the MTC treated group than others (NoT, STP and MT) near the lesion

area (Fig. 4.7). Therefore, it is possible that chABC treatment generated disaccharidic degradation products act as neuroprotective agents and trigger neuronal protective and survival signaling pathways.

4.5 CONCLUSIONS

In conclusion, this study clearly demonstrates that sustained local delivery of thermostabilized chABC digests CSPGs after SCI without aggravating the secondary injury response. Combinational therapy of chABC and neurotrophic factors via our delivery system could provide a synergic effect on axonal regrowth and functional recovery after SCI. This approach obviates the need for invasive, pump mediated delivery of chABC, elegantly enhances the thermostability and resultant efficacy of chABC *in vivo*, and overcomes an important technical hurdle for the *in vivo* application of chABC therapy after SCI.

4.6 REFERENCES

Baker JR, Christner JE, Ekborg SL (1991) An unsulphated region of the rat chondrosarcoma chondroitin sulphate chain and its binding to monoclonal antibody 3B3. Biochem J 273(Pt 1):237-239.

Barritt AW, Davies M, Marchand F, Hartley R, Grist J, Yip P, McMahon SB, Bradbury EJ (2006) Chondroitinase ABC promotes sprouting of intact and injured spinal systems after spinal cord injury. J Neurosci 26:10856-10867.

Bradbury EJ, Moon LD, Popat RJ, King VR, Bennett GS, Patel PN, Fawcett JW, McMahon SB (2002) Chondroitinase ABC promotes functional recovery after spinal cord injury. Nature 416:636-640.

Caggiano AO, Zimber MP, Ganguly A, Blight AR, Gruskin EA (2005) Chondroitinase ABCI improves locomotion and bladder function following contusion injury of the rat spinal cord. J Neurotrauma 22:226-239.

Chau CH, Shum DK, Li H, Pei J, Lui YY, Wirthlin L, Chan YS, Xu XM (2004) Chondroitinase ABC enhances axonal regrowth through Schwann cell-seeded guidance channels after spinal cord injury. FASEB J 18:194-196.

Chvatal SA, Kim YT, Bratt-Leal AM, Lee H, Bellamkonda RV (2008) Spatial distribution and acute anti-inflammatory effects of Methylprednisolone after sustained local delivery to the contused spinal cord. Biomaterials 29:1967-1975.

Dodla MC, Bellamkonda RV (2008) Differences between the effect of anisotropic and isotropic laminin and nerve growth factor presenting scaffolds on nerve regeneration across long peripheral nerve gaps. Biomaterials 29:33-46.

Houle JD, Tom VJ, Mayes D, Wagoner G, Phillips N, Silver J (2006) Combining an autologous peripheral nervous system "bridge" and matrix modification by chondroitinase allows robust, functional regeneration beyond a hemisection lesion of the adult rat spinal cord. J Neurosci 26:7405-7415.

Huang WC, Kuo WC, Cherng JH, Hsu SH, Chen PR, Huang SH, Huang MC, Liu JC, Cheng H (2006) Chondroitinase ABC promotes axonal re-growth and behavior recovery in spinal cord injury. Biochem Biophys Res Commun 349:963-968.

Iseda T, Okuda T, Kane-Goldsmith N, Mathew M, Ahmed S, Chang YW, Young W, Grumet M (2008) Single, high-dose intraspinal injection of chondroitinase reduces

glycosaminoglycans in injured spinal cord and promotes corticospinal axonal regrowth after hemisection but not contusion. J Neurotrauma 25:334-349.

Jain A, Kim YT, McKeon RJ, Bellamkonda RV (2006) In situ gelling hydrogels for conformal repair of spinal cord defects, and local delivery of BDNF after spinal cord injury. Biomaterials 27:497-504.

Jones LL, Margolis RU, Tuszynski MH (2003) The chondroitin sulfate proteoglycans neurocan, brevican, phosphacan, and versican are differentially regulated following spinal cord injury. Exp Neurol 182:399-411.

Jones LL, Yamaguchi Y, Stallcup WB, Tuszynski MH (2002) NG2 is a major chondroitin sulfate proteoglycan produced after spinal cord injury and is expressed by macrophages and oligodendrocyte progenitors. J Neurosci 22:2792-2803.

Kim YT, Caldwell JM, Bellamkonda RV (2009) Nanoparticle-mediated local delivery of Methylprednisolone after spinal cord injury. Biomaterials 30:2582-2590.

Lemons ML, Howland DR, Anderson DK (1999) Chondroitin sulfate proteoglycan immunoreactivity increases following spinal cord injury and transplantation. Exp Neurol 160:51-65.

McKeon RJ, Hoke A, Silver J (1995) Injury-induced proteoglycans inhibit the potential for laminin-mediated axon growth on astrocytic scars. Exp Neurol 136:32-43.

Meilander NJ, Yu X, Ziats NP, Bellamkonda RV (2001) Lipid-based microtubular drug delivery vehicles. J Control Release 71:141-152.

Meilander NJ, Pasumarthy MK, Kowalczyk TH, Cooper MJ, Bellamkonda RV (2003) Sustained release of plasmid DNA using lipid microtubules and agarose hydrogel. J Control Release 88:321-331.

Moon LD, Asher RA, Rhodes KE, Fawcett JW (2001) Regeneration of CNS axons back to their target following treatment of adult rat brain with chondroitinase ABC. Nat Neurosci 4:465-466.

Peng P, Massicotte EM (2004) Spinal cord compression from intrathecal catheter-tip inflammatory mass: case report and a review of etiology. Reg Anesth Pain Med 29:237-242.

Penn RD (2003) Intrathecal medication delivery. Neurosurg Clin N Am 14:381-387.

Rolls A, Cahalon L, Bakalash S, Avidan H, Lider O, Schwartz M (2006) A sulfated disaccharide derived from chondroitin sulfate proteoglycan protects against inflammation-associated neurodegeneration. FASEB J 20:547-549.

Rolls A, Avidan H, Cahalon L, Schori H, Bakalash S, Litvak V, Lev S, Lider O, Schwartz M (2004) A disaccharide derived from chondroitin sulphate proteoglycan promotes central nervous system repair in rats and mice. Eur J Neurosci 20:1973-1983.

Snow DM, Letourneau PC (1992) Neurite outgrowth on a step gradient of chondroitin sulfate proteoglycan (CS-PG). J Neurobiol 23:322-336.

Stichel CC, Kappler J, Junghans U, Koops A, Kresse H, Muller HW (1995) Differential expression of the small chondroitin/dermatan sulfate proteoglycans decorin and biglycan after injury of the adult rat brain. Brain Res 704:263-274.

Yick LW, Cheung PT, So KF, Wu W (2003) Axonal regeneration of Clarke's neurons beyond the spinal cord injury scar after treatment with chondroitinase ABC. Exp Neurol 182:160-168.

Yick LW, Wu W, So KF, Yip HK, Shum DK (2000) Chondroitinase ABC promotes axonal regeneration of Clarke's neurons after spinal cord injury. Neuroreport 11:1063-1067.

Zuo J, Neubauer D, Dyess K, Ferguson TA, Muir D (1998) Degradation of chondroitin sulfate proteoglycan enhances the neurite-promoting potential of spinal cord tissue. Exp Neurol 154:654-662.

CHAPTER 5

DELIVERY OF THERMOSTABILIZED CHABC AND NT-3 AND EVALUATION OF AXONAL REGENERATION AND FUNCTIONAL RECOVERY AFTER SPINAL CORD INJURY: LONG TERM STUDY

(Partially as published with R.J. McKeon and R.V. Bellamkonda, Proceedings of the National Academy of Science, 2009)

CSPGs are one major class of axon growth inhibitors which are upregulated after SCI and contribute to regenerative failure. Chondroitinase ABC (chABC) digests CS-GAG chains on CSPGs and can thereby overcome CSPG mediated inhibition and promote axonal regeneration when delivered at the site of injury. However, chABC loses its enzymatic activity rapidly at 37 ºC, necessitating the use of repeated injections or local infusions with a mini-pump or catheter for days to weeks. Maintaining these infusion systems is invasive, infection-prone and clinically problematic. To overcome this limitation, we thermostabilized chABC and developed a system for its sustained local delivery *in vivo*, obviating the need for chronically implanted catheters and pumps in chapter 3. When stabilized with trehalose, chABC remained active at 37 ºC *in vitro* for up to 4 weeks. A lipid microtube-agarose hydrogel system was used for controlled release of chABC over 2 weeks at the lesion site following a SCI in chapter 4. The enzymatic functionality of released chABC and the cellular and molecular responses were examined by immunostaining with 3B3, CS-56, GFAP and WFA two weeks after injury. The results demonstrate significant differences in CSPG

digestion between groups treated with the chABC-loaded hydrogel microtube delivery system and controls.

In this chapter, a long term study (45 days) was conducted to examine axonal regeneration and functional recovery after chABC treatment and combination treatment with a neurotrophic factor, NT-3. The resultant impact of the initial CSPG digestion during the first two weeks was still present at 6 weeks following SCI when delivered by a hydrogel-microtube delivery system. Axonal growth and functional recovery following the sustained local release of thermostabilized chABC versus a single treatment of unstabilized chABC demonstrated significant differences in CSPG digestion. Additionally, animals treated with stabilized chABC in combination with sustained NT-3 delivery showed significant improvement in locomotor function, enhanced growth of CTB-positive sensory axons, and sprouting of 5-HT serotonergic fibers at the lesion site. We suggest that this significant improvement of chABC thermostability facilitates development of a minimally invasive method for sustained, local delivery of chABC that is potentially effective in overcoming CSPG-mediated regenerative failure. Combination therapy of thermostabilized chABC and neurotrophic factors enhances axonal regrowth, sprouting and functional recovery after SCI.

5.1 INTRODUCTION

After injury to the central nervous system, the lesioned axons fail to re-grow or make functional connections (Schwab and Bartholdi, 1996). While the cellular and molecular mechanisms of axon growth failure are active areas of research, a breakthrough clinical therapy has yet to be developed. Injuries to the CNS induce a series of inflammatory events around the lesion site, typically resulting in permanent functional loss.

There are many factors contributing to the failure of spontaneous regeneration; a lack of sufficient neurotrophic support (Widenfalk et al., 2001), a lack of intrinsic regeneration capacity in CNS as compared to PNS microenvironment (Neumann and Woolf, 1999), inhibitory molecules such as myelin-associated proteins (Filbin, 2003; Schwab, 2004; Schwab et al., 2006) and glial scar-associated CSPGs (McKeon et al., 1995; Silver and Miller, 2004), which are upregulated after injuries to the CNS and contribute to regenerative failure. Strategies can be developed for each inhibitory factor to overcome the lack of repair capacity after spinal cord injury. In chapter 3 and 4, we focused on developing a chABC treatment to attenuate CSPG-mediated failure of axonal regeneration and provide permissive substrates prepared by chABC digestion for axonal outgrowth.

In this chapter a combination strategy was developed to provide a neurotrophic factor for chemo-attracting axons to the lesion site. Combination therapies with chABC have been previously investigated. Schwann cell-seeded guidance channels were implanted into hemisected adult rats after chABC treatment (Chau et al., 2004) and an autologous peripheral nervous system bridge with cellular matrix modified by chABC was grafted onto a hemisection lesion (Houle et al., 2006). Synergistic effects were observed on axonal sprouting into the dorsal column nuclei after combination treatment with chABC and NT-3 (Massey et al., 2008). Retinal fiber sprouting with combination treatment with chABC and BDNF after denervation of the superior colliculus has been also observed (Tropea et al., 2003). To encourage axonal outgrowth, we chose to use NT-3 with chABC. Removal of an unfavorable environment (CSPG) by chABC and presentation of the supporting neurotrophic factor NT-3 was expected to be a promising combination for SCI.

A longer 45 day study was designed to examine the functional consequences of CSPG digestion by chABC and a combination therapy with the neurotrophic factor NT-3 via implantation of a hydrogel-lipid microtube delivery system at the lesion site. We demonstrated that the enzymatic activity of chABC can be thermostabilized at 37 ºC due to the ability of trehalose to confer conformational stability, and that thermostabilized chABC delivered by a lipid microtube-hydrogel scaffold system is enzymatically active in situ for at least 2 weeks as described in Chapters 3 and 4. Here, a combination treatment of thermostabilized chABC and NT-3 was used to overcome the CSPG-rich astroglial barrier to axonal regeneration and encourage axonal outgrowth. Locomotor behavioral improvements with combination delivery of chABC and NT3 were observed, and correlated well to immunohistological evidence of axonal sprouting at the lesion site. Analysis of 5-HT sensory fibers and CTB-labeled fibers demonstrated that chABC treatment can induce plasticity of injured projections within the spinal cord and offers a possible mechanism of chABC-induced functional recovery. This study therefore demonstrated that a single administration of the hydrogel-microtube delivery system provides an effective alternative to chronically implanted, invasive catheters or mini-pumps typically used to deliver chABC after SCI. The combination therapy of chABC and NT-3 with our delivery method offers a potent approach for clinical application after SCI.

5.2   MATERIALS AND METHODS

5.2.1   TOPICAL DELIVERY OF HYDROGEL-MICROTUBE SCAFFOLDS IN A

DORSAL OVER HEMISECTION MODEL

Table 5.1 describes conditions and notations of experimental and control groups in the 45 day *in vivo* study. In the long term study, MTC (hydrogel-microtube delivery scaffold loaded with 1M trehalose/chABC; n=7), MTP (hydrogel-microtube delivery scaffold loaded with 1M trehalose/P'ase; n=6) and sham (n=4) treatment conditions were used, the other conditions used in the short term study were excluded, and three new treatments were added. In the short term study, a single injection of chABC did not show effective digestion of CSPGs, and there was no significant difference from no treatment animals in the 2 week study (in chapter 4, section 4.3.2). Therefore, single injection controls (SC − single injection of chABC, STC − single injection of 1M trehalose/chABC, STP − single injection of 1M trehalose/P'ase) were excluded.

MTN (hydrogel-microtube-1M trehalose/NT-3), MTCN (hydrogel-microtube-1M trehalose/chABC and 1M trehalose/NT-3) and GC (hydrogel mixed with an equal amount of 1M trehalose/chABC to the MTC treatment condition) treatment conditions were added for the long term study. As a control to probe the sustained release enabled by lipid microtubes embedded in the hydrogel, 1 % of SeaPrep agarose gel mixed with 10 mU of chABC/1M trehalose was implanted on the top of the lesion site (n=6; GC); the other conditions included lipid microtubes loaded with NT-3 (n=7; MTN; 100 ng per rat) or combination microtubes loaded with chABC and NT-3 (n=8; MTCN) to investigate effect of combination treatment of chABC and neurotrophic factor.

103

The surgical procedure followed to induce injury and the delivery methods of hydrogel-microtubes delivery scaffold were the same as for the 2-week short term study described in the chapter 4, section 4.2.2. Briefly, adult male Sprague-Dawley rats (Charles River) received a dorsal over-hemisection injury at the T-10 vertebral level. Sustained topical delivery was achieved using methods previously reported (Chvatal et al., 2008) and shown in the figure 4.1 and figure 4.3.

5.2.2   RETROGRADE NEUROAL TRACER INJECTION INTO THE SCIATIC NERVE

Six weeks post-injury and 3 days before sacrificing, cholera toxin B subunit (CTB; sigma) was injected into the right sciatic nerve for retrograde axonal tracing. Rats were anesthetized using isoflurane gas. The thigh region on the right leg was shaved, and 2 cm of incision was made through the skin and muscles to expose the sciatic nerve. 5 µl of 1% CTB was slowly injected into the nerve with a 34 gauge needle (NanoFil). The muscles were sutured and the skin closed using wound clips. 3 days after injecting the CTB, the animals were the animals were anesthetized with a ketamine-xylazine-acepromazine cocktail (1:0.17:0.37 ml/kg) and perfused transcardially with PBS followed by a mixture of 4% paraformaldehyde in PBS to facilitate fixation.

Table 2. Experimental design of 45 days study with notation		
Notation of groups	**Components**	**# of rats**
MTC	Agarose gel scaffold embedded with microtubes loaded with chABC/trehalose	7
MTN	Agarose gel scaffold embedded with microtubes loaded with NT-3	7
MTCN	Agarose gel scaffold embedded with microtubes loaded with chABC/trehalose and NT-3	8
GC	Agarose gel mixed with chABC/trehalose	6
MTP	Agarose gel scaffold embedded with microtubes loaded with penicillinase/trehalose	6
Sham	Conducted the same procedure except injury with other groups	4

M: lipid microtubes, S: single injection, T: trehalose, C: chABC and P: penicillinase

5.2.3 BEHAVIORAL ANALYSIS

Locomotion and thermal pain sensitivity were assessed to determine functional improvement in the 45 day long term study. The investigators were blinded with regard to animal groups throughout these tests. CatWalk (Noldus), a video-based analysis system, was used to assess locomotor deficits in voluntarily walking. Each rat voluntarily walked across the walkway three times every week after injury. After acquiring raw data, paw prints were labeled as right forepaw (RF), left forepaw (LF), right hindpaw (RH) and left hindpaw (LH) and measurements of locomotion were provided by the software. Stride length, paw print pattern and base support were chosen to examine behavior as a function of time after injury

for all experimental conditions. Stride length was defined as a distance between consecutive steps with the same limb. The distance in mm between the two hind paws was defined as the base of support and this distance is measured perpendicular to the direction of walking. The white boxes in figure 5.1 show abnormal hindpaw print patterns and the number of abnormal prints was counted for three step cycles.
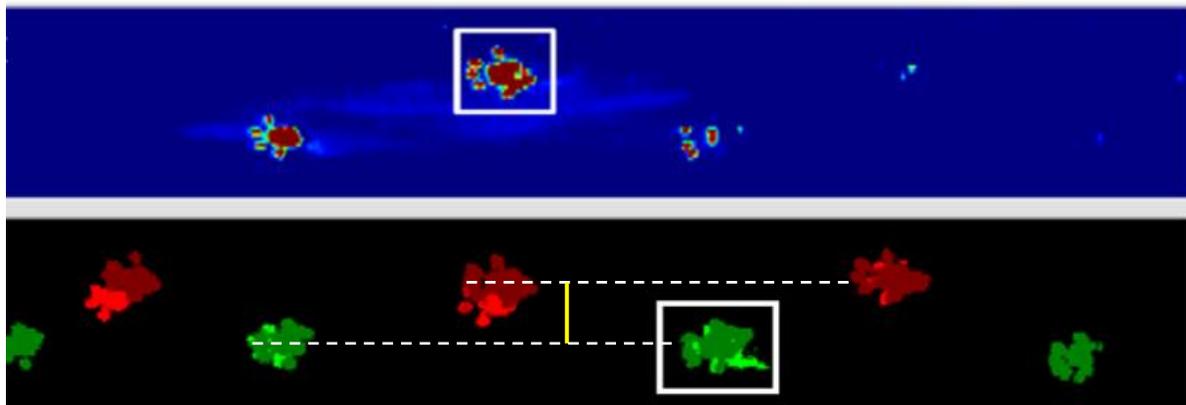
Figure 5.1. CatWalk raw data in false color mode. White boxes represent abnormal hindpaw print patterns. The dotted lines represent the stride length defined as a distance between consecutive steps with the same limb and the solid line represents the base of support defined as a distance between the two hind paws. (dark red – left hindpaw, light red – left forepaw, dark green – right hindpaw and light green – right forepaw)

Thermal sensitivity assessment by a dynamic plantar test (Ugo Basile) was used, identical to the method of Hargreaves et al (1988). The device measured the time taken to elicit a flexion reflex. Each hind-paw was tested three times every week and averaged. The animals were placed on a glass floor under which a mobile radiant infra-red heat source was positioned at the animal's hind paw. When the animal withdrew its paw, the source power turned off, triggered by an automatic sensor.

5.2.4   TISSUE PREPARATION AND IMMUNOHISTOCHEMISTRY

At 45 days post-surgery, the animals were perfused transcardially with PBS followed by 4% paraformaldehyde in PBS. The T9-T11 spinal cord was retrieved, post-fixed in 4% paraformaldehyde and placed in 30% sucrose at 4 ºC. Tissues were frozen and sagittal sections were cut with a cryostat (HM 560MV Cryostat) at 14 µm thickness. All sections were mounted in serial order onto charged microscope slides.

Sections were washed with 0.5% Triton X-100 PBS for 10 min and incubated with 4% of goat serum/0.5% Triton X-100 PBS (blocking solution) for 1 hour. The sections were incubated with primary antibodies diluted in the blocking solution at 4 ºC overnight. The following primary antibodies were applied against: CS-56 (1:250, mouse IgM; Sigma) to identify CSPGs; glial fibrillary acidic protein (GFAP) (1:600, polyclonal rabbit IgG; Chemicon) for astrocytes; anti-CTB (1:600; abcam); and serotonin (1:150, 5-HT, monoclonal mouse IgG1; Abcam) for serotonergic neurons. After primary antibody incubation, sections were washed three times with 0.5% Triton X-100 PBS and incubated with the appropriate secondary antibodies conjugated to fluorophores for 1 hour at room temperature. The following secondary antibodies were used: goat anti-rabbit IgG(H+L) Alexa Fluor 594 (1:200 dilution in 0.5% Triton X-100 PBS; Invitrogen) for GFAP; goat anti-mouse IgM Alexa Fluor 488 (1:200) for anti-CTB, 5-HT serotonin and CS-56. Sections treated with secondary antibody but without primary antibody were used as staining controls. The sections were washed three times with PBS and coverslipped using Fluoromount-G.

To evaluate the axonal sprouting, double staining was conducted with CTB and GFAP or 5-HT and GFAP. Double staining of 3B3 and GFAP was also conducted to examine the level of CSPGs. GFAP labeling was used to define the border of the astroglial

scar lining the lesion site (Fig. 4.4A). Images were taken on the Zeiss Axioskop 2 Plus microscope with an Olympus Microfire digital camera.

5.2.5   QUANTITATIVE ANALYSIS OF AXONAL SPROUTING

A montage of each tissue section stained for CTB labeled fibers was obtained at 10x magnification using Neurolucida software (MicroBrightField Bioscience). The 0 indicates the caudal lesion interface and defined by GFAP immunoreactivity (IR). The relative intensity of CTB labeled fibers were measured using ImagePro software (MediaCybernetics) at 1 and 0.5 mm caudal to the start of lesion, at the start of the lesion, and 0.5 and 1 mm rostral to the lesion. The intensity of CTB labeled fibers 1 mm caudal to the caudal edge of the lesion was assumed to represent the total CTB fibers approaching the lesion site and the percentage of CTB fibers stopped within the defined regions was determined by measuring the relative intensity. Background intensity was measured on each section and deducted from the measured CTB intensity.

To quantify 5-HT serotonin immunofluorescence, micrographs were taken at 20x magnification from two defined regions, ventral gray matter caudal and rostral to the lesion site, and relative fluorescent intensity was measured by ImagePro software package. The gross fluorescent intensity was measured for the region and mean value was obtained. Background intensity was measured on each section and deducted from the measured 5-HT IR intensity.

5.2.6 STATISTICAL ANALYSIS

Minitab software was used to determine the statistical differences existing between experimental conditions using analysis of variance (ANOVA). A p-value <0.05 was considered as statistically different.

All animal protocols were approved by the Institutional Animal Care & Use Committee at Georgia Institute of Technology. Animal welfare, including pre-care, surgeries, pain management, post-care and monitoring was supervised by the Animal Research Committee of the Georgia Institute of Technology.

5.3 RESULTS

5.3.1 LEVELS OF CSPG DEPOSITION AFTER SUSTAINED DELIVERY OF CHABC AT 6 WEEKS

To examine whether the resultant impact of the initial 2 weeks of CSPG digestion persists *in vivo* after 6 weeks, CS-56 immunostaining for intact CSPGs was conducted. Tissue sections from the MTCN treated animals showed that significantly less CS-56 expression compared to MTP treated controls (Fig. 5.2).
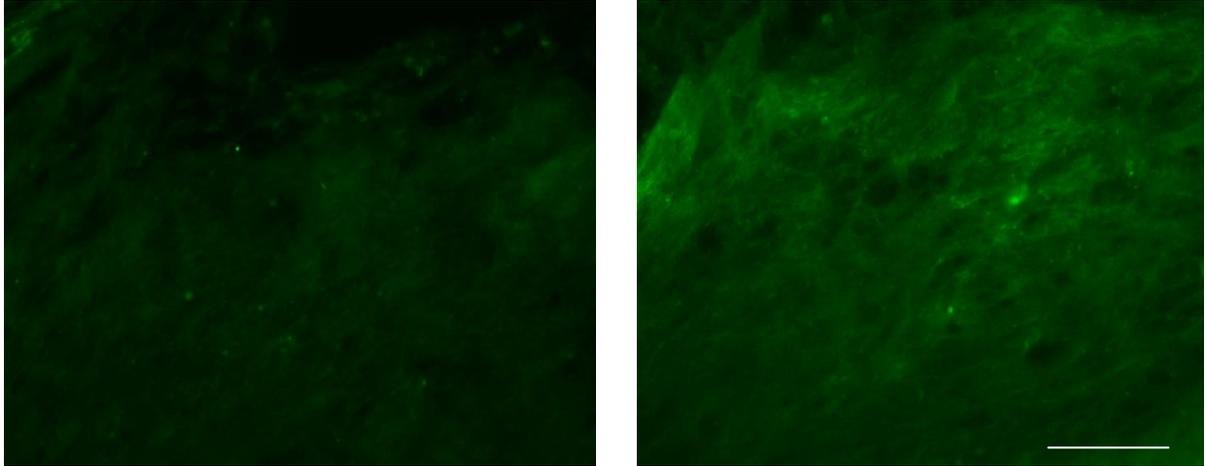
Figure 5.2. Micrograph of CS-56-IR around the lesion site at 6 weeks. (A) MTCN and (B) MTP. CSPG-IR is significantly less in the MTCN treated animals compared to MTP treated controls. Scale bar is 100 μm.

5.3.2   SUSTAINED DELIVERY OF CHABC AND NT-3 IMPROVES LOCOMOTOR FUNCTION

Functional recovery was assessed by using the CatWalk^{TM} and thermal plantar tests throughout the 45 day period. A significant difference in locomotor function was observed six weeks post-injury, but not earlier, and no improvement was observed with the thermal pain threshold test in any animal groups throughout the six week testing period. All the animal groups showed improved locomotor function throughout the testing period. At day 7 and day 14, all animals showed abnormal walking patterns, slow crossing, and abnormal paw prints, reflecting the SCI-mediated dysfunction. Four weeks post surgery, most animals showed a normal step sequence and the time necessary to cross the walkway decreased. A number of abnormal hind paw prints also decreased and stride length increased due to recovery from injury. However the differences between animals were not observed by 4 weeks.

Figure 5.3 showed CatWalk raw data of sham (A), MTCN (B) and MTP (C) treated animals on the walkway in false color mode at 6 weeks. Dark red represents left hindpaw; light red – left forepaw, dark green – right hindpaw and light green – right forepaw. As seen on figure 5.3, hindpaws step on the print of the consecutively previous forepaw. Animals with higher degree injuries generally fail to walk with a normal step sequence and step on the consecutively previous forepaw print. In this study, we used a relatively moderate injury (dorsal over hemisection), therefore, most animals showed normal step patterns. Six weeks post-SCI surgery, there were significant differences in the stride length between treatment conditions (Fig. 5.4). Average stride lengths (mean ± SEM) were 183.6 ± 6.91 mm for MTCN, 172.89 ± 20.8 mm for MTC, 157 ± 18.25 mm for MTN, 152.91 ± 13.13 mm for GC and 154.07 ± 10.11 mm for MTP at 6 weeks (See Table 2 for notation of groups). Significant differences were observed between MTCN and GC (p = 0.019), and MTCN and MTP (p = 0.035).

At 6 weeks, the MTCN, MTC and MTN treated animals had more normal foot prints (Fig. 5.3B) compared to MTP treated animals (white boxes in Fig. 5.3C). The sham animal had normal foot print and the MTP animal had abnormal hindpaw prints (white box in Fig. 5.3C.). The number of abnormal hindpaw prints was counted per three step cycles and the averages were 0.7 ± 0.3 for MTCN, 1.7 ± 0.6 for MTC, 1.8 ± 0.5 for MTN, 2.1 ± 1.3 for GC and 3.3 ± 1.3 for MTP. The mean number of abnormal print of the single treated animals, MTC and MTN, is less than that of animals treated by GC and MTP and the combination treatment MTCN group, on average had even fewer abnormal foot prints. However while these were strong trends, the differences were not significant between animal groups.

The distance in mm between the two hind paws was defined as the base of support and this distance is measured perpendicular to the direction of walking. Animals tend to show a larger base of support after SCI. At 6 weeks, the averages were 31.4 ± 4.8 mm for MTCN, 30.7 ± 4.4 mm for MTN, 39.8 ± 8.9 mm for GC and 38.5 ± 4.5 mm for MTP, and there was no statistical difference between animal groups.
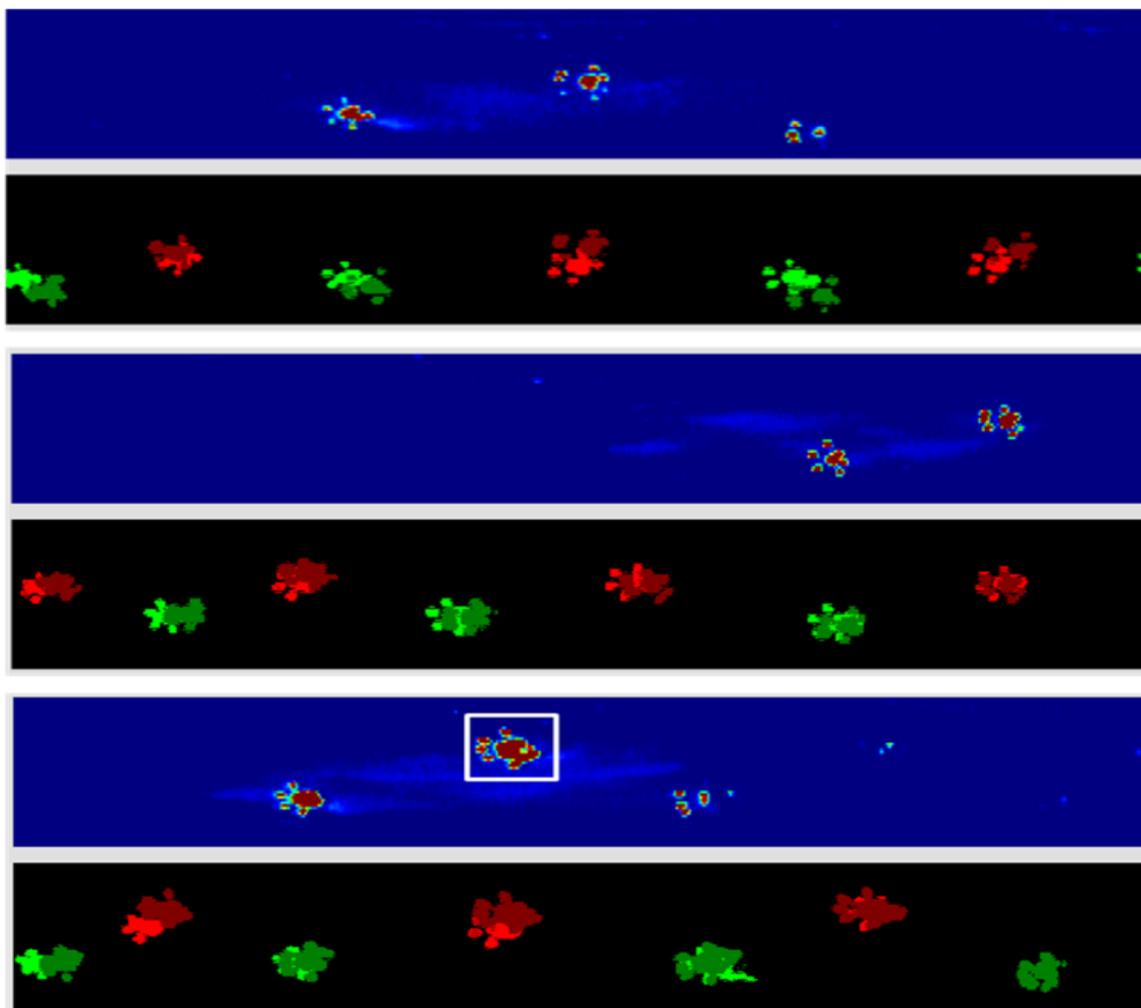
Figure 5.3. CatWalk raw data in false color mode, (A) Sham, (B) MTCN and (C) MTP treated animals on the walkway at 6 weeks. All animal groups show a normal step sequence. The white box in the figure C represents an abnormal hindpaw print. Red represents left paw prints and green represents right paw prints (dark red – left hindpaw, light red – left forepaw, dark green – right hindpaw and light green – right forepaw).
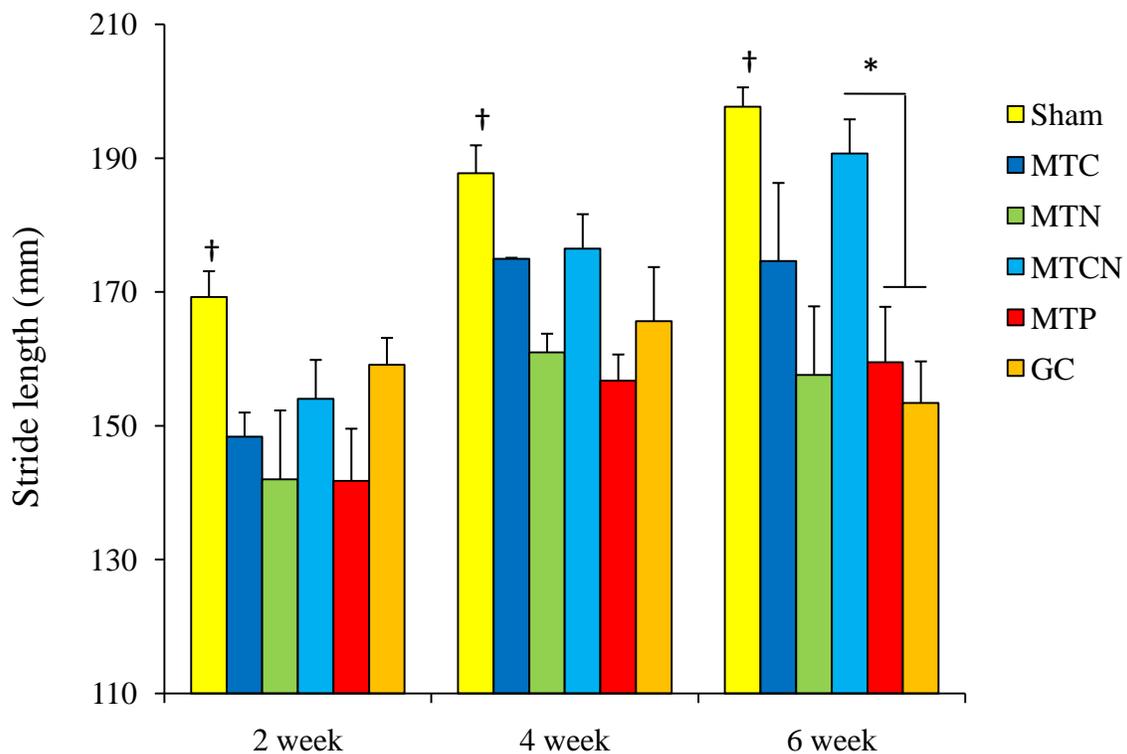
Figure 5.4. Stride length analysis for locomotion functional recovery. Data are mean ± SEM and asterisk denotes statistical significance between MTCN and MTP, and between MTCN and GC (P <0.05). Sham showed significant differences († < 0.05) compared to all other conditions throughout the testing period, except for MTCN at 4 and 6 weeks.

5.3.3   SUSTAINED DELIVERY OF CHABC AND NT-3 PROMOTES SPROUTING

5.3.3.1 AXONAL   SPROUTING   AROUND   THE   LESION   AREA: CTB-LABELED
        FIBERS

To examine anatomical regeneration in the dorsal column, CTB was injected into the sciatic nerve and resulted in labeling of the primary apparent within the spinal cord. The location of labeled fibers was examined; the MTP and GC treated animals had retracted CTB-labeled fibers in the glial scar area and few fibers approached the lesion site (Fig. 5.5A). However in the MTC, MTN and MTCN treated animals, more CTB-labeled fibers crossed the glial scar area and approached the lesion boundary (Fig. 5.5B). CTB-labeled fibers grew around cavities along the lesion interface (Fig. 5.5C and D; 0 to 0.5 mm interval in C and 0.5 to 1 mm interval in D) and a few fibers were observed after 0.5 mm rostral to caudal edge of the lesion in chABC and NT-3 treated animals. However no fibers entered the lesion cavity in any animal groups. Significantly more fibers crossed 0 and 0.5 mm rostral to the caudal edge of the lesion in the MTCN (p=0.03 and p=0.045; p=0.049 and p=0.045, respectively) animals compared to GC and MTP treated animals (Fig. 5.6). At one mm rostral to the caudal edge of the lesion start, a few fibers were observed in the MTC, MTN and MTCN treated animals, however most were not strong enough to be detected by the relative intensity measuring method described in section 5.2.5.
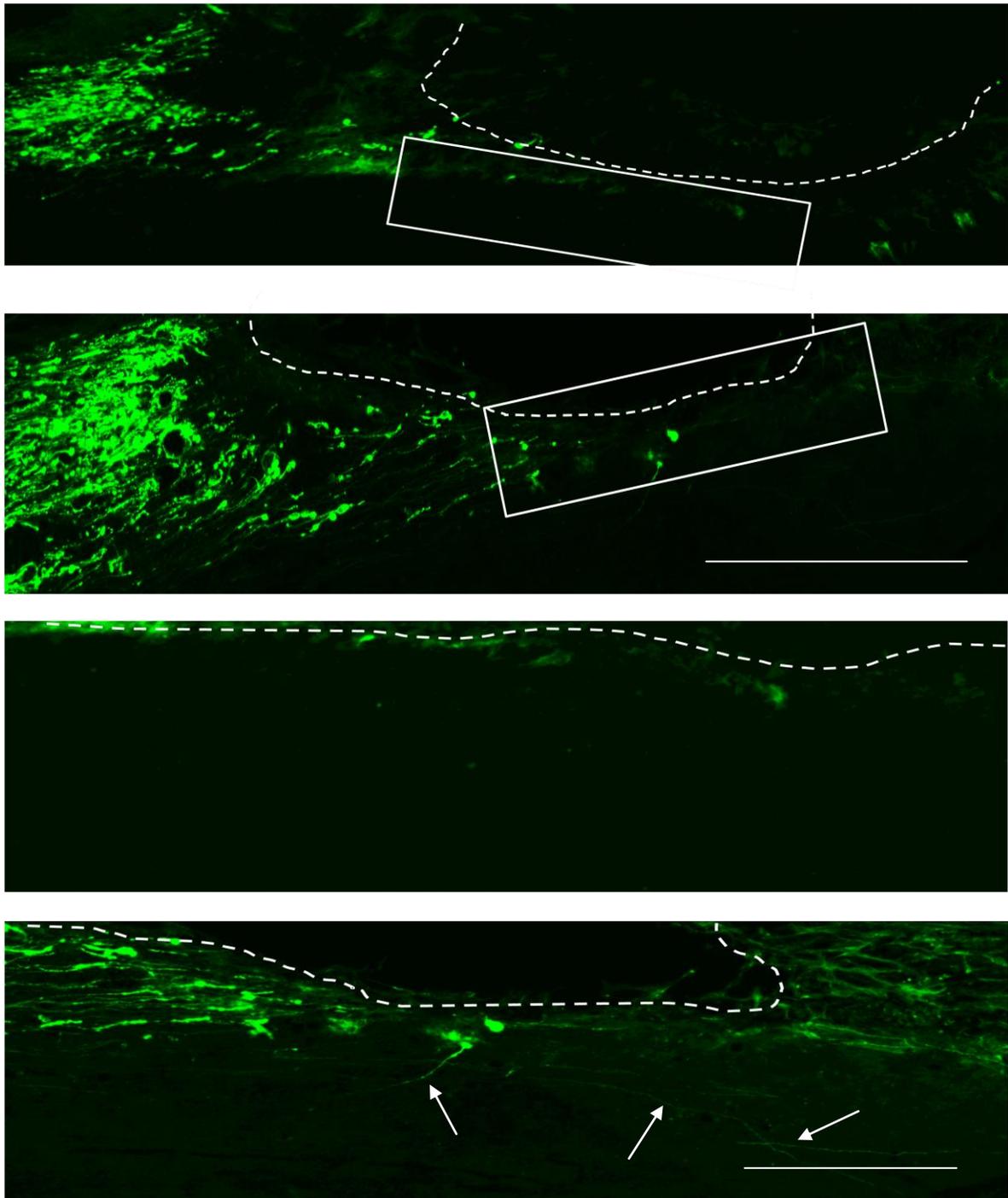
Figure 5.5. Micrographs of CTB labeled fibers (green) at the lesion site at 6 weeks. The dashed lines represent the lesion interface. (A) MTP and (B) MTCN at 10 x magnification. Scale bar is 500 μm (C) An expanded figure from the white box 0 to 0.5 mm interval in figure A, and (D) an expanded figure from the white box in 0.5 to 1 mm interval figure B at 20 x magnification. Arrows represent CTB labeled fibers. Scale bar is 100 μm.
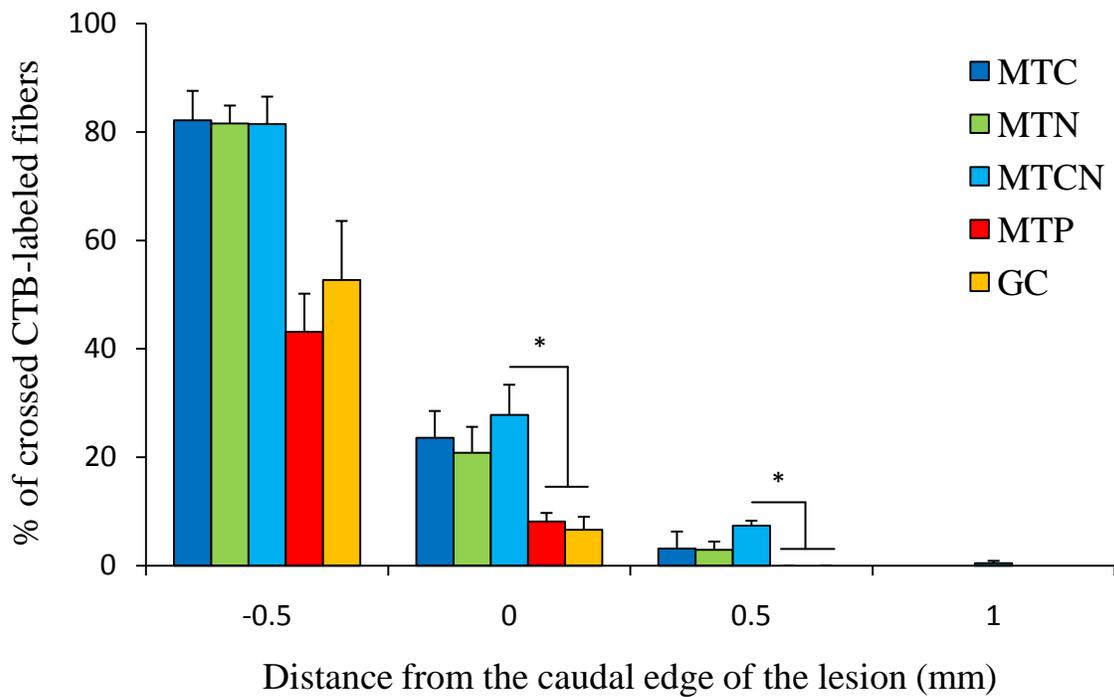
Figure 5.6. Quantification of CTB+ axon growth. The Y axis represents the percentage of crossed axons at the distance to the lesion interface and the X axis represents distance to the lesion (mm). The data represent the mean ± SEM. Asterisks denote a significant difference compared with MTCN ($P<0.05$).

5.3.3.2 AXONAL SPROUTING AROUND THE LESION AREA: 5-HT-IMMUNOREACTIVE FIBERS

5-HR-IR fibers in the ventral gray matter were measured to quantify the percentage of the lesion site. More 5-HT-IR fibers were observed in the gray matter of MTC, MTN and MTCN treated animals. The serotonergic fibers were observed in the gray mater, primarily in the ventral horn and lamina X, and more fibers were located rostral versus caudal to the lesion (Fig. 5.7A). The spinal cords tissues treated with chABC, NT-3 and combination of chABC and NT-3 had higher fluorescent intensity and the 5-HT-IR fibers extended closer to the lesion site than MTP and GC treated controls. Quantification confirmed that MTCN treatment showed significant sprouting of serotonergic fibers caudal to the lesion versus all other conditions ($p = 0.008$ for MTC, $p = 0.024$ for MTN, $p = 0.001$ for GC and $p = 0.001$ for MTP); and rostral to the lesion than MTN ($p = 0.015$), GC ($p = 0.002$) and MTP ($p = 0.001$) treatment (Fig. 5.8).
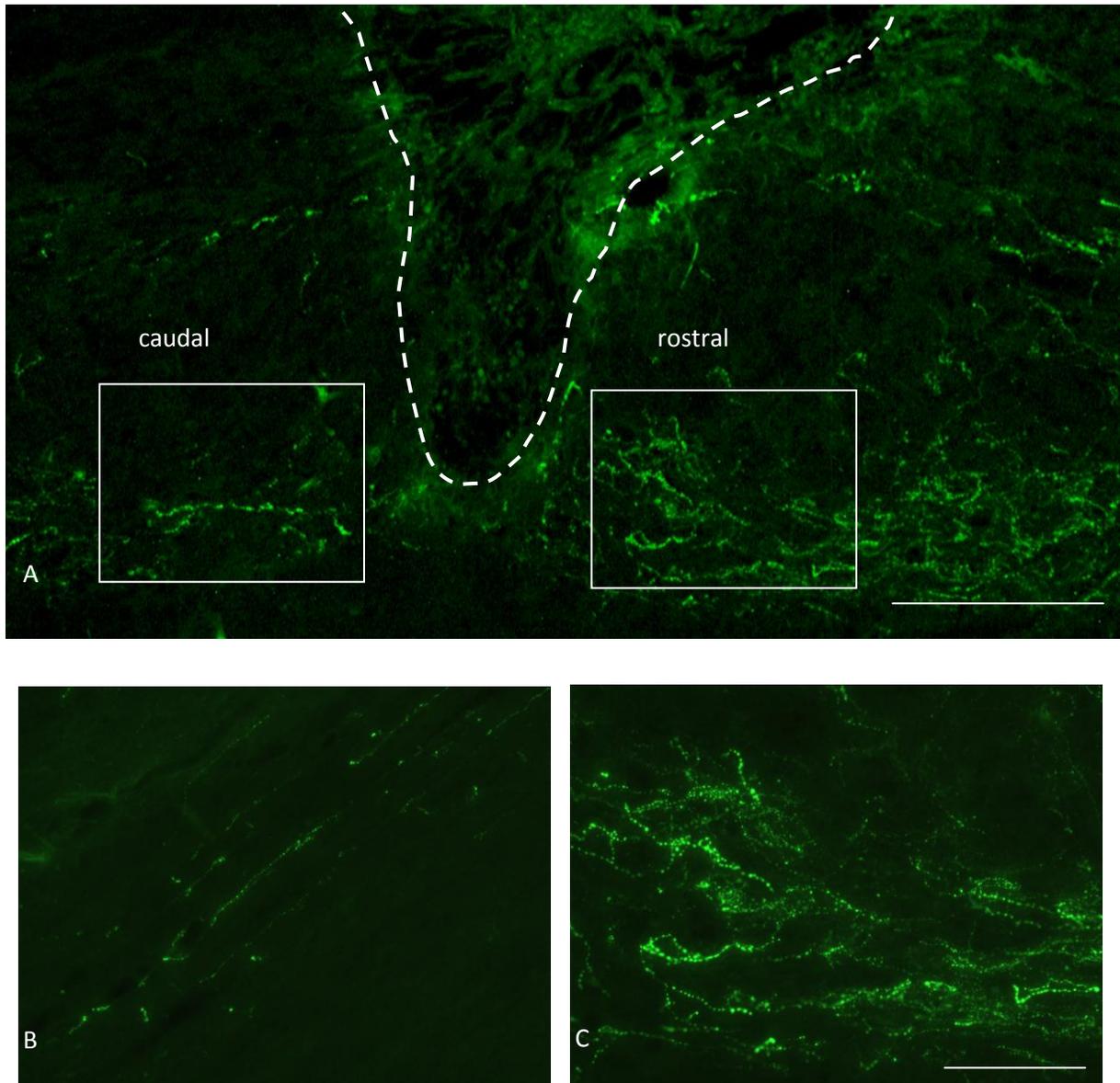
Figure 5.7. Immunohistological analysis of 5-HT-IR fibers. (A) Micrograph of 5-HT at 4× magnification in the MTCN treated animal tissue. The boxed areas in A denote regions selected for quantification and the solid white line represents the lesion interface. More fibers were located rostral versus caudal to the lesion. Scale bar is 500 μm. (B, C) Expanded figures from the white box in figure A. Serotonergic innervations rostral to the lesion in MTP (B) and MTCN (C) animals at 20× magnification. MTCN treated animal has higher fluorescent intensity and also had extended closer to the lesion site than MTP treated animal. Scare bar is 100 μm.
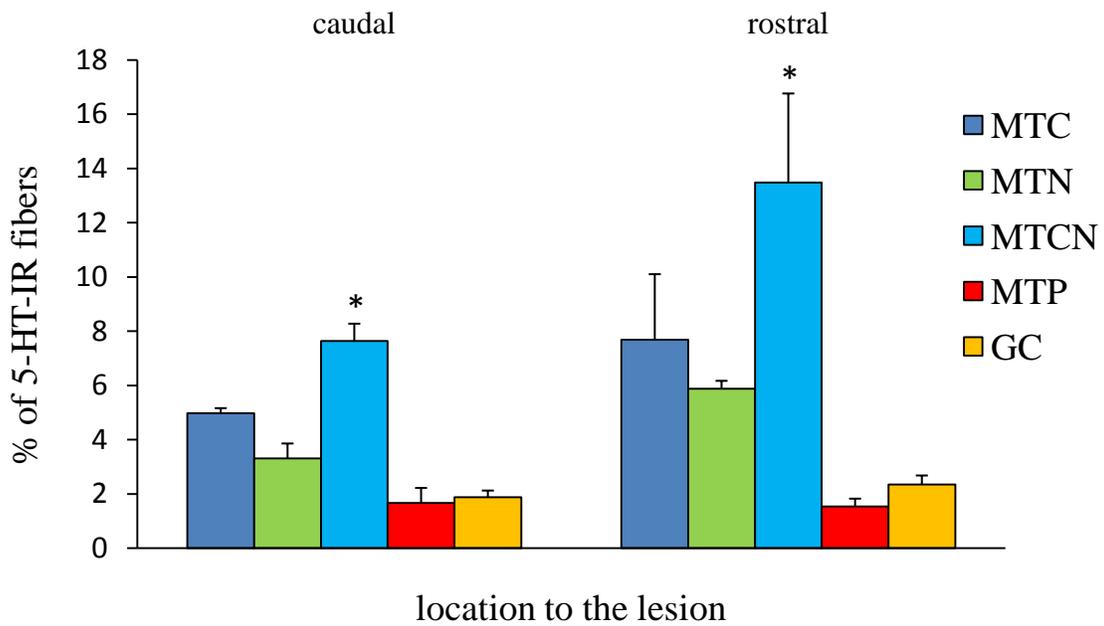
Figure 5.8. Quantitative analysis of 5-HT-IR intensity for the stained spinal cord. Quantification demonstrated that caudal to the lesion, MTCN showed significantly (* $p < 0.05$) increased 5-HT-IR compared to all other treatments, and rostral to the lesion, MTCN showed significantly (* $p < 0.05$) increased 5-HT-IR compared to all other treatments except for MTC. Data are mean ± SEM.

5.4   DISCUSSION

A six week long term study was performed to determine whether chABC or NT-3 delivered individually by using the hydrogel-microtube delivery system would encourage axonal sprouting/regeneration and improve functional recovery after SCI in the rodent model. Also, combination treatment of chABC and NT-3 was tested via our delivery system to evaluate whether the combination therapy can provide synergic effect on axonal regrowth and functional recovery. CSPG deposition, axonal sprouting and behavioral improvement were assessed to determine efficacy of the hydrogel-microtube delivery system and combination therapy. CS-56 immunostaining shows that the resultant impact of the initial CSPG digestion is still present at 6 weeks. Locomotor behavior improved with combinational chABC-NT3 delivery, and correlated well with increased axonal sprouting at the lesion site. This study demonstrates that a single treatment of thermostabilized chABC via the hydrogel-microtube delivery system provides an effective alternative to chronically implanted, invasive pumps typically used to deliver chABC *in viv*o. In addition, the combination treatment with NT-3 significantly enhanced functional recovery.

Once CSPGs are digested, the turn-over is relatively slow (Bruckner et al., 1998). In the short term study, significantly decreased CSPG-IR was observed in the animals treated with the chABC loaded hydrogel-microtube system. CS-56 immunostaining was performed to examine whether CSPG digestion during the first two week still present. CS-56 staining at 6 weeks (Fig. 5.2) shows that little CS-56 expression persists compared to untreated controls. This suggests that thermostabilized chABC digestion was effective early, at the peak of CSPG production and its turn-over is slow (more likely), or that chABC activity via microtubes is sustained for longer than 2 weeks (unlikely, but possible). In either case, the

121

chABC digestion via microtubes remains effective over a period of 6 weeks as is evident from little CS-56 positive tissue at the 6 week time point. CSPG levels remain low up to 6 weeks post-injury, thereby facilitating sprouting and regeneration. Another study reported similar results, showing that evidence of chABC digestion remained for at least 7 weeks in the spinal cord (Galtrey et al., 2007).

The results demonstrated that a single treatment of chABC and NT-3 enhanced sensory axonal sprouting, and the combination treatment enhanced more axonal sprouting around the lesion site. The CTB labeled fibers mainly represent ascending sensory pathways in the dorsal columns of the spinal cord. No CTB-labeled fibers entered the lesion cavity in any treatment condition, however a significantly higher percentage of axons were approached the lesion boundary and grew around the lesion site in the animals treated with single or combination delivery of chABC and NT-3 compared to other groups. While some sensory functional recovery was expected because of the result of CTB-fiber quantification, no improvement was observed using the thermal pain threshold test (hindpaw withdrawal latency to heat stimuli) in any of the animal groups during the 45 day test period. There are two possibilities to explain the results; first, after the dorsal over hemisection cutting there may be possibly spared fibers around the dorsal lateral fasciculus that help retain sensitivity in all groups independent of lesion. Second, despite the significant primary afferent sprouting in the treated animals, the sprouting was predominantly located in the dorsal white matter and no fiber entered into the lesion site in any animal groups. Therefore, the axonal sprouting was not enough to transmit stimuli to the dorsal horn where primary afferent terminals are located, explaining why no differences exist between experimental groups. Our observation is consistent with other studies. Despite robust primary afferent sprouting in

animals treated with chABC, no improvement of noxious thermal sensation (Barritt et al., 2006) was observed, and transgenic mice expressed chABC under the murine *gfap* promoter showed nearly complete digestion of CSPGs and robust axonal growth into the glial scar, but no axon crossing into the lesion or motor functional recovery (Cafferty et al., 2007).

Enhanced locomotor functions were observed in the MTC and MTCN animal groups and there were significant improvements in MTCN treated animals in terms of stride length, but not base support or number of abnormal hindpaw patterns. Stride length is an important parameter of locomotor efficacy as it impacts speed of locomotion (Hamers et al., 2001). The gains in other locomotor functions were probably obscured by our choice of the relatively mild hemisection injury model. Quantification of 5-HT serotonergic fiber sprouting demonstrated significantly higher sprouting in MTCN group relative to all other groups. As microtube-mediated delivery resulted in significant sprouting, with combinatorial delivery eliciting even more significant sprouting, it is possible that the sprouted local serotonergic spinal circuits facilitated observed locomotor improvements in stride length. This increase in sprouting is likely due to chABC mediated digestion of CSPG-rich PNNs that surround synapses (Vitellaro-Zuccarello et al., 1998). One of consequence of the chABC treatment is the digestion of CSPG-rich perineuronal nets (PNNs) (Massey et al., 2006; Galtrey et al., 2007; Massey et al., 2008). There is evidence that this structure regulates neuronal plasticity (Pizzorusso et al., 2002), protects encapsulated neurons (Bruckner et al., 1999) and supports ion homeostasis (Bruckner et al., 1993). This observation is consistent with other reports that PNN digestion by chABC leads to increased plasticity and functional improvement due to reinnervation and sprouting; PNN breakdown in the cuneate nucleus promoted collateral sprouting/plasticity, resulting in axonal sprouting in the forelimb afferents after SCI (Massey

et al., 2006) and increasing plasticity in the spinal cord improved peripheral nerve regeneration (Galtrey et al., 2007). CSPG removal by chABC delivery in the adult visual cortex to treat monocular deprivation increased ocular dominance plasticity by significant recovery of dendritic spine density (Pizzorusso et al., 2006). In this study we observed that the PNN breakdown around the lesion area after chABC treatment (Fig. 4.5); motor neurons and many interneurons are surrounded by PNNs. It may possibly have caused the increased sprouting of serotonergic fibers, thereby increasing plasticity of spinal locomotor circuits and resulting in functional locomotor recovery.

The de-stabilized PNNs by chABC digestion would promote anatomical plasticity by increasing the density of newly-grown processes in the adult CNS ECM, and it could lead functional plasticity. chABC-induced plasticity, such as collateral sprouting (Massey et al., 2006) or aberrant sprouting (Barritt et al., 2006), is one major mechanism of chABC treatment. Therefore, possible negative effects are aberrant sprouting and neuropathic pain due to the aberrant plasticity (Woolf and Salter, 2000) or autonomic dysreflexia due to increased plasticity (Weaver et al., 2006). These concerns have been raised previously. Studies reported that no evidence of hyperalgesia was observed after chABC injection in to the spinal cord (Pizzorusso et al., 2006), and no increase of connectivity of nociceptive neurons and development of mechanical allodynia or thermal hyperalgesia was observed even after aberrant sensory fiber sprouting (Barritt et al., 2006). Therefore, it is very important to balance between detrimental sprouting and beneficial sprouting, and the molecular mechanism involved in chABC-mediated improvement of plasticity needs to be proven to develop the optimized chABC treatment after SCI.

In the short term study, there appears to be significant impact of chABC digestion at 2 weeks, though evidence of functional recovery for *in vivo* studies was not seen until at least 6 weeks. With regard to the time lag between peak CSPG deposition and first evidence of functional recovery, axonal regrowth and sprouting can occur after CSPG digestion – hence the lag in time between CSPG digestion and functional recovery. After injury, severed axons retract from the lesion site, therefore, functional recovery requires axonal regrowth and sprouting to reconnect/regain the functional pathway. Once our chABC treatment removes inhibitory molecules (CSPGs), the CSPG/astroglial-inhibitory region becomes permissive for axonal outgrowth, and axons can then regrow and sprout through the region. After SCI, animals are typically allowed 6 weeks or longer to assess axonal regeneration and functional recovery.

Our data is consistent with other studies where successful digestion of CSPGs does not automatically lead to improved behavioral outcomes (Barritt et al., 2006; Cafferty et al., 2007). Transgenic mice having a *gfap* promoter to express chABC demonstrated almost complete CSPG digestion at the reactive astrocyte-region. Significant sensory axon sprouting was observed, however it was not sufficient to improve motor function (Cafferty et al., 2007). It suggests that providing a permissive environment by removing inhibitory components is not enough to induce significant functional improvement; combination therapy needs to provide to favorable environment for sufficient axon regeneration. When chABC delivery is combined with NT-3 lentivirus delivery, dramatically increased axonal extension was observed compared to single delivery of chABC or NT-3 (Massey et al., 2008). In this study, combination treatment of chABC and NT-3 resulted in significantly increased axonal sprouting as compared to a single treatment of each.

To apply this method as a clinical therapy, the practicality of chABC treatment needs to be considered. In this study, the chABC activity was limited to 1 mm away from lesion site and it is not clear whether this area is large enough to be clinically useful. Because chABC is a relatively large molecule, diffusion through neural tissue and extracellular space is limited. However, we believe that compared to intrathecal delivery of chABC by a mini-pump, chABC delivered via the hydrogel-microtube system diffuses deeper into the tissue (up to 1mm). This is because mini-pump delivery affects a larger region, diluting the chABC, whereas our delivery system enables local delivery into the tissue. As CSPG deposition tapers off exponentially from the lesion border, the local delivery of chABC is relevant and effective, and sufficient diffusion (again as evident from our 6 week CS-56 staining) occurs to effectively digest the CSPGs deposited near the lesion site. In humans, there might be a need for greater diffusion distances as the CSPG deposition zone may be deeper, but whether or not chABC diffusion into injured human cord will be a limitation or not remains to be determined. The minimum clinically relevant chABC concentration required to elicit behavioral recovery also remains to be determined.

5.5   CONCLUSIONS

In conclusion, we demonstrate that sustained local delivery of thermostabilized chABC digests CSPGs after SCI without aggravating secondary injury response. Combination therapy of chABC and NT-3 facilitated by our sustained delivery system enhanced axonal sprouting and functional recovery after SCI. This approach elegantly

obviates the need for invasive, indwelling catheter/pump-mediated delivery of chABC, enables combinatorial therapy with neurotrophic factors, and represents a promising approach to implementing chABC therapy after SCI.

5.6 REFERENCES

Barritt AW, Davies M, Marchand F, Hartley R, Grist J, Yip P, McMahon SB, Bradbury EJ (2006) Chondroitinase ABC promotes sprouting of intact and injured spinal systems after spinal cord injury. J Neurosci 26:10856-10867.

Bruckner G, Bringmann A, Hartig W, Koppe G, Delpech B, Brauer K (1998) Acute and long-lasting changes in extracellular-matrix chondroitin-sulphate proteoglycans induced by injection of chondroitinase ABC in the adult rat brain. Exp Brain Res 121:300-310.

Bruckner G, Hausen D, Hartig W, Drlicek M, Arendt T, Brauer K (1999) Cortical areas abundant in extracellular matrix chondroitin sulphate proteoglycans are less affected by cytoskeletal changes in Alzheimer's disease. Neuroscience 92:791-805.

Bruckner G, Brauer K, Hartig W, Wolff JR, Rickmann MJ, Derouiche A, Delpech B, Girard N, Oertel WH, Reichenbach A (1993) Perineuronal nets provide a polyanionic, glia-associated form of microenvironment around certain neurons in many parts of the rat brain. Glia 8:183-200.

Cafferty WB, Yang SH, Duffy PJ, Li S, Strittmatter SM (2007) Functional axonal regeneration through astrocytic scar genetically modified to digest chondroitin sulfate proteoglycans. J Neurosci 27:2176-2185.

Chau CH, Shum DK, Li H, Pei J, Lui YY, Wirthlin L, Chan YS, Xu XM (2004) Chondroitinase ABC enhances axonal regrowth through Schwann cell-seeded guidance channels after spinal cord injury. FASEB J 18:194-196.

Chvatal SA, Kim YT, Bratt-Leal AM, Lee H, Bellamkonda RV (2008) Spatial distribution and acute anti-inflammatory effects of Methylprednisolone after sustained local delivery to the contused spinal cord. Biomaterials 29:1967-1975.

Filbin MT (2003) Myelin-associated inhibitors of axonal regeneration in the adult mammalian CNS. Nat Rev Neurosci 4:703-713.

Galtrey CM, Asher RA, Nothias F, Fawcett JW (2007) Promoting plasticity in the spinal cord with chondroitinase improves functional recovery after peripheral nerve repair. Brain 130:926-939.

Hamers FP, Lankhorst AJ, van Laar TJ, Veldhuis WB, Gispen WH (2001) Automated quantitative gait analysis during overground locomotion in the rat: its application to spinal cord contusion and transection injuries. J Neurotrauma 18:187-201.

128

Hargreaves K, Dubner R, Brown F, Flores C, Joris J (1988) A new and sensitive method for measuring thermal nociception in cutaneous hyperalesia. *Pain* 32:77-88.

Houle JD, Tom VJ, Mayes D, Wagoner G, Phillips N, Silver J (2006) Combining an autologous peripheral nervous system "bridge" and matrix modification by chondroitinase allows robust, functional regeneration beyond a hemisection lesion of the adult rat spinal cord. J Neurosci 26:7405-7415.

Massey JM, Hubscher CH, Wagoner MR, Decker JA, Amps J, Silver J, Onifer SM (2006) Chondroitinase ABC digestion of the perineuronal net promotes functional collateral sprouting in the cuneate nucleus after cervical spinal cord injury. J Neurosci 26:4406-4414.

Massey JM, Amps J, Viapiano MS, Matthews RT, Wagoner MR, Whitaker CM, Alilain W, Yonkof AL, Khalyfa A, Cooper NG, Silver J, Onifer SM (2008) Increased chondroitin sulfate proteoglycan expression in denervated brainstem targets following spinal cord injury creates a barrier to axonal regeneration overcome by chondroitinase ABC and neurotrophin-3. Exp Neurol 209:426-445.

McKeon RJ, Hoke A, Silver J (1995) Injury-induced proteoglycans inhibit the potential for laminin-mediated axon growth on astrocytic scars. Exp Neurol 136:32-43.

Neumann S, Woolf CJ (1999) Regeneration of dorsal column fibers into and beyond the lesion site following adult spinal cord injury. Neuron 23:83-91.

Pizzorusso T, Medini P, Berardi N, Chierzi S, Fawcett JW, Maffei L (2002) Reactivation of ocular dominance plasticity in the adult visual cortex. Science 298:1248-1251.

Pizzorusso T, Medini P, Landi S, Baldini S, Berardi N, Maffei L (2006) Structural and functional recovery from early monocular deprivation in adult rats. Proc Natl Acad Sci U S A 103:8517-8522.

Schwab JM, Tuli SK, Failli V (2006) The Nogo receptor complex: confining molecules to molecular mechanisms. Trends Mol Med 12:293-297.

Schwab ME (2004) Nogo and axon regeneration. Curr Opin Neurobiol 14:118-124.

Schwab ME, Bartholdi D (1996) Degeneration and regeneration of axons in the lesioned spinal cord. Physiol Rev 76:319-370.

Silver J, Miller JH (2004) Regeneration beyond the glial scar. Nat Rev Neurosci 5:146-156.

Tropea D, Caleo M, Maffei L (2003) Synergistic effects of brain-derived neurotrophic factor and chondroitinase ABC on retinal fiber sprouting after denervation of the superior colliculus in adult rats. J Neurosci 23:7034-7044.

Vitellaro-Zuccarello L, De Biasi S, Spreafico R (1998) One hundred years of Golgi's "perineuronal net": history of a denied structure. Ital J Neurol Sci 19:249-253.

Weaver LC, Marsh DR, Gris D, Brown A, Dekaban GA (2006) Autonomic dysreflexia after spinal cord injury: central mechanisms and strategies for prevention. Prog Brain Res 152:245-263.

Widenfalk J, Lundstromer K, Jubran M, Brene S, Olson L (2001) Neurotrophic factors and receptors in the immature and adult spinal cord after mechanical injury or kainic acid. J Neurosci 21:3457-3475.

Woolf CJ, Salter MW (2000) Neuronal plasticity: increasing the gain in pain. Science 288:1765-1769.

CHAPTER 6

CONCLUSION AND FUTURE PERSPECTIVES

Our delivery method of chABC provides an alternative treatment to spinal cord injury. The results showed enhanced axonal sprouting around the lesion site and improved functional recovery in locomotion. However the ultimate goal is to develop treatment strategies to promote axonal regrowth through the lesion site to regain functional pathways, and apply this method for clinical treatment. In this study no axon enters the lesion site and complete functional recovery was not achieved yet. Therefore, further studies will be discussed in this chapter to overcome these challenges.

6.1 OPTIMIZATION OF CHABC TREATMENT FOR CLINICAL APPLICATION

To investigate clinical relevance of our method, we need to optimize chABC treatment. There are several factors that need to be investigated and determined in order to design the optimized chABC administration: 1) characterize release profile of chABC with various concentrations of chABC, 2) different lengths of lipid microtube, and 3) then determine total amount of chABC for a certain delivery period.

For example, with our delivery method the chABC activity was limited to 1 mm away from lesion site and it is not clear whether the area is a large enough to induce axonal sprouting and functional improvement in clinical study. Because chABC is a relatively large molecule, diffusion through neural tissue and extracellular space is limited. chABC delivered via the hydrogel-microtube system has advantages and diffuses deeper into the tissue (up to

1mm) compared to intrathecal delivery of chABC. However in humans, there might be a need for greater diffusion distances as the CSPG deposition zone may be deeper and larger, but whether or not chABC diffusion into injured human cord will be a limitation remains to be determined. The minimum clinically relevant chABC concentration required to elicit behavioral recovery also remains to be determined.

6.2 EFFECTS OF CHABC ON NERVE TISSUE AND IMMUNE SYSTEM

In this study, single injection of chABC and sustained delivery of chABC did not increase inflammatory response compared to other controls (no treatment and P'ase delivery) after injury. However the effects of chABC on nerve tissue and immune system need to be considered. When chABC was delivered intrathecally to intact spinal cord, robust sprouting of descending projects and primary afferents were observed (Barritt et al., 2006). However, in that study, it did not lead an increase in mechanical allodynia (noxious response to a usually non-painful stimulus) or thermal hyperalgesia (increased sensitivity to thermal pain). Other studies also reported that intrathecal delivery of chABC (0.2 ~ 1 ml of 200 U/ml) showed any morphologic changes in the spinal cord and any neurophysiologic changes in tibial nerves in rabbits (Olmarker et al., 1991). No adverse effects on nerve tissue and blood vessels were observed after intrathecal delivery in pig except a slight intrathecal fibrotic reaction (Olmarker et al., 1996). In those studies, they expected that approximately 1/40 diluted concentration of chABC might be used clinically for chemonucleoysis: however, as we mentioned previously, the clinically relevant dosage still needs to be determined.

chABC is an enzyme produced from bacteria, so there is a chance to evoke immune response. In this study, chABC was delivery locally at the lesion site with lipid microtube

and hydrogel, however antigenicity and immunogenicity of chABC and the delivery system still need to be tested. The safety test of chABC for side effects on nerve tissues and immune response needs to be investigated with the relevant dosage range for clinical application and sustained delivery system for prolonged delivery period.

6.3   LONGER MICROTUBE: OPTIMIZATION OF DELIVERY VEHICLE

A prolonged sustained delivery would be clinically desirable as increasing the duration of release agents. To prolong the period of sustained delivery, longer lipid microtubes can be considered as a delivery vehicle *in vivo*. The length and properties of microtube can be controlled by modifying a cooling procedure, varying concentration of lipid solution and changing ratio between ethanol and water for the solution to dissolve lipid (Lando et al., 1990; Thomas et al., 1995; Meilander et al., 2001). With the original protocol, average 37 micron length of microtube is fabricated. The adjustments were made to the original protocol. 70% ethanol and 1 mg lipid per 1 ml ethanol solution were fixed and a part of cooling process modified; the rate of decreasing temperature (53-23 deg) changed from 1deg/40min to 1 deg/10 min. The measured average length of microtube was approximately 100 micron (Fig. 6.1). We demonstrated that the length of microtube is controllable and since the release profile of loaded agents is dependent on the length of microtube, it facilitates to control drug delivery. The release duration and rate of agent from the delivery scaffold also can be controlled by modifying the gel. The release profiles are dependent on the type and concentration of gel (Meilander et al., 2001; Meilander et al., 2003).
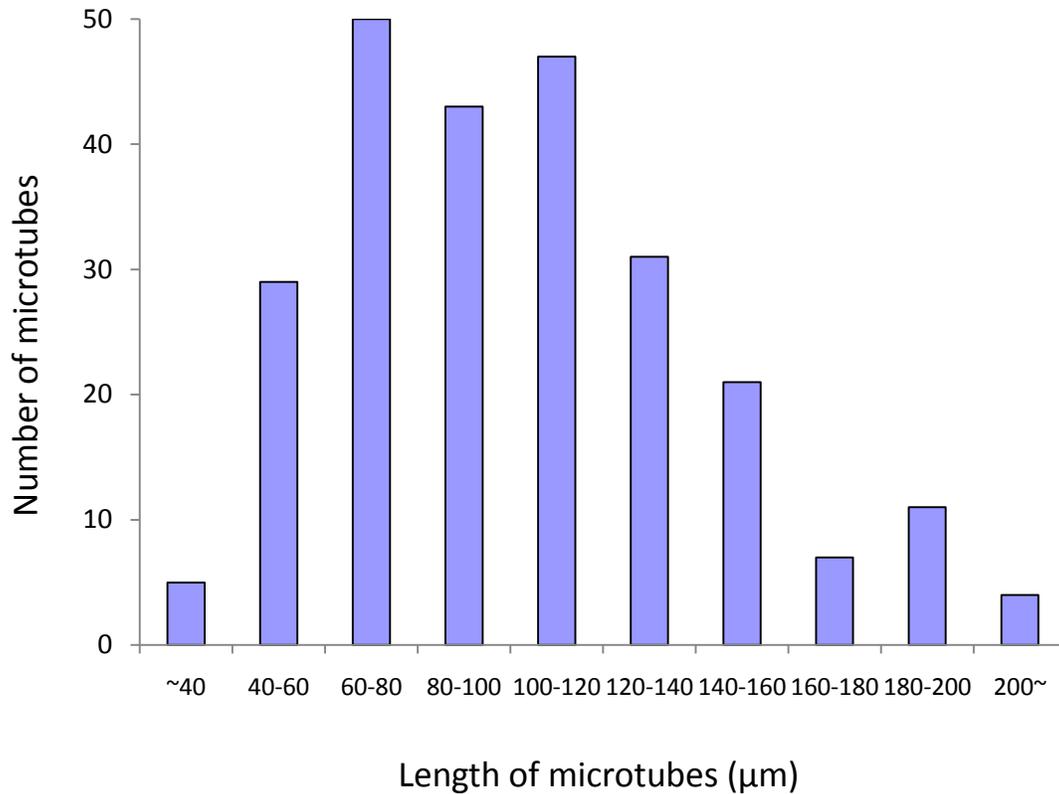
Figure 6.1. Histogram of microtube length distribution with a modified fabrication procedure. The average length is about 100 μm.

6.4   OPTIMIZATION OF DOSAGE

In this *in vivo* study presented in Chapter 4 and 5, one concentration/total amount of chABC and NT-3 was delivered to examine the effect on levels of CSPG deposition, axonal regeneration and functional recovery after SCI in rats. We demonstrated that there are significant differences in CSPG digestion, axonal sprouting and functional recovery between single injection and sustained delivery. Some other studies reported that there is no significant difference in sprouting axons between chABC treatment and untreated groups after SCI (Iaci et al., 2007). This implicates that the amount/concentration of delivered chABC and delivery frequency/period are important to elicit relevant axonal regeneration

and behavioral recovery. Therefore, it is necessary to conduct experiments to optimize the concentration and total amount, and delivery period. The optimal dosage delivered in combination of chABC and NT-3 also needs to be determined, because combining each optimal dosage for individual delivery of chABC or NT-3 might not be the best possible dosage for the combination therapy. For example, other study showed that dramatically improved (~40 times) axonal sprouting was observed with combination therapy of chABC and NT-3 (Massey et al., 2008). In this long term *in vivo* study, even more enhanced axonal sprouting and functional recovery were observed in chABC/NT-3 treated animals than individually treated animals. If the concentration and ratio between chABC and NT-3 are modified, it could synergistically enhance effects on axonal regeneration.

6.5 LONGER *IN VIVO* STUDY

To evaluate the effects of chABC two animal studies were conducted; a 2 week study to evaluate of functionality of our chABC-delivery system in Chapter 4 and a 6 week study to examine axonal sprouting/regeneration and functional recovery as discussed in Chapter 5. The duration of the *in vivo* study is a critical factor to determine whether the administrated therapy is effective or not to treat injuries or diseases. For example, in this study if we had terminated earlier than 6 weeks, we would not observe the significantly improved functional recovery in locomotion assessed by stride length between animal groups. Similarly, if we conduct longer period animal study, such as 8 or 12 weeks, more fibers might outgrow closer to the lesion and even completely grow through/around the lesion site to reconstruct synaptic connections. This would lead to improvement of more precise locomotion controls.

6.6   RATE AND AMOUNT OF CSPG DEPOSITION *IN VIVO* AFTER SCI

In the *in vivo* study, significant differences were observed in the CS-56-IR and 3B3-IR intensity at 2 weeks, and CS-56-IR intensity at 6 weeks between the chABC-hydrogel-microtube treated groups and controls. These results suggested that the enzyme, chABC, still retains its enzymatic activity after being released from the hydrogel-microtube delivery scaffold *in vivo*, and digests CSPGs more effectively than the controls, chABC-hydrogel or chABC-single injection treated groups. However, it is not clear how constant the enzymatic activity of released chABC remains over this time period and how much chABC is released from the delivery scaffold and diffused into the tissue. Once chABC is released from the hydrogel-microtube delivery scaffold, it can be assumed that the activity of chABC will be similar to fresh, unstabilized chABC, because the ratio of trehalose to chABC becomes a lot diluted. It is shown that the production of several CSPGs is differentially regulated following spinal cord injury (Jones et al., 2003) by immunohistological analysis. However, the rates and amount of CSPG deposition are not known and depend on injury models, degree of injury and age (Gilbert et al., 2005). Therefore, it would be clinically desirable if the CSPG deposition rate can be determined for specific injury models and degree of injury.

6.7 COMBINATION STRATEGIES: CHABC AND STEM CELL TRANSPLANTATION

This study showed that combination therapy with thermostabilized chABC and NT-3 significantly enhanced axonal sprouting and functional recovery. Our hydrogel-microtube delivery system with thermostabilized chABC could provide permissive environment for neurite outgrowth and can be combined with other strategies, such as delivery of neurotrophic factor, cell transplantation (NSC, olfactory, Schwann cell, autologus peripheral

nerve graft, etc), and acellular scaffold implantation. This combination therapy can be a potent treatment for many neurodegenerative diseases by promoting axonal regeneration and restoring complete functional recovery after neuronal injuries. One cell transplantation strategy, neural stem cell (NSC) therapy, is very promising; however, this approach needs to be further elucidated before proceeding with clinical trials.

Factors regulating NSC have been investigated, and studies showed that the modulation of local environment is important in regulating NSC. Evidences have been provided that CSPGs regulate neural stem/progenitor cell proliferation and intervene in fate decision making between the neuronal and glial lineage. *In vitro* experiments showed that CSPGs inhibit migration of neural stem/progenitor cell (NSPC)-derived cells and chABC treatment attenuated the inhibitory effect (Ikegami et al., 2005; chABC). Also, cell-surface soluble GAGs involve in internalization of extracellular proteins for some progenitor cell to facilitate differentiation; an example would be of heparin sulfate proteoglycan for pancreatic stem cells (Ueda et al., 2008; heparin). As explained above, chABC can be used to modify the local environment in CNS via digesting CS-GAGs and also to selectively degrade GAGs for investigating biological roles of CSPGs *in vitro*.

The use of NSCs in conjunction with chABC may prove to be therapeutic in repairing CNS by modulating cellular matrix and CSPGs, which act as a barrier for stem cell migration after transplantation. In many cases, however, transplanted stem cells fail to migrate and integrate into the host tissue and CSPGs are considered as a putative inhibitor of stem cell migration *in vivo*. chABC treatment combined with NSPC transplantation into injured spinal cord promoted migration of the transplanted cell into the host spinal cord and resulted in increased sprouting of growth-associated protein -43-positive fibers at the lesion site

(Ikegami et al., 2005; chABC). When Müller stem cells were implanted with chABC into degenerating retina , this resulted in dramatic increase of migration of stem cell into all of the retina cell layers (Singhal et al., 2008; CSPGs; Fawcett) and differentiation into retinal neurons and glia (Bull et al., 2008; glaucoma stem).

Studies suggest that chABC treatment can facilitate migration and differentiation of transplanted NSPCs. Therefore, when the sustained local delivery of thermostabilized chABC by our hydrogel-microtube system is combined with NSPCs transplantation, it will be a promising strategy for the regeneration of injured or degenerated CNS tissues. Also, our chABC treatment can be combined with delivery of other neurotrophic factors and cell transplantations.

6.8   DIFFERENCES BETWEEN HUMAN CASES AND RAT INJURY MODEL

It is hard to simulate the human cases of SCI in animal experiments: first, human SCI occurs in the closed vertebral system generally under conscious state and a combination force of flexion, extension, rotation and compression works on the cord when the injury happens (Sharma et al., 1993; Choi, 1996). Most human SCI results from fracture of vertebral column or luxation of vertebrae. In contrast, in animal models, injury or compression is always conducted on the posterior side of the cord with laminectomy (opened vertebra system) under anaesthetized state and one force, such as contusion, compression or incision, is applied to produce injury for high reproducibility (Sharma, 2005a). Therefore, human SCI cases are more complex and only few cases are similar to experimental models in terms of the magnitude and severity of the injury (Sharma, 2005b; Onifer et al., 2007). Table 3 summarizes different facts between human and rat spinal cord.

Parameters	Human	Rat
Number of neurons	10^9	0.3^6
Length (cm)	43-45	8-10
Weight (g)	34	0.7
Proportion to brain (volume %)	2	35
Glial/neuron ratio	12-16	10-14
Weight drop injury (g)	2438	50*
	971	20*
	485	10*

Table 3. A comparison between human and rat spinal cord.
* Weight for rat SCI is about one fifth to human SCI. Table from Sharma, 2007.

Our study required an SCI model allowing for behavioral and immunohistological analysis to examine functional recovery and axonal regeneration. There are several commonly used models for spinal cord injury and each has advantages and disadvantages: complete spinal transection, dorsal over hemisection, lateral hemisection injury, compression and contusion.

The complete transection model removes any overlap between spared and regenerated fibers. However, the animal undergoes severe pain and various syndromes, such as bowel and bladder dysfunction and no functional recovery with hindlimbs, because the transection completely eliminates functions below the injury site. Therefore, it requires relatively long term management with various post-surgical complications and morbidity is higher than other injury models.

The contusion model could be the most clinically relevant model, although it still lacks some of the absent factors described above. A fluid filled cyst forms at the impacted area and is surrounded by tissue containing spared/intact axons (Kwon et al., 2002). Because

of the spared axons around the cyst, it is hard to distinguish between spared and regenerated axons (Steward et al., 2003) and it is a limitation for studies focusing on regeneration.

The lateral transection model is a complete transection of one side of the spinal cord. In this model all pathways in one side of the cord are severed. However, intact axons in the non-lesioned side can sprout into the lesioned side and make it hard to distinguish from regenerated axons (Kwon et al., 2002).

The dorsal over hemisection model has relatively moderate severity of injury. In this injury model, damage is limited in the dorsal column and animals undergo less stress and pain with less post-surgery dysfunctions than other injury models. Axonal regeneration can be easily quantified by injection of anterograde tracer (i.e. BDA) to the corticospinal tract (CST) or retrograde tracer to the primary sensory pathway (i.e. cholera toxin subunit B), and spared fiber is not a critical issue. Therefore, the dorsal over hemisection model was chosen for our study. There is a chance of spared fibers in the bilateral transected CST (Vavrek et al., 2006), and the primary sensory pathway was chosen in this study to examine regenerating axons.

As a further study, contusion injury model can be used to examine the delivery efficiency of our topical delivery method with chABC and develop a more relevant delivery method for human therapy. In the contusion model, it would be difficult to deliver drugs deep through the surrounding tissue to the cyst with our topical delivery model if the drug is not small enough. Diffusion efficiency of chABC needs to be examined in this model. If the diffusion is not enough to remove CSPGs and promote axonal outgrowth, alternative delivery methods should be developed, such as a direct injection of mitcrotube-trehalose/chABC into the cyst by needle.

6.9 REFERENCES

Barritt AW, Davies M, Marchand F, Hartley R, Grist J, Yip P, McMahon SB, Bradbury EJ (2006) Chondroitinase ABC promotes sprouting of intact and injured spinal systems after spinal cord injury. J Neurosci 26:10856-10867.

Bull ND, Limb GA, Martin KR (2008) Human Muller stem cell (MIO-M1) transplantation in a rat model of glaucoma: survival, differentiation, and integration. Invest Ophthalmol Vis Sci 49:3449-3456.

Choi DW (1996) Ischemia-induced neuronal apoptosis. Curr Opin Neurobiol 6:667-672.

Gilbert RJ, McKeon RJ, Darr A, Calabro A, Hascall VC, Bellamkonda RV (2005) CS-4,6 is differentially upregulated in glial scar and is a potent inhibitor of neurite extension. Mol Cell Neurosci 29:545-558.

Iaci JF, Vecchione AM, Zimber MP, Caggiano AO (2007) Chondroitin sulfate proteoglycans in spinal cord contusion injury and the effects of chondroitinase treatment. J Neurotrauma 24:1743-1759.

Ikegami T, Nakamura M, Yamane J, Katoh H, Okada S, Iwanami A, Watanabe K, Ishii K, Kato F, Fujita H, Takahashi T, Okano HJ, Toyama Y, Okano H (2005) Chondroitinase ABC combined with neural stem/progenitor cell transplantation enhances graft cell migration and outgrowth of growth-associated protein-43-positive fibers after rat spinal cord injury. Eur J Neurosci 22:3036-3046.

Jones LL, Margolis RU, Tuszynski MH (2003) The chondroitin sulfate proteoglycans neurocan, brevican, phosphacan, and versican are differentially regulated following spinal cord injury. Exp Neurol 182:399-411.

Kwon BK, Oxland TR, Tetzlaff W (2002) Animal models used in spinal cord regeneration research. Spine (Phila Pa 1976) 27:1504-1510.

Lando JB, Hansen JE, Sudiwala RV, Rickert SE (1990) The formation of polymerizable tubules. Polym Adv Technol 1:27-32.

Massey JM, Amps J, Viapiano MS, Matthews RT, Wagoner MR, Whitaker CM, Alilain W, Yonkof AL, Khalyfa A, Cooper NG, Silver J, Onifer SM (2008) Increased chondroitin sulfate proteoglycan expression in denervated brainstem targets following spinal cord injury creates a barrier to axonal regeneration overcome by chondroitinase ABC and neurotrophin-3. Exp Neurol 209:426-445.

Meilander NJ, Yu X, Ziats NP, Bellamkonda RV (2001) Lipid-based microtubular drug delivery vehicles. J Control Release 71:141-152.

Meilander NJ, Pasumarthy MK, Kowalczyk TH, Cooper MJ, Bellamkonda RV (2003) Sustained release of plasmid DNA using lipid microtubules and agarose hydrogel. J Control Release 88:321-331.

Olmarker K, Danielsen N, Nordborg C, Rydevik B (1991) Effects of chondroitinase ABC on intrathecal and peripheral nerve tissue. An in vivo experimental study on rabbits. Spine (Phila Pa 1976) 16:43-45.

Olmarker K, Stromberg J, Blomquist J, Zachrisson P, Nannmark U, Nordborg C, Rydevik B (1996) Chondroitinase ABC (pharmaceutical grade) for chemonucleolysis. Functional and structural evaluation after local application on intraspinal nerve structures and blood vessels. Spine (Phila Pa 1976) 21:1952-1956.

Onifer SM, Rabchevsky AG, Scheff SW (2007) Rat models of traumatic spinal cord injury to assess motor recovery. ILAR J 48:385-395.

Sharma HS (2005a) Pathophysiology of blood-spinal cord barrier in traumatic injury and repair. Curr Pharm Des 11:1353-1389.

Sharma HS (2005b) Neuroprotective effects of neurotrophins and melanocortins in spinal cord injury: an experimental study in the rat using pharmacological and morphological approaches. Ann N Y Acad Sci 1053:407-421.

Sharma HS, Olsson Y, Nyberg F, Dey PK (1993) Prostaglandins modulate alterations of microvascular permeability, blood flow, edema and serotonin levels following spinal cord injury: an experimental study in the rat. Neuroscience 57:443-449.

Singhal S, Lawrence JM, Bhatia B, Ellis JS, Kwan AS, Macneil A, Luthert PJ, Fawcett JW, Perez MT, Khaw PT, Limb GA (2008) Chondroitin sulfate proteoglycans and microglia prevent migration and integration of grafted Muller stem cells into degenerating retina. Stem Cells 26:1074-1082.

Steward O, Zheng B, Tessier-Lavigne M (2003) False resurrections: distinguishing regenerated from spared axons in the injured central nervous system. J Comp Neurol 459:1-8.

Thomas BN, Safinya CR, Plano RJ, Clark NA (1995) Lipid Tubule Self-Assembly: Length Dependence on Cooling Rate Through a First-Order Phase Transition. Science 267:1635-1638.

Trounson A (2009) New perspectives in human stem cell therapeutic research. BMC Med 7:29.

Ueda M, Matsumoto S, Hayashi S, Kobayashi N, Noguchi H (2008) Cell surface heparan sulfate proteoglycans mediate the internalization of PDX-1 protein. Cell Transplant 17:91-97.

Vavrek R, Girgis J, Tetzlaff W, Hiebert GW, Fouad K (2006) BDNF promotes connections of corticospinal neurons onto spared descending interneurons in spinal cord injured rats. Brain 129:1534-1545.